TRIBHUVAN UNIVERSITY
INSTITUTE OF ENGINEERING
PULCHOWK CAMPUS

THESIS NO: 079/MSPSE/024

Voltage Impact Analysis for VSC-Based DGs Connected to the Primary Distribution System

by

Upendra Bhattarai

A THESIS
SUBMITTED TO THE DEPARTMENT OF ELECTRICAL ENGINEERING IN PARTIAL FULFILLMENT OF THE REQUIREMENTS FOR THE DEGREE OF
MASTER OF SCIENCE IN POWER SYSTEM ENGINEERING

DEPARTMENT OF ELECTRICAL ENGINEERING
LALITPUR, NEPAL

APRIL, 2025

Voltage Impact Analysis for VSC-Based DGs Connected to the Primary Distribution System

by

Upendra Bhattarai

Roll No: PUL079MSPSE024

Thesis Supervisor:

Dr. Sujan Adhikari

Associate Professor, Hillside College of Engineering

Balkumari, Kathmandu

A thesis

submitted to the Department of Electrical Engineering

in partial fulfillment of the requirements for the degree of

Master of Science in Power System Engineering

Department of Electrical Engineering

Institute of Engineering, Pulchowk Campus

Tribhuvan University

Lalitpur, Nepal

APRIL, 2025

COPYRIGHT©

The author has agreed that the library, Department of Electrical Engineering, Pulchowk Campus, Institute of Engineering, Tribhuvan University, Nepal may make this dissertation freely available for inspection. Moreover, the author has agreed that the permission for extensive copying of this dissertation work for scholarly purpose may be granted by the professor(s), who supervised the dissertation work recorded herein or, in their absence, by the Head of the Department, wherein this dissertation was done. It is understood that the recognition will be given to the author of this dissertation, and the Department of Electrical Engineering, Pulchowk Campus, Institute of Engineering, Tribhuvan University, Nepal in any use of the material of this dissertation. Copying or publication or other use of this dissertation for financial gain without approval of the Department of Electrical Engineering, Pulchowk Campus, Institute of Engineering, Tribhuvan University, Nepal and author's written permission is prohibited. Request for permission to copy or to make any use of the material in this dissertation in whole or part should be addressed to:

Head of Department
Department of Electrical Engineering
Tribhuvan University, Institute of Engineering
Pulchowk Campus, Pulchowk, Lalitpur, Nepal

Accredited by University Grants Commission (UGC) Nepal 2020

त्रिभुवन विश्वविद्यालय
TRIBHUVAN UNIVERSITY
इन्जिनियरिङ्ग अध्ययन संस्थान
INSTITUTE OF ENGINEERING
पुल्चोक क्याम्पस
PULCHOWK CAMPUS
DEPARTMENT OF ELECTRICAL ENGINEERING
Pulchowk, Lalitpur

Institute of Engineering Electrical Engineering Department Pulchowk Campus

CERTIFICATE OF APPROVAL

The undersigned certify that they have read and recommended to the Institute of Engineering for acceptance, a dissertation entitled "**Voltage Impact Analysis for VSC-Based DGs Connected to the Primary Distribution System**" submitted by **Upendra Bhattarai** in partial fulfilment of the requirement for the award of the degree of **Master of Science in Power System Engineering.**

Dr. Sujan Adhikari
Associate Professor, Hillside College of Engineering, Balkumari, Kathmandu
(Supervisor)

Dr. Laxman Maharjan
Former Assistant Manager, Corporate R&D Headquarters, Fuji Electric Co., Ltd., Japan
(External Examiner)

Asst. Prof. Dr. Bishal Silwal
Program Coordinator
M. Sc. in Power System Engineering
Pulchowk Campus, Lalitpur

Assoc. Prof. Dr. Basanta Kumar Gautam
Head of Department
Department of Electrical Engineering
Pulchowk Campus, Lalitpur

APRIL, 2025

ACKNOWLEDGEMENT

I would like to extend my heartfelt gratitude to a number of individuals and institutions whose support and encouragement have been instrumental in the completion of this thesis. First and foremost, I owe a profound debt of gratitude to my supervisor, **Dr. Sujan Adhikari**, whose exceptional guidance, insightful feedback, and unwavering commitment have shaped this research from its inception to its final form. His expertise in electrical engineering and his willingness to provide constructive advice during every stage of this journey have been invaluable, inspiring me to push the boundaries of my understanding and refine my work to meet the highest academic standards.

I am also deeply thankful to the entire faculty and staff of the **Department of Electrical Engineering** at the Institute of Engineering (IoE), Pulchowk Campus. They have created a supportive academic environment that greatly enriched my learning experience and enabled me to conduct this research effectively. I am particularly grateful to my colleagues and peers within the department, whose collaborative spirit and intellectual exchanges have broadened my perspective and motivated me to excel.

Beyond the academic sphere, I wish to express my sincere appreciation to my friends, who have offered endless encouragement, shared in my challenges, and celebrated my progress. Their companionship has been a vital source of motivation during moments of doubt. Above all, I am deeply grateful to my family for their unconditional love, patience, and understanding, which sustained me through the demanding phases of this endeavor. Their belief in my abilities and their constant moral support have been the bedrock of my perseverance.

This thesis stands as a testament to the collective efforts and belief of all those mentioned above. I am truly honored to have been supported by such a remarkable network of individuals and institutions. Thank you all for being an integral part of this rewarding academic journey and for helping me turn my aspirations into reality.

ABSTRACT

The rapid integration of renewable Distributed Energy Resources (DERs), particularly photovoltaic (PV) systems using Voltage Source Converters (VSCs), into primary distribution networks poses significant challenges for maintaining voltage stability and power quality. This thesis examines the voltage impacts of VSC-based PV systems in high-DER environments, focusing on steady-state overvoltage and Rapid Voltage Change (RVC). A comprehensive simulation framework is developed using the IEEE 8500-node test feeder in CYMDIST to analyze the effects of PV placement, feeder impedance (R/X ratio), and loading conditions on voltage profiles and RVC due to sudden drops in PV output. Two mitigation strategies—fixed power factor (PF) operation and Volt-VAR operation, both leveraging smart inverter capabilities—are evaluated under high, medium, and low load conditions with high PV penetration. The study first applies fixed PF operation to assess voltage impact mitigation, followed by a practical Volt-VAR curve with appropriate settings for performance comparison. Results show that steady-state voltage rise is most severe during low load conditions, while RVC is most pronounced during peak load, underscoring the need to evaluate both phenomena across diverse load scenarios. PV placement near substations significantly reduces both steady-state voltage rise and RVC, especially in feeders with high R/X ratios. Fixed PF operation exhibits limited effectiveness in dynamic conditions due to its static nature, whereas Volt-VAR operation, aligned with IEEE 1547-2018 standards, effectively mitigates voltage violations by dynamically adjusting to a non-unity power factor, maintaining steady-state voltage within ANSI C84.1 limits (114–126 V) under varying conditions. These findings highlight the importance of strategic PV placement and advanced smart inverter technologies in supporting high PV penetration while ensuring grid reliability. This research offers practical guidance for utilities to study DER impacts across various loading scenarios and select effective mitigation strategies, while guiding developers in choosing site locations to minimize voltage impact mitigation costs, emphasizing the critical role of smart inverter capabilities for both stakeholders.

Keywords: *Distributed Energy Resources (DERs), IEEE 8500-Node Test Feeder, Photovoltaic (PV) Systems, Power Quality, Primary Distribution System, Rapid Voltage Change (RVC), Reactive Power Control, Smart Inverter Control, Volt-VAR Operation, Voltage Rise, Voltage Source Converter (VSC).*

TABLE OF CONTENTS

LIST OF FIGURES

LIST OF TABLES

LIST OF ABBREVIATIONS

DERs	Distributed Energy Resources
DGs	Distributed Generations
ECG	Electronically Coupled Generator
GSU	Generator Step-Up Transformer
IEEE	Institute of Electrical and Electronics Engineers
MV	Medium Voltage
MW	Mega-Watt
MVA	MegaVolt-Amperes
POI	Point of Interconnection
PF	Power Factor
PV	Photovoltaic Systems
RVC	Rapid Voltage Change
Volt-VAR	Voltage - Reactive Power Operation
VSC	Voltage Source Converter

CHAPTER ONE: INTRODUCTION

1.1 Background

The integration of renewable energy sources (RES) into modern power distribution systems has accelerated significantly, driven by global efforts to reduce carbon emissions and enhance energy sustainability. Among these, Photovoltaic (PV) systems and Battery Energy Storage Systems (BESS), interfaced through Voltage Source Converters (VSCs), have emerged as key Distributed Energy Resources (DERs) within primary distribution networks. These VSC-based DGs offer substantial benefits, including reduced reliance on fossil fuels and improved grid flexibility to handle fluctuating demand. However, their intermittent generation profiles introduce pronounced challenges in voltage regulation, particularly in the context of high penetration levels. Two critical issues dominate: steady-state voltage rise due to excess power injection during low demand, and Rapid Voltage Change (RVC), often manifesting as voltage flicker, caused by abrupt fluctuations in PV output from environmental or grid-related factors. Addressing these phenomena is essential to ensure grid stability, power quality, and compliance with operational standards in contemporary distribution systems.

1.2 Problem Statement

The rapid integration of distributed energy resources (DERs), such as photovoltaic (PV) systems, into modern distribution systems has introduced significant challenges in maintaining voltage stability and power quality. As DER penetration increases, primary distribution networks face two prominent issues: overvoltage and voltage flicker. Overvoltage occurs when excessive active power from Voltage Source Converter (VSC)-based Distributed Generations (DGs), particularly PV systems, is injected into feeders with high impedance, especially during low-load conditions. This phenomenon is exacerbated in long radial feeders, typical of U.S. utility systems operating at 12.47 kV, where the voltage rise can exceed acceptable limits, such as those defined by ANSI C84.1 (114–126 V). Additionally, sudden drops in DER output—caused by environmental factors like cloud cover or system faults—lead to rapid voltage changes (RVC), manifesting as voltage flicker at customer premises. This flicker, often exceeding IEEE 1547-2018 limits ($\leq 3\%$), negatively impacts power quality and poses operational challenges for utilities. Traditional mitigation approaches, such as upgrading infrastructure or deploying additional voltage

regulation devices, often impose substantial financial burdens on PV developers, making them cost-prohibitive. Consequently, there is a pressing need to investigate the root causes of these voltage issues, considering factors like PV placement, feeder impedance (e.g., R/X ratio), and loading variations, while exploring advanced mitigation strategies, such as Volt-VAR operation with smart inverters, to ensure grid reliability and stability in high-DER environments.

1.3 Scope of this Thesis

This research focuses on analyzing the voltage impacts of Voltage Source Converter (VSC)-based Distributed Energy Resources (DERs), specifically photovoltaic (PV) systems, within primary distribution systems, using the IEEE 8500-node test feeder as a realistic simulation framework to represent large-scale networks. The study examines voltage regulation challenges under three distinct loading scenarios—Peak (100%), Normal (60%), and Off-Peak (15%)—with a constant PV output of 10 MVA across all cases to simulate worst-case conditions, ensuring that mitigation strategies developed for extreme scenarios, where voltage rise and rapid voltage changes (RVC) are most pronounced, remain robust across intermediate operating states, despite real-world variations in PV generation and feeder loading due to environmental and temporal factors. The scope is limited to steady-state phenomena, excluding transient dynamics, focusing on persistent voltage regulation issues such as overvoltage and RVC during extreme loading conditions and maximum PV output. This work involves evaluating the effectiveness of advanced mitigation strategies, specifically fixed power factor (PF) and Volt-VAR operations as smart inverter capabilities, with fixed PF applied first to assess voltage impact mitigation, followed by the implementation of a practical Volt-VAR curve with appropriate settings for performance comparison, highlighting Volt-VAR's effectiveness due to its ability to dynamically adjust the reactive power injection/absorption.

The scope of this study is further refined to focus exclusively on the voltage impacts of PV systems exporting power to the grid, rather than incorporating Battery Energy Storage Systems (BESS) within VSC-based DGs. A key aspect of this research is the analysis of Rapid Voltage Change (RVC), where frequent drops in PV output due to cloud coverage can significantly affect voltage at the Point of Interconnection (POI) and regulating devices, potentially exceeding RVC limits. For this purpose, the study prioritizes the specific impact of PV generation. While BESS could also export power similarly to PV, its charging scenario deviates towards a load interconnection study, necessitating an emphasis on undervoltage conditions and known charging

limits—areas outside this thesis's focus on overvoltage and flicker from DG export. Moreover, in practical applications, developers often pair BESS with PV (e.g., DC-coupled BESS charged by co-located PV systems), minimizing direct grid impact during charging. Thus, this study concentrates on PV exporting to the grid as the primary case, with BESS charging impacts deferred to future research.

1.3.1 Objectives of the Thesis

This thesis aims to address the voltage regulation challenges posed by high Distributed Energy Resource (DER) penetration in distribution systems through the following objectives:

- **To analyze the combined impact of PV location, feeder impedance, and feeder loading conditions on voltage rise and flicker:** This objective focuses on quantifying the effects of photovoltaic (PV) placement, feeder impedance (specifically the R/X ratio), and loading conditions on steady-state overvoltage and Rapid Voltage Change (RVC) in large-scale networks. Using the IEEE 8500-node test feeder as the simulation platform in CYMDIST, the study examines Peak, Normal, and Off-Peak scenarios to understand how these factors interact and exacerbate voltage issues.

- **To evaluate voltage impact mitigation using fixed power factor (PF) operation and practical Volt-VAR operation with appropriate settings, comparing their effectiveness as smart inverter capabilities:** This objective focuses on assessing voltage impact mitigation by first applying fixed PF operation, a smart inverter capability, to establish a baseline for managing voltage violations in high-DER environments. Subsequently, a practical Volt-VAR curve with suitable settings—such as deadband width, VAR limits, and regulation region—is implemented to dynamically adjust reactive power, leveraging the smart inverter's ability to operate at a non-unity power factor as needed. The study compares the performance of these two mitigation strategies using simulation results on the IEEE 8500-node test feeder, validating their effectiveness in maintaining grid voltage stability during high PV penetration scenarios.

1.4 Thesis Organization

This dissertation is structured into six chapters, followed by References and Appendices, systematically addressing the voltage regulation challenges posed by Voltage

Source Converter (VSC)-based Distributed Energy Resources (DERs) in primary distribution systems. Below is a brief outline of each chapter and its contents:

- Chapter 1: Introduction provides an overview of the integration of renewable energy sources, specifically photovoltaic (PV) systems, into modern distribution networks. It introduces the key challenges of voltage rise and rapid voltage changes (flicker), defines the problem statement, outlines the scope and objectives of the thesis, and discusses its limitations. The problem statement, detailed in Section 1.2, highlights the critical voltage stability issues in high-DER environments.

- Chapter 2: Literature Review reviews existing research, standards, books related to the integration of renewable Distributed Generations (DGs), particularly photovoltaic (PV) systems, into distribution networks, focusing on voltage stability and power quality challenges. It explores the impact of high DGs penetration on voltage regulation, including overvoltage and rapid voltage changes (RVC), and evaluates mitigation strategies such as energy storage, reactive power support, and smart inverter-based fixed PF and Volt-VAR operations. The chapter also introduces the IEEE 8500-node test feeder as a benchmark for large-scale analysis, identifies gaps in the literature regarding the combined effects of PV placement, R/X ratio, and loading conditions, and outlines how this thesis addresses these gaps using CYMDIST simulations.

- Chapter 3: Theoretical Background establishes the theoretical framework for voltage impact analysis. It explores the causes and effects of voltage flicker and voltage rise, supported by mathematical models, and discusses mitigation strategies, encompassing both conventional and advanced inverter-based techniques. The chapter provides a detailed comparison of reactive power compensation methods defined by IEEE 1547-2018, including Constant Power Factor (PF), Volt-VAR, Watt-VAR, Constant Reactive Power, and Volt-Watt operations, evaluating their operational principles and suitability for high-DER penetration scenarios. It also explains the rationale for focusing on Constant PF and Volt-VAR operations in this study, as these methods are widely adopted by local standards for mitigating voltage violations, offering a practical basis for performance evaluation in subsequent chapters.

- Chapter 4: Methodology describes the research design and simulation setup. It details the IEEE 8500-node test feeder model, case study scenarios based

on PV placement and loading conditions, evaluation metrics, simulation parameters in CYMDIST, and the development of Volt-VAR operation settings, providing a structured approach to achieving the thesis objectives.

- Chapter 5: Results and Discussion presents the simulation results for steady-state voltage and rapid voltage change (RVC) analyses conducted on the IEEE 8500-node test feeder using CYMDIST. It discusses the impacts of PV placement, loading conditions, and R/X ratios on voltage profiles, highlighting the distinct behavior of voltage rise and RVC across different scenarios. The chapter evaluates the effectiveness of fixed power factor (PF) and Volt-VAR operations as smart inverter capabilities for voltage impact mitigation, with fixed PF applied first to establish a baseline, followed by a practical Volt-VAR curve with appropriate settings for performance comparison. Volt-VAR operation is shown to be highly effective due to its dynamic adjustment to a non-unity power factor, while fixed PF exhibits limitations under varying loading conditions. Additionally, the chapter provides an integrated analysis of steady-state and dynamic voltage impacts, emphasizing the need for simulataneous analysis, and proposes future research directions to enhance grid stability in high-DER networks.

- Chapter 6: Conclusion and Recommendation synthesizes the study's key findings, highlighting the effectiveness of placing PV systems near substations to mitigate steady-state overvoltage and the critical role of smart inverter controls in managing high PV penetration while ensuring grid reliability. It emphasizes the distinct behavior of voltage rise and RVC under various loading conditions, underscoring the need to evaluate impacts across all scenarios. The chapter details the performance comparison of fixed power factor (PF) and Volt-VAR operations as smart inverter capabilities, with fixed PF applied first, followed by a practical Volt-VAR curve, demonstrating Volt-VAR's superior effectiveness due to its dynamic non-unity power factor adjustment. It offers practical recommendations for engineers and utilities, including strategic PV placement, adoption of Volt-VAR operation, and adaptive control strategies, while proposing future research directions—such as exploring adaptive Volt-VAR settings, BESS integration, and real-world feeder studies—to address evolving grid challenges.

- The References section lists all cited works, providing a comprehensive bibliography of standards, journal articles, Books and technical reports relevant to voltage regulation and DER integration.

- The Appendices include supplementary data, such as system modeling information and simulation settings to support the findings of the thesis. Additionally, the section includes the Conference Paper publication confirmation and plagiarism report to further verify the integrity of the research.

CHAPTER TWO:LITERATURE REVIEW

The integration of renewable Distributed Generations (DGs), particularly photovoltaic (PV) systems, into distribution networks has gained significant momentum globally, driven by the need for sustainable energy solutions. However, this rapid adoption introduces complex technical challenges, especially in maintaining voltage stability and power quality. A substantial body of research has explored these issues, focusing on the interaction between DGs and existing network infrastructure, as well as the development of mitigation strategies.

Awad et al. [1] investigate the impact of high DG penetration on the operation of under-load tap changers (ULTCs) in Canadian rural distribution feeders, using OpenDSS simulations. Their study highlights how variable DG output leads to rapid voltage fluctuations, straining ULTC tap operations designed for slow load variations. They conclude that DG concentrations near ULTC secondary terminals exacerbate tap operations, while constant power factor (PF) mode offers a practical trade-off between simplicity and effectiveness in reducing tap changes, compared to more complex modified ULTC controllers. Similarly, Hamza et al. [2] provide a comprehensive overview of PV integration effects on low-voltage distribution networks (LVDNs), emphasizing overvoltage as a critical concern. Their analysis compares mitigation strategies such as energy storage systems (ESSs), load shedding methods (LSM), reactive power support (RPS), active power curtailment (APC), on-load tap changers (OLTCs), reactive power compensation (RPC), and hybrid methods (HMs). They note that while ESSs enhance reliability and voltage regulation, their high installation costs are a drawback, whereas RPC and HMs, though effective, involve significant expenses due to FACTS devices and coordination complexities.

Haque and Wolfs [3] review the global expansion of PV systems, reaching 177 GW by 2014, and their impact on low-voltage (LV) networks with high R/X ratios. They categorize mitigation techniques into commercially available (e.g., OLTCs) and emerging methods (e.g., VAr control of PV inverters, distributed batteries, FACTS controllers), concluding that FACTS devices, particularly unified power flow controllers (UPFCs), are more effective, though VAr control is limited by current standards, and batteries are cost-prohibitive. Petinrin and Shaaban [4] examine the voltage variations caused by reverse power flow from renewable generation, advocating for smart grid technologies like demand-side integration (DSI) and energy storage (ES) to mitigate these issues with minimal network reinforcement. Their

work suggests that coordinating voltage control devices with renewable generation could improve voltage profiles, though further investigation is needed.

Sharma et al. [5] propose a method to reduce overvoltage-induced PV curtailment in distribution networks by leveraging reactive power support from battery and smart PV inverters, focusing on an 11-kV feeder in South Australia. Their approach prioritizes reactive power from battery inverters to mitigate overvoltage without affecting active power flow, activating PV inverter response modes (as per Australian standard AS/NZS 4777.2.2020) only when battery support is insufficient. Simulation results demonstrate that this method can eliminate overvoltage events and active power curtailment when a high percentage of PV systems ($\geq 50\%$) are paired with batteries, reducing financial losses for utilities. They also find that lowering the source bus voltage during high solar radiation periods further mitigates overvoltage issues, offering a complementary strategy for voltage regulation in high PV penetration scenarios.

Balogun et al. [6] conduct a systematic review and bibliometric analysis on the coordination of smart inverter-enabled distributed energy resources (DERs) for optimal PV and battery energy storage system (BESS) integration in modern distribution networks. Their study emphasizes the role of smart inverters in enhancing voltage stability through grid support functions like Volt/VAr control. They identify optimal inverter settings and strategic PV-BESS placement as key factors in mitigating voltage violations and increasing PV hosting capacity. The authors also highlight research gaps, such as the need for robust algorithms to enable dynamic DER coordination and better integration with legacy grid systems, suggesting future directions for improving grid stability in high-DER scenarios.

The IEEE 8500-node test feeder, as introduced by Arritt and Dugan [7], serves as a critical benchmark for the power systems analysis community, offering a realistic and challenging radial distribution feeder for large-scale studies. Comprising approximately 8500 nodes and 4800 buses, this test feeder incorporates typical North American medium voltage (MV) distribution elements such as multiple feeder regulators, per-phase capacitor control, and feeder secondaries, making it an ideal platform for evaluating voltage regulation and power flow under complex conditions. Developed to address the limitations of smaller test cases like the 123-node feeder, the 8500-node system enables researchers to assess the scalability of distribution analysis methods, particularly for unbalanced systems and high-penetration renewable scenarios. Its potential for advanced applications, including voltage and VAR

control simulation, further underscores its relevance to modern grid challenges, providing a robust foundation for studies on the impacts of distributed energy resources (DERs) like photovoltaic (PV) systems on voltage stability.

Seguin et al. [8] develop a handbook for distribution engineers, addressing impacts of high-penetration PV (1-5 MW) on overload, voltage, reverse power flow, protection, and circuit configuration. Their study process, validated with case studies, proposes mitigation measures using PV inverters, though specific thresholds depend on utility standards.

The circuit voltage limits during steady-state analysis should remain within the acceptable 114-126 volt range (120-volt base) at the distribution transformer's high side during normal operation, ensuring reliable customer service. These voltage limits are described in ANSI C84.1 [9], which provides the American National Standard for electric power systems and equipment voltage ratings. This framework supports the evaluation of voltage stability under varying conditions, a critical aspect for assessing the impact of high PV penetration in distribution networks.

The IEEE 1547-2003 standard [10] initially lacked requirements for reactive power capability, prohibiting DERs from regulating voltage at the point of common coupling (PCC). However, the updated IEEE 1547-2018 standard [11] mandates voltage regulation through reactive power adjustments, reflecting the need for DERs to support larger-scale integrations. Fuchs and Masoum [12] provide a foundational text on power quality in distribution systems, offering insights into voltage rise and flicker mitigation, which remain relevant for modern high-DER networks.

Varma [13] explores the impacts of high-penetration solar PV systems, noting that by 2050, PV systems could provide 35% of global electricity generation. The study details the adverse effects of PV integration on both transmission and distribution systems, such as voltage instability and frequency deviations, and introduces smart inverter developments that enable reactive and active power control to mitigate these issues. In a subsequent chapter, Varma [14] elaborates on key smart inverter functions, including reactive power exchange at zero active power output and ramp rate control, which allows DERs to adjust active power in response to voltage deviations, ensuring grid stability. Varma [15] further discusses the modeling and control of three-phase smart PV inverters, focusing on power and control circuit constituents, which are critical for accurate power flow analysis in high-DER networks.

Varma [16] introduces the concept of PV-STATCOM, a technology that leverages PV inverters as STATCOMs during nighttime or system disturbances, providing dynamic voltage regulation and power factor correction. The applications of PV-STATCOM in distribution systems are explored by Varma [17], demonstrating its effectiveness in reducing line losses and supporting grid voltage control, particularly during daytime disturbances when active power can be curtailed for STATCOM operation. In transmission systems, Varma [18] highlights PV-STATCOM's role in improving power transfer capacity, damping power oscillations, and mitigating fault-induced delayed voltage recovery, with case studies showing its simultaneous support for frequency response and oscillation damping.

Varma [19] examines the role of smart inverters in increasing the hosting capacity of PV systems in distribution networks, presenting methodologies for selecting optimal inverter settings and showcasing field implementations that enhance grid reliability. Additionally, Varma [20] addresses the coordination of smart PV inverters with conventional voltage control equipment, noting potential interactions with FACTS controllers and the importance of autonomous PCC voltage control through active and reactive power exchange. Finally, Varma [21] discusses emerging trends in smart PV inverters, including grid-forming capabilities and financial compensation mechanisms for grid support functions, which could significantly enhance overall grid stability.

Wan et al. [22] propose a two-layer adaptive control strategy for distributed PV systems in low-voltage distribution networks, addressing the limitations of rigid control methods. Their approach adjusts active and reactive power reference values based on grid demands and PV regulation capabilities, using single and compound control modes to adapt to diverse scenarios. A case study validates this strategy, demonstrating improved grid support and stability under varying conditions, offering a flexible framework for DER integration.

Sitompul et al. [23] enhance Volt-VAR control by incorporating voltage sensitivity in grid-connected PV systems, addressing voltage rise at the point of common coupling (PCC) due to reverse power flow. Their method adjusts reactive power based on changes in PCC voltage caused by PV active power, ensuring the voltage profile remains within desired limits even under high PV output. This approach demonstrates the potential of adaptive Volt-VAR control to improve voltage stability in high-penetration scenarios.

Despite these contributions, several gaps persist in the existing research. The combined effects of PV placement, feeder R/X ratio, and loading conditions on voltage rise and rapid voltage changes (RVC) have received limited attention. The impact of these factors on the point of interconnection (POI) and regulating devices, such as OLTCs and voltage regulators, remains underexplored. Furthermore, detailed analyses in large-scale systems are scarce, particularly using the IEEE 8500-node test feeder with accurate commercial load flow software like CYMDIST, limiting the applicability of findings to real-world complexities. Many researchers currently rely on the 123-node test feeder as a "large" system to test methods for distribution power flow and analysis; however, its small scale fails to prove scalability to realistic large systems, underscoring the need for a more robust benchmark like the 8500-node test feeder to evaluate impacts on distribution systems comprehensively.

This thesis addresses these gaps by investigating the integrated impact of PV location, feeder R/X ratio, and varying loads (Peak, Normal, Off-Peak) on voltage rise and flicker, utilizing the complex IEEE 8500-node test feeder for a comprehensive study in CYMDIST. Unlike other software packages such as ETAP, PSS/ADEPT, and OpenDSS, CYMDIST holds a significant market share among utilities and consulting firms for distribution system analysis, excelling in DER integration with its comprehensive and user-friendly features, ensuring accurate and practical analysis. This work offers actionable recommendations for selecting Volt-VAR operation settings, enhancing grid stability in real-world applications. It also provides practical insights into mitigating voltage issues in high-DER networks by comparing the performance of Volt-VAR operation with fixed PF operation as mitigation strategies, validating their effectiveness through simulations to ensure grid reliability.

CHAPTER THREE:THEORETICAL BACKGROUND

3.1 Voltage Impact Analysis

3.1.1 Voltage Flicker: Causes and Impact

Voltage flicker, interchangeably referred to as Rapid Voltage Change (RVC) in subsequent sections of this paper, denotes short-term voltage fluctuations in distribution systems arising from rapid variations in PV generation. These fluctuations primarily stem from two sources: sudden shading due to cloud coverage, which induces abrupt reductions in PV output and corresponding power swings, and grid faults, such as short circuits or line tripping, which prompt immediate PV disconnections and significant voltage drops. The magnitude of these changes can be approximated as $\Delta V \approx \frac{R \cdot \Delta P + X \cdot \Delta Q}{V_n}$ [12], where R and X are the feeder resistance and reactance, ΔP and ΔQ represent the changes in active and reactive power due to PV variability, and V_n is the nominal voltage. The impacts of voltage flicker are multifaceted, degrading power quality by causing perceptible flickering in lighting systems, which diminishes customer satisfaction, and inducing malfunctions in sensitive industrial and medical equipment due to voltage instability. Furthermore, sustained flicker levels exceeding thresholds, such as the 3% limit at the Point of Interconnection (POI) specified by IEEE Std 1547-2018 [11], may result in regulatory non-compliance, exposing PV owners to penalties and necessitating robust mitigation measures to maintain grid reliability.

3.1.2 Voltage Rise: Causes and Impact

Voltage rise occurs when excess active power from PV systems is injected into the grid, exceeding local demand. This phenomenon is particularly significant in weak rural distribution feeders, where high impedance amplifies voltage deviations. The effect of connecting distributed generation systems on the voltage of a distribution network is explained in [4].

Figure 3.1 shows a simple distribution system with both load and PV generation.

The voltage change along a feeder without external generation (PV) can be expressed as:

$$\Delta V = V_1 - V_2 = \frac{R_{LN} P_L + X_{LN} Q_L}{V_2} \tag{3.1}$$

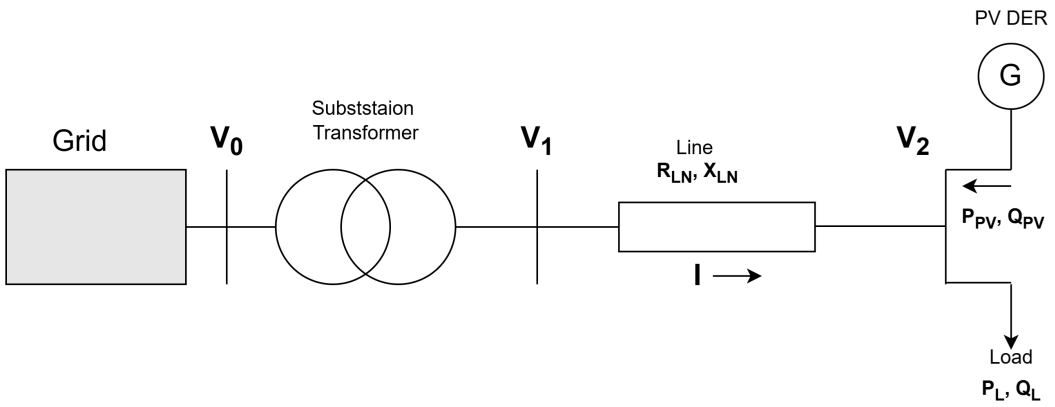

Figure 3.1: Distribution system with load and PV generation.

where P_L and Q_L are the active and reactive power loads, and R_{LN} and X_{LN} represent feeder impedance.

When a PV system is connected to the distribution network, the voltage equation modifies to:

$$\Delta V = V_1 - V_2 = \frac{R_{LN}(P_L - P_{PV}) + X_{LN}(Q_L - Q_{PV})}{V_2} \tag{3.2}$$

When the generation from PV systems exceeds the power consumed by the load (i.e., $P_{PV} > P_L$), the ΔV given by Equation 3.2 becomes negative, indicating that the voltage at the load side becomes higher than that at the source side. This results in a voltage rise, which may violate grid standards such as IEEE Std 1547-2018 [11] and ANSI C84.1 [9].

This voltage rise is more pronounced when the PV is interconnected further away from the source, as the values of R_{LN} and X_{LN} are higher in those cases. Consequently, a PV system connected close to the source causes minimal voltage rise, whereas the same system placed at the end of the network may lead to serious overvoltage issues. This phenomenon is further explained and validated in the *Results and Discussion* section.

Various strategies have been developed to address these issues, ranging from traditional methods to advanced inverter-based techniques. The following section explores these mitigation strategies, focusing on their theoretical principles and applicability in high-DER penetration scenarios, such as those analyzed using the IEEE

8500-node test feeder under varying loading conditions (Peak, Normal, Off-Peak) and PV placement configurations, as detailed in Chapter FOUR.

3.2 Conventional Mitigation Strategies

Traditional voltage regulation in distribution systems relies on methods such as capacitor banks, installation of new voltage regulators and network reinforcements. Capacitor banks provide reactive power compensation to support voltage levels but lack the dynamic response needed to handle rapid variations in PV output, such as those caused by cloud transients. This can lead to over- or under-compensation, potentially failing to maintain voltages within the ANSI C84.1 standard range of 114–126 V (on a 120 V base) used in this study. Network reinforcements, such as upgrading to larger conductors or adding voltage regulators, reduce feeder impedance or step down the voltage and enhance voltage control. However, these solutions are often cost-prohibitive, particularly for large-scale systems like the IEEE 8500-node test feeder with extended primary conductor lengths, and may discourage investment in renewable energy projects like PV DERs.

3.3 Smart Inverter Capability and Regulatory Requirement

Advanced mitigation strategies leverage the capabilities of smart inverters to dynamically regulate voltage through reactive and active power control. The IEEE 1547-2018 standard, titled "IEEE Standard for Interconnection and Interoperability of Distributed Energy Resources with Associated Electric Power System Interfaces," marks a significant evolution in DER requirements [11]. Unlike the IEEE 1547-2003 standard, which prohibited DERs from actively regulating voltage at the Point of Common Coupling (PCC) and did not mandate reactive power capabilities [10], IEEE 1547-2018 requires DERs to support voltage regulation through reactive power adjustments. This shift addresses the growing penetration of DERs, which increases the demand on utilities to manage reactive power for transformer support and maintain stable voltages at the PCC.

This study evaluates advanced inverter-based methods using the IEEE 8500-node test feeder, considering diverse loading conditions (Peak, Normal, Off-Peak) and PV placement scenarios (near and far from the substation). While IEEE 1547-2018 defines multiple reactive power control modes—including Constant Power Factor (PF), Volt-VAR, Volt-Watt, Watt-VAR, and Constant Reactive Power—this thesis focuses on Constant PF and Volt-VAR operations. These methods are selected

because they are widely adopted by local standards and regulations for mitigating voltage violations, offering a practical basis for comparing their effectiveness in maintaining grid stability.

3.3.1 Reactive Power Capability of Inverters

The reactive power capability of a DER defines its ability to inject or absorb reactive power, directly impacting the effectiveness of voltage regulation strategies. According to IEEE 1547-2018, this capability is represented by a P-Q (active power vs. reactive power) curve, as shown in Figure 3.2 [11]. The curve illustrates the relationship between active power (P) and reactive power (Q), constrained by the DER's rated apparent power (S_{rated}), where $S_{\text{rated}} = \sqrt{P^2 + Q^2}$. The horizontal axis represents active power output up to the rated active power (P_{rated}), while the vertical axis shows reactive power, with positive values indicating injection (over-excited) and negative values indicating absorption (under-excited).

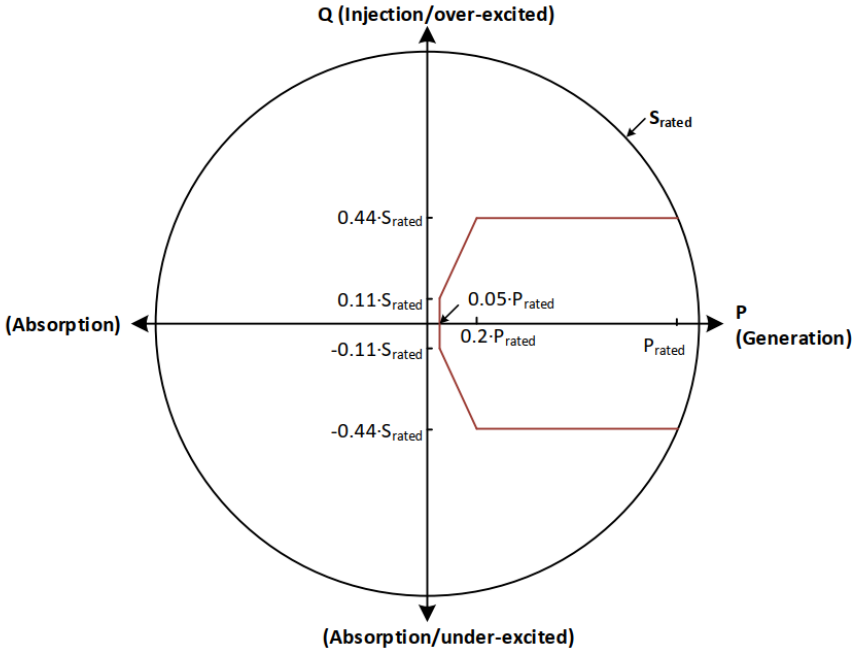

Figure 3.2: Reactive power capability of DER as per IEEE 1547-2018

The DER must have the ability to supply reactive power (in an over-excited state) and consume reactive power (in an under-excited state) when its active power output is at or above the minimum steady-state active power threshold (P_{min}), or 5% of its rated active power (P_{rated}, measured in kW), whichever value is higher. IEEE 1547-2018 defines the reactive power injection/absorption capability for Category B DER to be minimum 44% of S_{rated}.

The outer boundary of the P-Q curve represents the apparent power limit (S_{rated}). For active power outputs of at least 20% of P_{rated}, the DER must inject or absorb reactive power up to 44% of S_{rated} (i.e., $\pm 0.44 \cdot S_{\text{rated}}$). For active power between 5% and 20% of P_{rated}, the reactive power capability scales linearly as $0.44 \cdot S_{\text{rated}} \times \frac{P}{0.2 \cdot P_{\text{rated}}}$, reducing to $\pm 0.111 \cdot S_{\text{rated}}$ at 5% of P_{rated}. The standard allows active power curtailment to prioritize reactive power delivery within the S_{rated} limit, ensuring voltage regulation takes precedence.

3.4 Advanced Mitigation Strategies

Smart inverters employ various reactive power compensation methods to mitigate voltage violations, as defined by IEEE 1547-2018. These methods include Constant Power Factor (PF), Volt-VAR, Volt-Watt, Watt-VAR, and Constant Reactive Power operations, each utilizing distinct mechanisms to regulate voltage by adjusting reactive power, active power, or both, in response to grid conditions. This subsection provides a theoretical overview of these methods, comparing their operational principles and suitability for high-DER penetration scenarios. However, this thesis focuses on Constant PF and Volt-VAR operations, as these are the most commonly implemented methods in local standards by most of the utilities for addressing voltage violations, with their practical performance evaluated in Chapter FIVE.

3.4.1 Constant Power Factor Operation

Constant Power Factor (PF) operation involves the inverter maintaining a fixed power factor by adjusting reactive power output proportionally to its active power production. At higher active power levels, the inverter injects or absorbs more reactive power, while at lower levels, the reactive power exchange decreases accordingly. IEEE 1547-2018 specifies a default power factor of unity (1.0), meaning no reactive power is exchanged unless the setting is adjusted, typically to a value between 0.95 and 1.00 leading or lagging [11]. Smart inverters support adjustable power factors ranging from ± 0.8 to 1.0, allowing flexibility in reactive power management.

To mitigate voltage violations, the inverter can operate at a non-unity power factor that absorbs reactive power (lagging PF), counteracting the voltage rise caused by active power injection. This method is effective in scenarios with high PV penetration, particularly when PV systems are located far from the substation, as it increases reactive power absorption with rising active power output. Constant PF operation is straightforward to implement, requiring minimal dynamic control, but

its static nature limits its ability to adapt to varying grid conditions, potentially leading to over- or under-compensation.

3.4.2 Volt-VAR Operation

Volt-VAR operation enables smart inverters to dynamically regulate voltage by adjusting reactive power output based on the measured voltage at the Point of Interconnection (POI). A generic Volt-VAR curve, as shown in Figure 3.3, consists of three distinct regions, each governing the inverter's behavior under different voltage conditions.

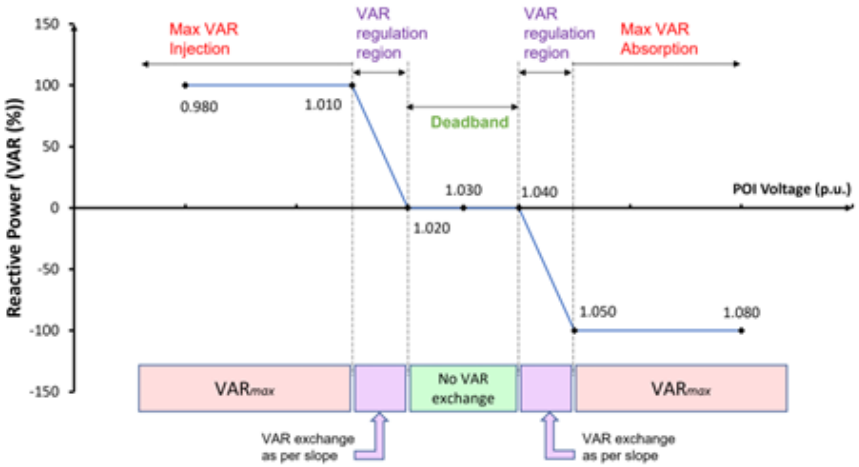

Figure 3.3: Volt-VAR Curve Explanation

1. **Max VAR Injection:** If the voltage at the monitored location falls in this region, the inverter will inject the maximum VAR of which it is calibrated.

2. **VAR Regulation Region:** If the voltage at the monitored location falls in this region, the inverter will inject VAR as per the slope. Understanding this region is important as the inverter will try to find an equilibrium point in this region while injecting VAR. The details are discussed in the following section.

3. **Dead-Band:** If the voltage at the monitored location falls in this region, the inverter will operate with unity PF and will not exchange VAR with the grid. The deadband is desired to be kept larger to prevent the inverter from continuous operation. The continuous operation of the inverter in the VAR regulation region might cause possible heating and other unforeseen problems. One should be careful while selecting the deadband, considering all the possible

operating characteristics to avoid possible malfunction of the inverter due to excessive heating.

The Volt-VAR characteristic, as defined by IEEE 1547-2018, follows a piecewise linear curve with four key points (V_1, Q_1 to V_4, Q_4), expressed in per-unit (p.u.) voltage and percentage of the DER's available reactive power capability, as shown in Figure 3.4 [11]:

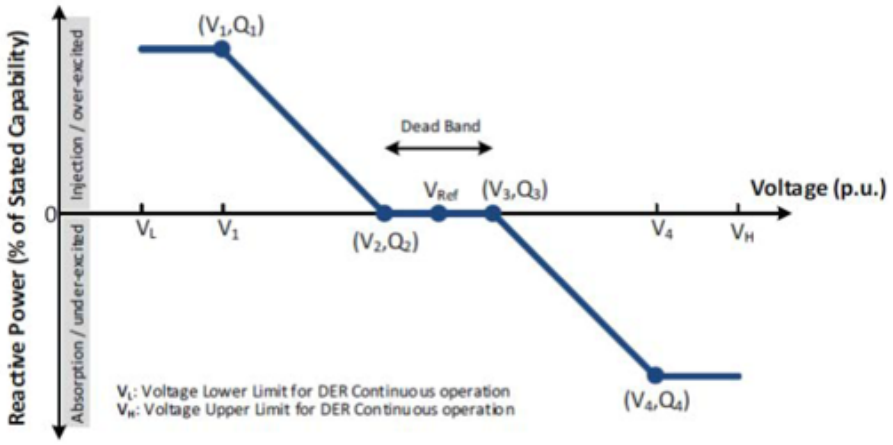

Figure 3.4: IEEE example of voltage-reactive power characteristic

- **(V1, Q1)**: At V_1 p.u., the DER injects the maximum capacitive reactive power (Q_1) to raise the voltage.
- **(V2, Q2)**: V_2 marks the lower deadband boundary, where $Q_2 = 0\%$, with no reactive power adjustment.
- **(V3, Q3)**: V_3 is the upper deadband boundary, with $Q_3 = 0\%$.
- **(V4, Q4)**: At V_4 p.u., the DER absorbs the maximum inductive reactive power (Q_4) to lower the voltage.

The deadband between V_2 and V_3 prevents reactive power adjustments for minor voltage deviations, while outside this range, reactive power adjusts linearly to support voltage regulation. IEEE 1547-2018 mandates that Q_1 and Q_4 be at least 44% of the inverter's nameplate apparent power rating for Category B performance [11].

Volt-VAR operation is highly effective for mitigating voltage violations due to its dynamic response to voltage changes. However, it is constrained by the 44% reactive power capability limit, which may be insufficient in extreme scenarios, and requires

careful coordination with legacy devices like capacitor banks and voltage regulators to avoid operational conflicts, such as hunting behavior.

Further details on the Volt-VAR curve and operating point selection are provided in Chapter FOUR.

3.4.3 Watt-VAR Operation

Watt-VAR operation adjusts reactive power output based on the inverter's active power production, following a predefined characteristic curve as shown in Figure 3.5 [11]:

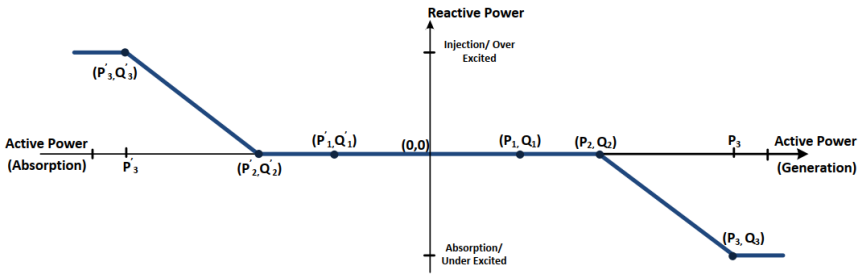

Figure 3.5: IEEE example of active power-reactive power characteristic

In a typical Watt-VAR curve, reactive power output scales with active power. For example, at low active power levels (e.g., below 20% of P_{rated} - *P_2 in Figure 3.5*), reactive power output may be zero, while at full active power (P_{rated}) - (*P_3 in Figure 3.5*), the inverter absorbs the maximum reactive power (e.g., 44% of the nameplate rating - *Q_3 in Figure 3.5*) to mitigate voltage rise. This method is effective when voltage violations correlate with active power injection, as it automatically adjusts reactive power absorption without requiring voltage measurements. However, its reliance on active power output means it may not respond effectively to voltage violations that are not directly tied to active power levels, such as those caused by grid conditions or load variations.

For PV systems interconnecting to the grid, the primary concern is often voltage violations, which can occur due to the intermittent nature of PV generation and its impact on the distribution system. In such scenarios, a control method that directly monitors voltage and adjusts reactive power to compensate for deviations—such as Volt-VAR operation—offers a more effective approach to voltage regulation compared to Watt-VAR. Volt-VAR operation dynamically responds to real-time voltage

measurements at the Point of Interconnection (POI), injecting or absorbing reactive power to maintain voltage within acceptable limits, as defined by standards like ANSI C84.1. This direct voltage-based control makes Volt-VAR more suitable for addressing the voltage challenges associated with PV integration, ensuring grid stability even under varying operating conditions.

3.4.4 Constant Reactive Power Operation

Constant Reactive Power operation, another method defined by IEEE 1547-2018, involves the inverter maintaining a fixed level of reactive power injection or absorption, regardless of active power output or system voltage [11]. This mode is typically used in scenarios where a consistent reactive power contribution is needed to support the grid. However, its lack of dynamic adjustment makes it less suitable for scenarios with variable PV output or fluctuating grid conditions, as it may lead to over- or under-compensation, potentially exacerbating voltage violations in high-DER penetration systems.

3.4.5 Volt-Watt Operation

Volt-Watt operation regulates voltage by adjusting the inverter's active power output based on the measured voltage at the POI. Unlike Volt-VAR, which manipulates reactive power, Volt-Watt curtails active power as voltage increases, directly reducing the contribution to voltage rise. The Volt-Watt characteristic, as defined by IEEE 1547-2018, is shown in Figure 3.6 [11]:

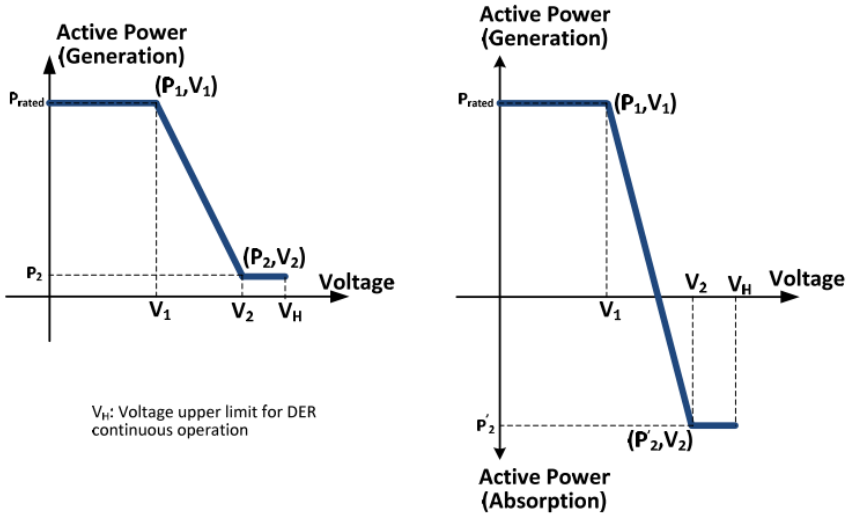

Figure 3.6: IEEE example of voltage-active power characteristic

Typically, the inverter operates at full active power (P_{rated}) up to a voltage threshold (e.g., 1.05 p.u.). Beyond this threshold, active power is linearly reduced to a minimum (e.g., 0% of P_{rated}) at a higher voltage (e.g., 1.10 p.u.), mitigating excessive voltage rise. This method is effective in high PV penetration scenarios where active power injection significantly contributes to voltage violations. Since Volt-Watt operation does not rely on reactive power, it avoids the 44% reactive power capability limit specified by IEEE 1547-2018. This method can result in higher risk of active power curtailment during abnormal circuit configurations. However, curtailing active power reduces energy export, potentially leading to economic losses for PV owners.

Although the reactive power modes described earlier cannot be used simultaneously, the volt-watt mode can be activated alongside one of these reactive power control modes. Generally, the starting point of the watt-var curve, denoted as V_1, is set after the boundary of the reactive power absorption region on the Volt-VAR curve (*i.e V_4 in the Figure 3.4*). That means volt-watt mode can be activated when the available reactive power capability of inverter can't resolve the voltage violations.

3.4.6 Selection Criteria for Reactive Power Compensation Methods

Selecting the appropriate reactive power compensation method for mitigating voltage violations depends on several criteria, including effectiveness, adaptability, inverter constraints, coordination with legacy devices, and practical considerations. These criteria are evaluated in the context of the IEEE 8500-node test feeder with high PV penetration, focusing on maintaining voltages within the ANSI C84.1 range of 114–126 V (120 V base).

1. Effectiveness in Voltage Regulation: The primary objective is to mitigate voltage violations effectively. Constant PF operation is effective for consistent PV output scenarios but lacks dynamic response to varying conditions. Volt-VAR operation excels due to its ability to adjust reactive power based on real-time voltage measurements, as demonstrated in Chapter FIVE. Volt-Watt control directly addresses voltage violations by curtailing active power but does not utilize reactive power, limiting its versatility. Watt-VAR is effective when voltage issues correlate with active power but may underperform otherwise. Constant Reactive Power operation provides steady support but is less effective in dynamic scenarios.

2. Adaptability to Varying Grid Conditions: Constant PF and Constant Reactive Power operations lack adaptability, as their fixed settings do not respond

to real-time changes across loading conditions (Peak at 100%, Normal at 60%, Off-Peak at 15%). Volt-VAR operation adapts effectively by adjusting reactive power based on voltage, while Volt-Watt control is limited to mitigate extreme overvoltage scenarios. Watt-VAR adapts moderately but it lacks the use of reactive power capability of modern smart-inverters and curtails the active power output of the PV DER instead.

3. Inverter Capability Constraints: IEEE 1547-2018 mandates a 44% reactive power capability limit for Category B performance, affecting Constant PF, Volt-VAR, Watt-VAR, and Constant Reactive Power methods [11]. Volt-VAR provides precise control within this limit, while Volt-Watt avoids reactive power constraints but at the cost of active power curtailment. Watt-VAR and Constant Reactive Power may underperform at low active power levels (below 20% of P_{rated}), where reactive power capability scales down.

4. Coordination with Legacy Utility Devices: Constant PF, Watt-VAR, Volt-VAR and Constant Reactive Power's static or active power-based adjustments may trigger unnecessary tap changes in legacy devices like voltage regulators, increasing wear. risks conflicts with slower mechanical devices if not properly tuned, as observed in simulations where regulator taps were locked. Volt-Watt has minimal direct interaction with reactive power devices but may indirectly affect regulator operation.

5. Practical Implementation and Economic Considerations: Constant PF and Constant Reactive Power are the simplest to implement but may lead to active power curtailment, reducing PV owner revenue. Volt-VAR requires sophisticated settings but offers superior regulation without sacrificing active power, as shown in Chapter FIVE. Volt-Watt is simple but economically disadvantageous due to active power curtailment. Watt-VAR is moderately complex for voltage control as voltage is not directly monitored for fine control, with economic impacts depending on active power export.

Table 3.1 summarizes the evaluation of these methods based on the selection criteria.

Table 3.1: Comparison of Reactive Power Compensation Methods

Criterion	Constant PF	Volt-VAR	Volt-Watt	Watt-VAR	Constant Q
Effectiveness	Moderate	High	High	Moderate	Low
Adaptability	Low	High	Moderate	Moderate	Low
Inverter Constraints	Within 44% limit	Within 44% limit	No reactive power use	Within 44% limit	Within 44% limit
Coordination with Legacy Devices	Poor	Moderate (with tuning)	Good	Poor	Poor
Implementation Complexity	Low	High	Low	Moderate	Low
Economic Impact	Moderate (possible curtailment)	Low	High (active power loss)	Moderate	Moderate

Selected Methods: Volt-VAR operation is selected for the IEEE 8500-node test feeder due to its effectiveness in mitigating voltage violations, adaptability to varying conditions, and ability to utilize the full 44% reactive power capability. Constant PF is suitable due to its simplicity to select the mitigation method without focusing on much complexity with operating condition of the system.

This study focuses on Constant Power Factor (PF) and Volt-VAR operations, as these methods are widely adopted by local standards for mitigating voltage violations. Their theoretical principles are discussed in this section, with practical implementation and performance analyzed in Chapter FIVE.

CHAPTER FOUR:METHODOLOGY

This chapter outlines the methodology employed to investigate voltage regulation challenges in high-DER distribution networks, focusing on the integration of photovoltaic (PV) systems. The research approach is structured into three main phases: data acquisition and scenario definition, voltage impact analysis, and mitigation development and evaluation. The study leverages the IEEE 8500-node test feeder in CYMDIST to simulate realistic large-scale distribution scenarios, enabling a comprehensive analysis of steady-state overvoltage and rapid voltage change (RVC). The methodology aims to quantify the combined effects of PV placement, feeder impedance (R/X ratio), and loading conditions, while developing and validating practical mitigation strategies, such as Volt-VAR operation and fixed power factor (PF) operation, to enhance grid stability.

The overall summary of the research methods is reflected in Table 4.1 below.

Study Steps
Data Acquisition and Scenario Definition
- Acquire IEEE 8500-node test feeder model and CYMDIST data
- Identify PV placement locations (Near and Far from Substation)
- Define study scenarios (Peak, Normal, Off-Peak loading)
↓
Voltage Impact Analysis
- Analyze steady-state voltage rise on the circuit
- Analyze the rapid voltage change effects on POI and regulators
- Assess voltage violations across different PV locations and at different loading conditions
- Evaluate the worst scenario for PV interconnection comparing the integrated voltage rise and RVC impact
↓
Mitigation Development and Evaluation
- Develop mitigation for voltage violations (Fixed PF Operation and Volt-VAR operation settings)
- Compare Volt-VAR operation vs. fixed PF operation
- Validate mitigation effectiveness using simulation results

Figure 4.1: Methodology Outline for Voltage Regulation in High-DER Networks

4.1 System Modeling and Simulation Setup

This thesis employs the **IEEE 8500-node test feeder** as the primary simulation platform to investigate voltage impacts across a radial primary distribution system under varying PV locations and feeder loading conditions. Selected for its realistic representation of large-scale North American medium voltage (MV) distribution networks, the feeder includes approximately 8500 nodes and 4800 buses, featuring elements such as multiple feeder regulators, per-phase capacitor control, and a 170km primary conductor length, which pose significant challenges for voltage regulation analysis. Its moderate difficulty in power flow solution and approximately 10% loss at peak load (high side) make it an ideal test case for evaluating the scalability and robustness of voltage impact assessments, particularly when integrating high PV penetration levels. The feeder's design, which supports the simulation of unbalanced systems and diverse loading scenarios (Peak, Normal, Off-Peak), aligns perfectly with the thesis objective to quantify the effects of PV placement and loading variations on steady-state overvoltage and rapid voltage changes (RVC). Figure 4.2 shows the standard IEEE 8500-node test feeder with existing feeder regulating devices.

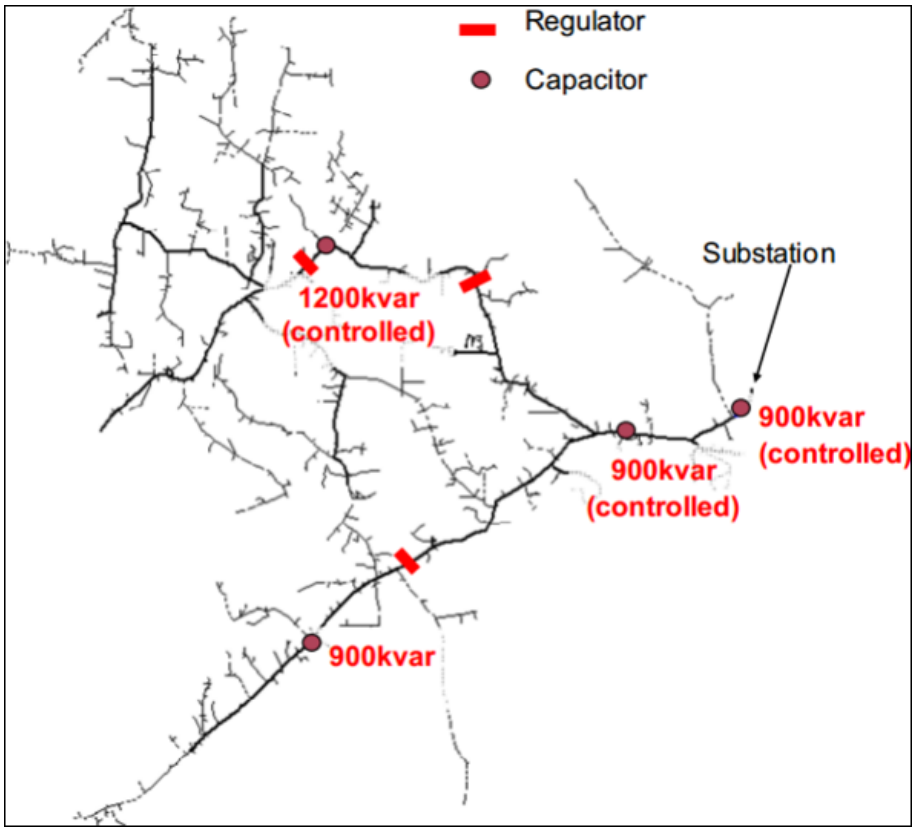

Figure 4.2: IEEE 8500-node test feeder with existing devices

The peak loading in the standard feeder is 11.836 MVA at 99.60% PF, which is considered as 100% loading. Normal and off-peak loadings are considered 60% and 15% of the peak loading, respectively. The DG (PV) output is set at 10 MVA and is modeled at a 12.47 kV voltage level along the feeder at two different locations: near the substation and at the end of the feeder, as shown in Figure 4.3. The 10 MVA PV output is assumed to represent High PV penetration, considering the generation comparable to the peak load. The voltages presented in this study are based on a standard base voltage of 120 V, which is considered the nominal voltage.

Simulation Details:

- **Software:** CYMDIST, Python (CYMPY libraries).
- **DER Configurations:** VSC-based PVs.
- **DER Placement:** Near Substation (G_{NS}) & Far from Substation (G_{FS}).
- **Loading Scenarios:** Peak (100%), normal (60%), and off-peak (15%) conditions.
- **High PV Penetration Level**

In this simulation setup, the VSC-based DG is modeled solely as a PV system exporting 10 MVA to the grid, without explicitly incorporating BESS dynamics. This choice is driven by the study's focus on voltage impacts during DG export, particularly for Rapid Voltage Change (RVC) analysis, where frequent PV output drops (e.g., due to cloud coverage) challenge voltage stability at the POI and regulating devices. While BESS could similarly export power, its charging mode shifts the analysis towards load interconnection studies, requiring exploration of undervoltage scenarios and specific charging limits—beyond the scope of this research, which targets overvoltage and flicker from grid export. Additionally, real-world BESS projects are often DC-coupled with PV, charging from co-located systems rather than the utility grid, thus having minimal direct grid impact during charging. Consequently, only PV export scenarios are simulated here, with BESS charging impacts reserved for potential future studies.

4.2 Case Study Scenarios

This study evaluates different PV placement scenarios under varying loading conditions. Table 4.1 presents the case study scenarios analyzed, considering varying loading conditions and different DG placement locations along the primary distribution feeder.

Table 4.1: Case Study Scenarios Based on PV Placement and Loading Conditions

Loading	PV Placement	Scenario Name
Peak (P)	No PV (Off) (B)	P-B
	PV Far from Substation (G_{FS})	P-G_{FS}
	PV Near Substation (G_{NS})	P-G_{NS}
Normal (N)	No PV (Off) (B)	N-B
	PV Far from Substation (G_{FS})	N-G_{FS}
	PV Near Substation (G_{NS})	N-G_{NS}
Off-Peak (O)	No PV (Off) (B)	O-B
	PV Far from Substation (G_{FS})	O-G_{FS}
	PV Near Substation (G_{NS})	O-G_{NS}

Figure 4.3 illustrates the two PV placement scenarios considered and the names and locations of existing feeder regulating devices.

4.3 Evaluation Metrics

The impact of DG on distribution circuit voltage is evaluated through steady-state and rapid voltage change (RVC or flicker) analyses. The steady-state analysis is employed to verify that circuit voltage remains within the acceptable 114-126 volt range (120-volt base) at the distribution transformer's high side during normal operation, ensuring reliable customer service. These voltage limits are established in accordance with ANSI C84.1 [9]. The rapid voltage change analysis assesses instantaneous voltage fluctuations (flicker) at the Point of Interconnection (POI) upon sudden project output transitions (full to no output and vice versa), with a limit of $\leq 3\%$. This analysis also examines voltage changes at the substation and in-series line regulators, requiring them to be $\leq$ half of their bandwidths (typically 1.5 V). The rapid voltage change (RVC) limits are in accordance with IEEE Std 1547-2018 [11].

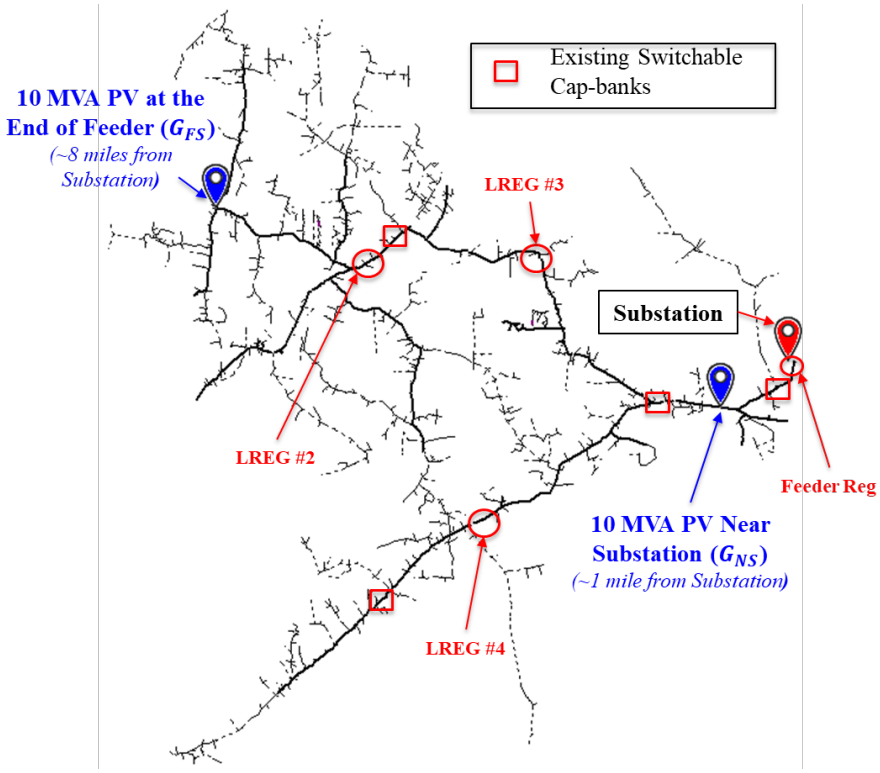

Figure 4.3: IEEE 8500-node test feeder with existing devices and new DG (PV) locations.

- **Voltage Rise Limit:** Percentage voltage rise above the standard nominal voltage ($\leq$5%)
- **RVC Limit:** Voltage flicker within limits at POI ($\leq$3%) and existing regulating equipment ($\leq$ half of the bandwidth).

The detailed workflows for these analyses are illustrated in the following sections.

4.4 Steady-State Voltage Analysis

Figure 4.4 presents the flowchart for the steady-state voltage analysis, outlining the steps to assess voltage rise and violations using the CYMDIST 'Load Flow Analysis' module.

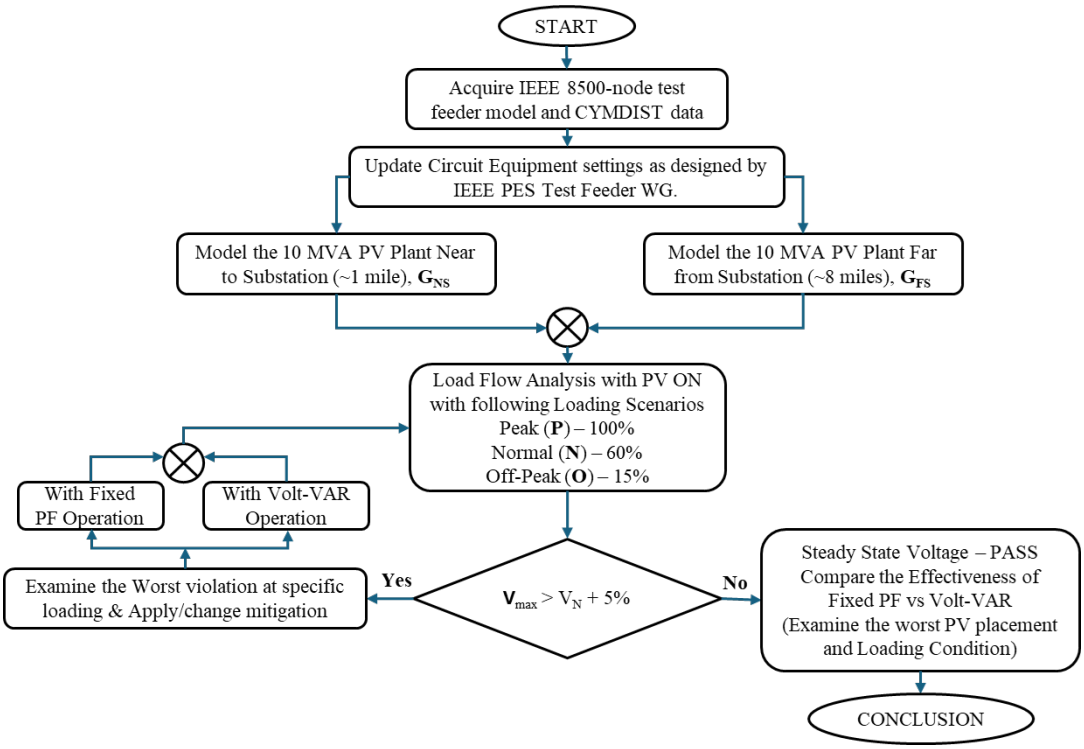

Figure 4.4: Flowchart for Steady-State Voltage Analysis

4.4.1 Load Flow Parameters for Overvoltage Analysis

- Load flow method used in this study is: "Voltage Drop – Unbalanced"
- Convergence Parameters:
  - Tolerance: 0.01%
  - Iterations: 60
- Transformers, regulators & switchable cap-banks taps at normal operation.

4.5 Rapid Voltage Change (RVC) Analysis

Figure 4.5 depicts the flowchart for the rapid voltage change analysis, detailing the process to evaluate flicker and voltage fluctuations using the 'Long Term Dynamics' module.

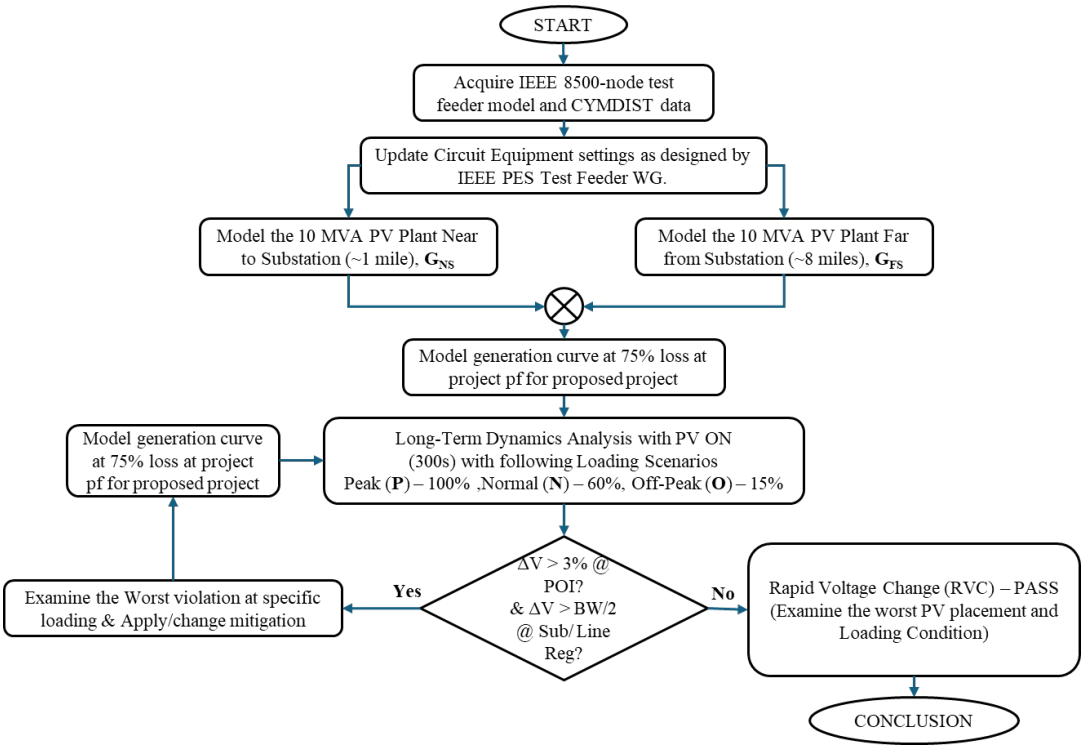

Figure 4.5: Flowchart for Rapid Voltage Change Analysis

4.5.1 Load Flow Parameters for Voltage Flicker Analysis

The long term dynamics module of CYMDIST software is used for the RVC analysis with following parameters.

- Total Simulation Time: 300s
- Simulation time step: 1s
- Load flow method used in this study is: "Voltage Drop – Unbalanced"
- Voltage change monitoring locations:
  - PV POI
  - Feeder and Line Regulators
- Transformers and regulators tap positions were locked at their respective tap positions.
- Switchable cap-banks locked at their current state.

Time (s)	P (%)	PF (%)
0	100	100.0
150	100	100.0
151	25	100.0
300	25	100.0

Table 4.2: PV Generation Curve Data

The snapshot of simulation settings is provided at the appendix section at the end of this document.

4.6 The Volt-VAR Curve

To ensure stability, the Volt-VAR curve must be carefully designed to avoid hunting (oscillatory behavior). The equilibrium point theory is used to select the operating points on the curve, ensuring that the inverter's reactive power response converges to a stable voltage. The settings for the Volt-VAR curve are detailed in the simulation setup, reflecting the practical constraints of the IEEE 8500-node test feeder and the 10 MVA PV system.

4.6.1 Finding the Equilibrium Point

In the VAR regulation region, the inverter would hunt for an equilibrium point once it senses the voltage at the monitored location is outside of the deadband. Let's define some terms which will be used while discussing the topic.

Characteristic Slope: It is the slope of the curve for the required change in VAR for per unit (1%) change in voltage, i.e., for a given loading of the circuit and at a given location: the slope is the VAR required to change the voltage at the monitored location by 1 unit (%). We will consider this as the 'Characteristic slope' for the given condition. For example: say 1.5 MVAR is required to change the voltage at the monitored location by 1.2 V or 1.0%; then the characteristic slope is 1.5 MVAR or 1.0%. The figure 4.7 shows the volt-VAR curve with characteristic slope 1.

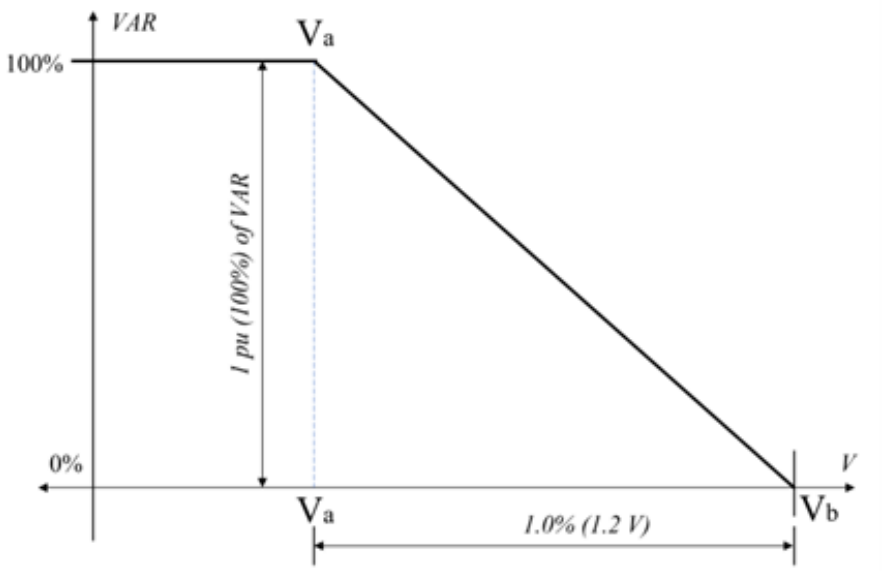

Figure 4.6: Characteristic Slope

Here, 1.5 MVAR has nothing to do with the possible limit of VAR exchange (injection/absorption). The topic of concern here is the slope and not the limit itself. Say for the above example: The circuit has the max VAR exchange limit as 2.5 MVAR and if we wish to maintain the 1.0% slope, then the VAR regulation region needs to be wide, 2V (see below).

$\frac{2.5}{1.5} * 1.0 = 1.67\% = 120 * \frac{1.67}{100} = 2V$

If we constrain the voltage change (ΔV) to 1.0% for the given VAR exchange limit (2.5 MVAR), then the slope will increase.

Equilibrium Point: The figure 4.7 shows the different iterations/attempts of the inverter to converge to the final equilibrium point.

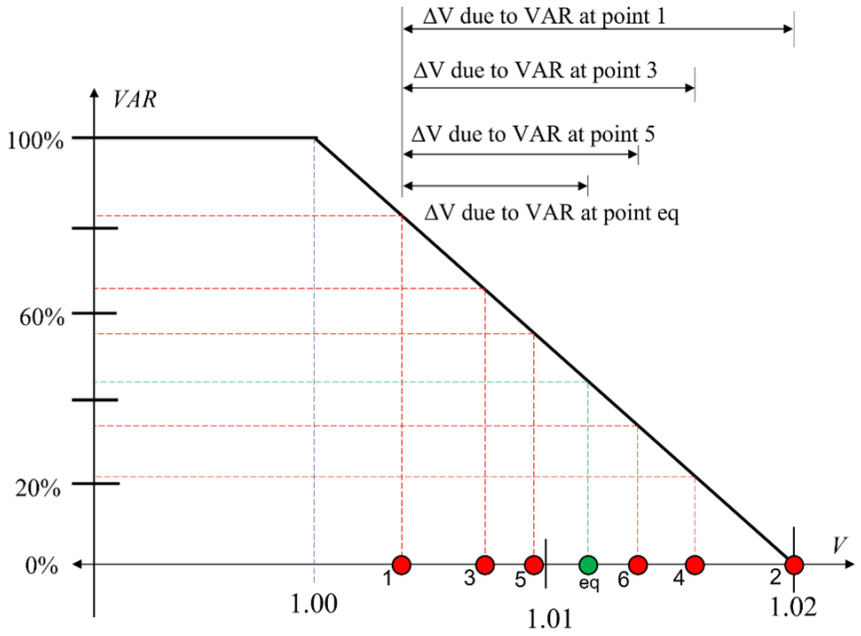

Figure 4.7: Finding Equilibrium Point

As seen in the figure 4.7, the slope is equal to the characteristic slope. Now, due to a sudden change in loading, the voltage at the monitored location changes. For the voltage at the monitored location between 1.00–1.02 pu (say 1.004), the point corresponding to this voltage (1.004 pu) is shown as point 1 on the curve. Sensing this voltage, the inverter will inject a little more than 80% of the VAR limit. With VAR injected, the voltage at the POI will increase and will reach point 2. Here, the inverter will reduce its VAR injection as per the slope to a minimum, resulting in the voltage at point 1. In the succeeding attempt, the inverter will inject lesser VAR. Suppose the inverter will inject less VAR corresponding to the voltage at point 3, which will again increase the voltage as of point 4. In a similar fashion, eventually, the inverter will find the equilibrium point where the injected VAR and the resulting voltage lie on the same vertical line. That point corresponding to the equilibrium ('eq' in the figure) in this case is at $V = 1.012\,\text{pu}$. Here,

$$\text{Avg}(1.004, 1.02) = 1.012\,\text{pu}$$

For this case, the equilibrium point is found at the midpoint as the VAR injected and the voltage will fall on the same vertical line only for this value. Based on the above arguments, we can say there always exists a characteristic curve with a unit

slope corresponding to the loading of the circuit at the given instant, which can be compared against to confirm the possible equilibrium point of stable operation for a sudden change in voltage.

The above-discussed theory assumes the continuum of VAR availability; however, in a real case, there is a minimum step size the inverter can operate with, i.e., the VAR availability can be considered as a discrete function of voltage. The figure below 4.8 shows the attempts of the inverter to find the stable operating point. The number of attempts before finding the equilibrium will depend on the initial voltage at the monitored location.

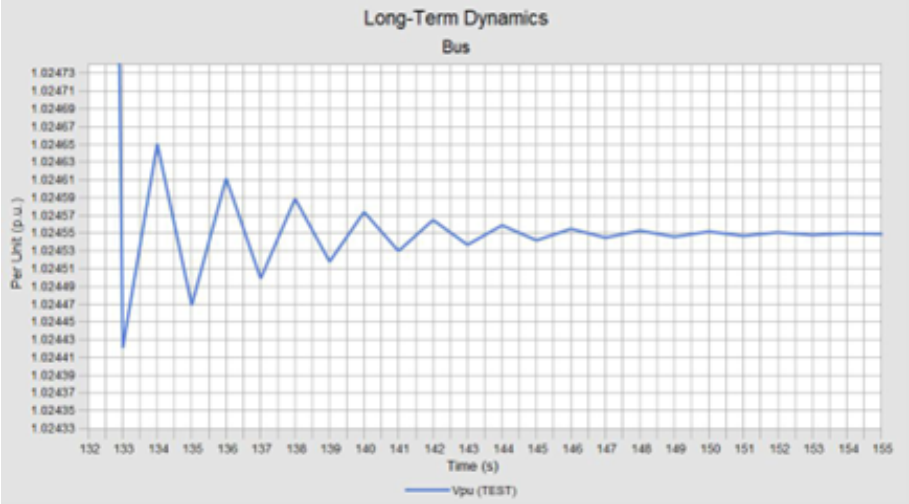

Figure 4.8: Attempts for Equilibrium Point

If the VAR required cannot be found due to this, then the inverter would hunt for the equilibrium and will constantly keep changing its VAR output. However, the voltage change is too small to notice. This can be verified with simulation results from CYMDIST. The figure below 4.9 shows the hunting observed.

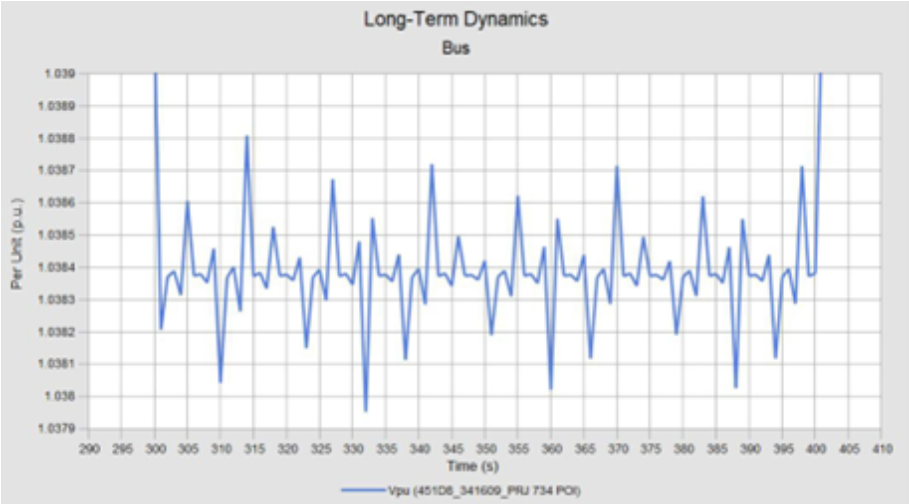

Figure 4.9: Hunting of Inverter

Curve with Higher Slope: If the chosen curve has a slope greater compared to the characteristic curve, then the equilibrium point found will be nearer to the nearest deadband limit. For example, illustrated in figure 4.7, the equilibrium point found is at 1.012 pu. However, for a curve with a higher slope and the same initial voltage (1.004 pu), the equilibrium point found will be more near to the lower deadband limit (i.e., greater than 1.012 pu). If the initial voltage change is in the other VAR regulation region (i.e., VAR absorption region), then the voltage will fall near to the upper deadband limit compared to the characteristic slope.

Curve with Lower Slope: If the chosen curve has a lower slope compared to the characteristic curve, then the equilibrium point found will be further from the nearest deadband limit. For the example illustrated in figure 4.7, the equilibrium point found is at 1.012 pu. However, for a curve with a lower slope and the same initial voltage (1.004 pu), the equilibrium point found will be further away from the lower deadband limit (i.e., smaller than 1.012 pu). If the initial voltage change is in the other VAR regulation region (i.e., VAR absorption region), then the voltage will go further away than the upper deadband limit compared to the characteristic slope.

One important point worth noting is: The voltage will always converge in the VAR regulation region. However, if the voltage is far beyond the nearest deadband limit and the maximum VAR exchange would not drag the voltage into the regulation region, then the DG will continue to operate with the maximum VAR exchanged, with the resulting voltage lying in the maximum VAR exchange region. If the max

VAR exchange results in the voltage falling into the VAR regulation region, then the inverter will adjust its VAR output based on the slope of the curve.

4.6.2 Qn, Vn Selection

Extreme Points on the Volt-VAR Curve

A generic curve is shown in figure 4.10. The four points ABCD are needed to define the nature of the curve. The height of AB implies the maximum VAR injection limit, the length of BC implies the deadband, and the height of CD implies the maximum VAR absorption limit. Generally, the height of AB and the height of CD are desired to be kept equal to make the curve symmetric. However, it can be asymmetric if needed.

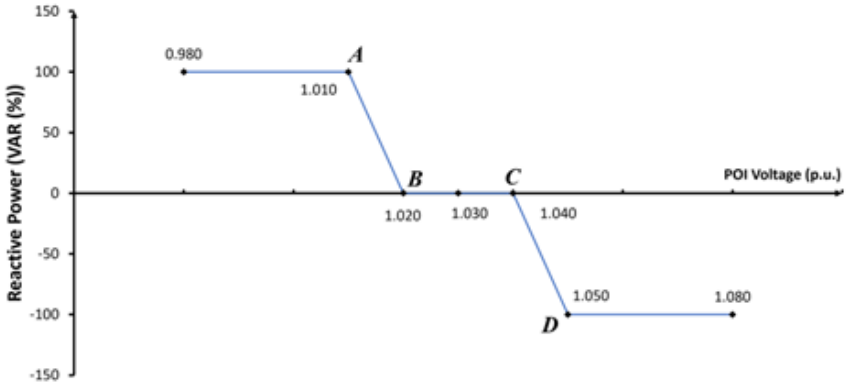

Figure 4.10: A typical Volt-VAR Curve

Section 4.6.1 suggests the location of the stable operating point will be found in the VAR regulation region. From this fact, we can infer that the extreme point A and D need to be the lower (114.0 V) and upper (126.0 V) allowable voltage respectively. Generally, point A is selected higher than the lower allowable limit of 95% (generally 116.0 V or higher); however, the upper limit (point D) should not be more than 105% (126.0 V) of the nominal voltage, considering a 10% voltage range. The deadband should be the maximum allowable for a given set of requirements. The slope and VAR limit can be determined as follows.

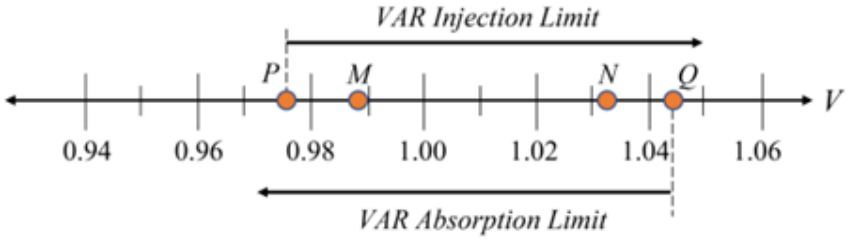

Figure 4.11: Consideration of VAR Limit

Figure 4.11 shows the possible voltage at Peak (M) and at Off-Peak (N) without other voltage regulating devices in action. Let's consider a PV project which will discharge, giving a full capacity of DG. For the worst-case scenario, we can consider discharging the full PV output to the feeder in the off-peak case. With DG injecting the maximum rated active power (discharging), the voltage will rise to Q. The VAR absorption limit can be determined as the VAR required to drag the voltage at the monitored location to the possible minimum such that no under-voltage is seen in any part of the circuit. Similarly, if we consider DG (BESS) charging during the peak load, the voltage will fall to P. The VAR injection limit can be determined as the VAR required to raise the voltage at the monitored location to the possible highest value such that no over-voltage is seen in any part of the circuit. This process will give the maximum VAR limit in each case. The suggested VAR exchange limit must be equal to or less than this VAR limit. While injecting or absorbing VAR for the limit consideration, if an overload of any equipment is observed, then the VAR less than the overload limit should be considered.

Minimizing the Tap Change of Voltage Regulators

The regulator action will be affected by the projects operating with Volt-VAR settings. The location of the project (with Volt-VAR) also affects the voltage regulator action. The idea is presented below with supporting justifications. Figure 4.12 shows the cumulative action of Volt-VAR operation and regulator. The regulator will always try to keep the voltage in between its bandwidth (region m-n in figure 4.12).

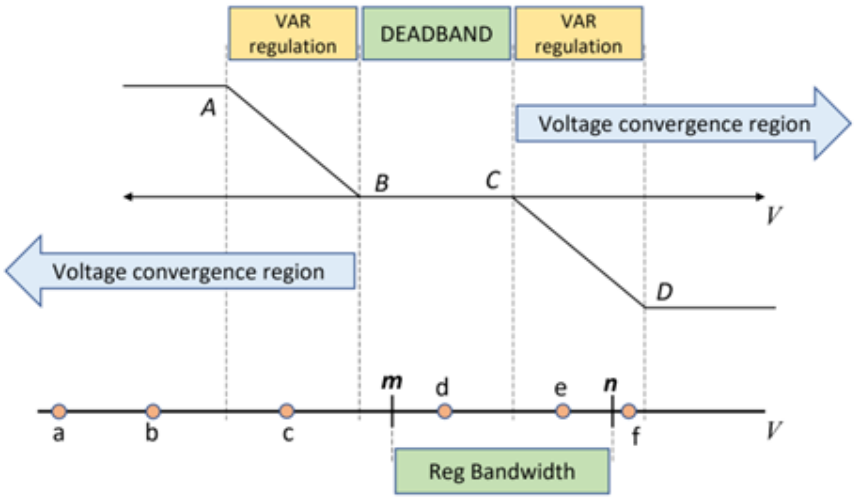

Figure 4.12: Volt-VAR operation along-with Regulator Action

Suppose the Volt-VAR operation is given to a DG very near to a voltage regulator. The regulator will always try to bring the voltage in between its bandwidth. The DG will respond faster to any voltage change; however, the DG will only bring the voltage in the 'Voltage convergence region'. For a given stable operating point 'c', the regulator will increase its tap to bring the voltage in between the 'm-n' region. Hence, for a lower voltage than point 'm', the regulator will change its tap as if there is no Volt-VAR operation in the DG. The catch here is the regulator tap change will remain unaltered if the DG's Volt-VAR operation contains the voltage regulator bandwidth in its operating region (deadband to be exact). If we wish not to let the regulator tap change, it requires the Volt-VAR curve (ABCD) to be squished in between the regulator bandwidth m-n, which won't be a feasible solution as it will significantly reduce the VAR-regulation and deadband region of the Volt-VAR curve. The regulator action won't be altered if the voltage falls (or stabilizes with VAR exchange) in the region from 'a' to 'm' and from 'n' to beyond. The initial voltage at point 'e' will stabilize above the deadband limit 'C'. The voltage at points 'd' and 'e' falling within 'm-n' won't trigger the regulator to operate its taps.

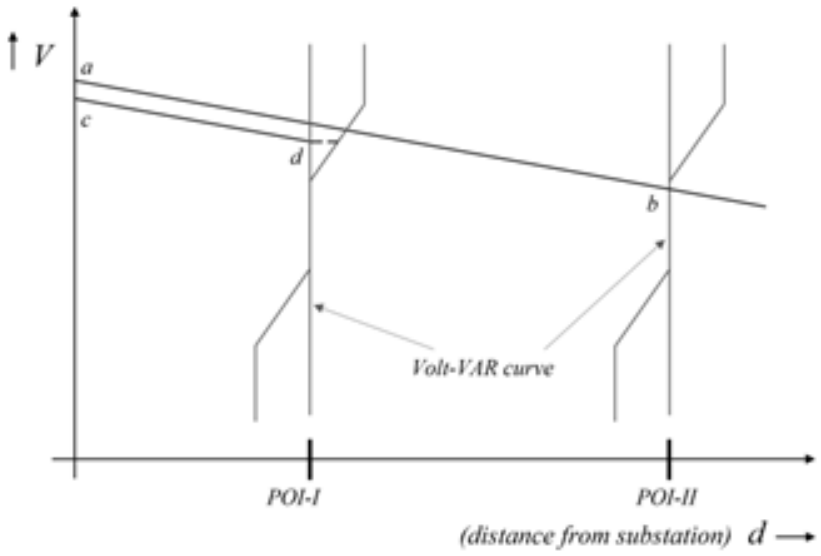

Figure 4.13: Voltage profile of circuit (DG POI location)

Also, the DG POI will have a direct impact on curve selection. Figure 4.13 shows a simplified voltage profile of a circuit. As seen in figure 4.13, the POI at location POI-I results in a lower voltage profile (c-d) for the initial voltage profile (a-b). However, if the POI is at POI-II, then the voltage at the monitored location (POI) will fall in the deadband limit, and the DG will continue to operate with unity PF.

4.6.3 Summary on Volt-VAR Curve Parameters Selection Algorithm

The Volt-VAR curve, as shown in Figure 4.14, is defined by four key points (V_1, Q_1), (V_2, Q_2), (V_3, Q_3), and (V_4, Q_4), with a deadband between V_2 and V_3. The following algorithm outlines the process for selecting these parameters to ensure stable voltage regulation at the Point of Interconnection (POI).

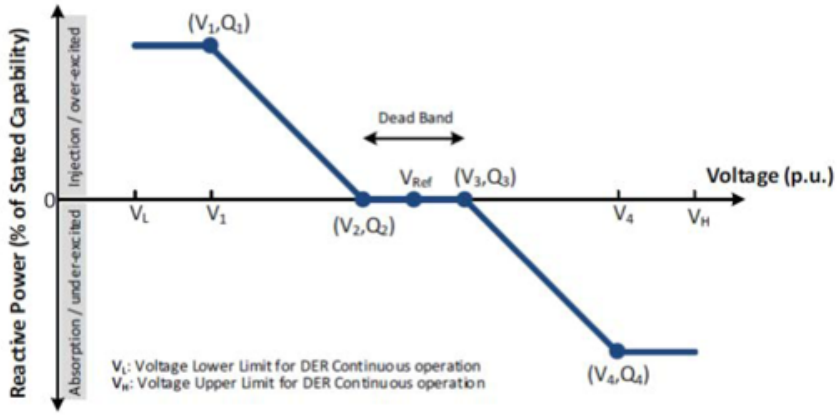

Figure 4.14: A typical Volt-VAR Curve

Algorithm 4.1: Volt-VAR Curve Parameters Selection process

Require: Nominal voltage $V_{\text{nom}} = 1.0$ p.u., allowable voltage limits $V_L = 0.95$ p.u., $V_H = 1.05$ p.u., IEEE 8500-node test feeder model, Peak and Off-Peak loading conditions.

Ensure: Volt-VAR curve parameters (V_1, Q_1), (V_2, Q_2), (V_3, Q_3), (V_4, Q_4).

1: **Step 1: Determine Extreme Voltage Points (V_1 and V_4)**
2: Set $V_1 \geq 0.99$ p.u. (typically 0.99 p.u., or above V_L).
3: Set $V_4 \leq 1.05$ p.u. (typically 1.05 p.u., or below V_H).
4: Set $Q_1 = 44\%$ of nameplate kVA rating (maximum reactive power injection).
5: Set $Q_4 = -44\%$ of nameplate kVA rating (maximum reactive power absorption).
6: **Step 2: Perform Load Flow Analysis**
7: Run load flow analysis on the IEEE 8500-node test feeder without PV.
8: Simulate Peak (100%) and Off-Peak (15%) loading conditions.
9: Record voltage at POI (V_{POI}) for both conditions.
10: **Step 3: Define Deadband (V_2 to V_3)**
11: Set V_{ref} as the nominal voltage adjusted by average V_{POI}.
12: Set Bandwidth, BW $(V_3 - V_2) = (V_{\text{O-POI}} - V_{\text{P-POI}})$
13: Define deadband: $V_2 = V_{\text{ref}} - BW/2$ p.u., $V_3 = V_{\text{ref}} + BW/2$ p.u.
14: Set $Q_2 = Q_3 = 0$ (no reactive power in deadband).
15: **Step 4: Set VAR Regulation Region Width**
16: Set injection region width: $V_2 - V_1$
17: Set absorption region width: $V_4 - V_3$
18: Adjust V_1 and V_4 to maintain symmetry while respecting limits.
19: **Step 5: Ensure Stable Operating Point**
20: Run load flow with PV and Volt-VAR operation enabled.
21: Verify operating point lies within VAR regulation regions.
22: If hunting occurs, adjust deadband or region width iteratively.
23: **Step 6: Output Volt-VAR Curve Parameters**
24: Return (V_1, Q_1), (V_2, Q_2), (V_3, Q_3), (V_4, Q_4).

CHAPTER FIVE:RESULTS AND DISCUSSION

Voltage impact analysis was conducted using the CYMDIST distribution load flow software to evaluate both steady-state and rapid voltage change (RVC) effects, ensuring that the photovoltaic (PV) interconnection complies with established voltage standards. This dual analysis is critical to assess the holistic impact of Voltage Source Converter (VSC)-based PV systems on the distribution network, addressing both long-term voltage stability and instantaneous voltage fluctuations (flicker) that could affect grid reliability and equipment performance.

5.1 Steady-State Voltage Analysis Under Different Scenarios

A steady-state voltage analysis was performed to evaluate the project's impact on the distribution circuit voltage, ensuring it remains within the acceptable range of 114 to 126 volts (on a 120-volt base) as measured at the high side of the distribution transformer during normal operation. This range, defined by ANSI C84.1 [9], ensures acceptable voltages at all nodes under all anticipated load conditions, regardless of PV operation. The analysis utilized the IEEE 8500-node test feeder, integrating a 10 MVA PV system under Peak (P), Normal (N), and Off-Peak (O) loading conditions, with PV placements at no PV (B), far from the substation (G_{FS}), and near the substation (G_{NS}).

The simulation results, presented in Figures 5.1, 5.2, and 5.3, illustrate the voltage profiles across these scenarios without mitigation. These profiles reveal significant variations influenced by PV location and loading conditions. Over voltage regions (highlighted in green, exceeding 126 V) are prominently observed in the $O-(G_{FS})$ case, as shown in Figure 5.4 (5.4c).

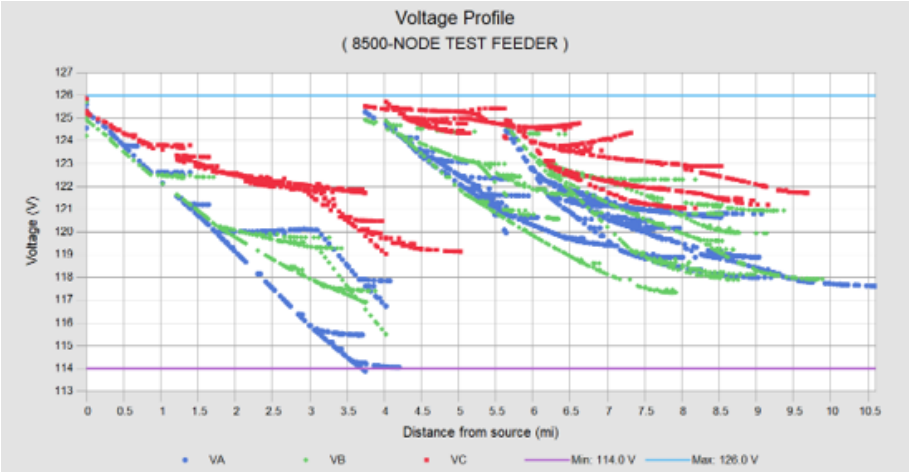

(a) P-B Voltage profile without mitigation.

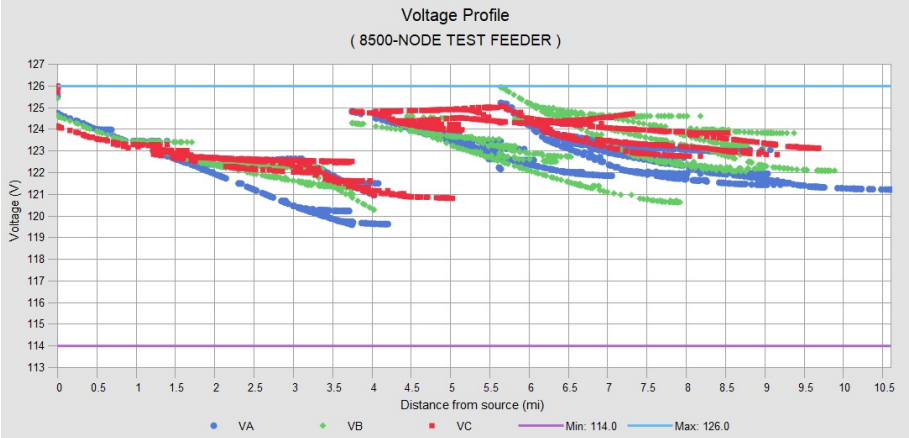

(b) N-B Voltage profile without mitigation.

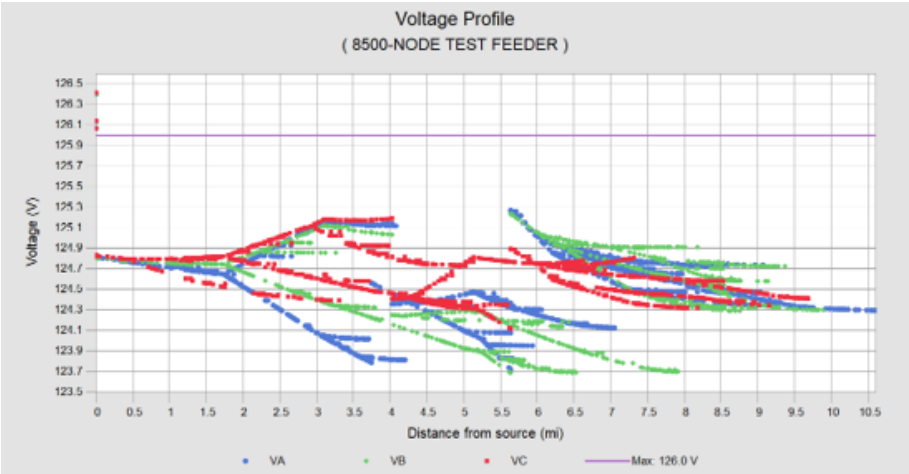

(c) O-B Voltage profile without mitigation.

Figure 5.1: Voltage Profiles for Base Case

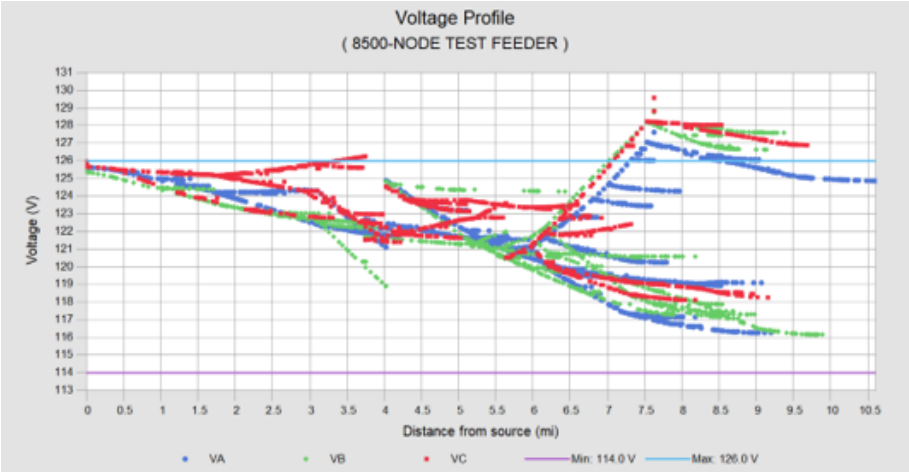

(a) P-G_{FS} Voltage profile without mitigation.

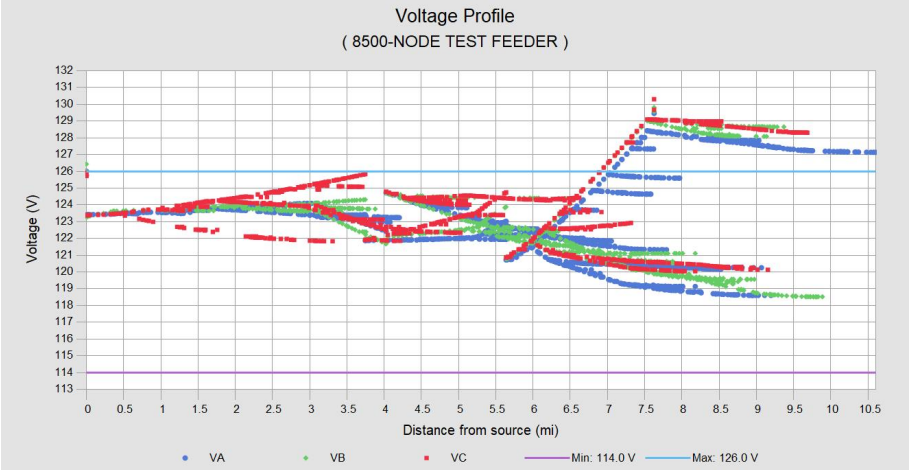

(b) N-G_{FS} Voltage profile without mitigation.

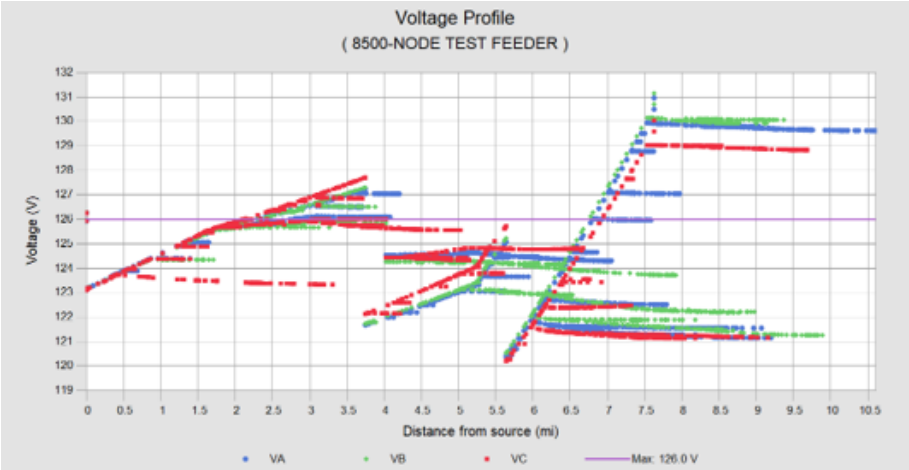

(c) O-G_{FS} Voltage profile without mitigation.

Figure 5.2: Voltage Profiles for G_{FS} Case

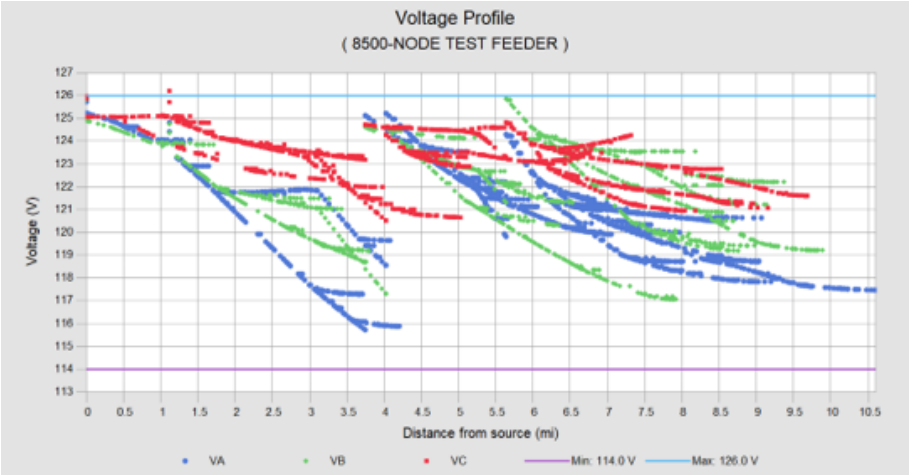

(a) P-G_{NS} Voltage profile without mitigation.

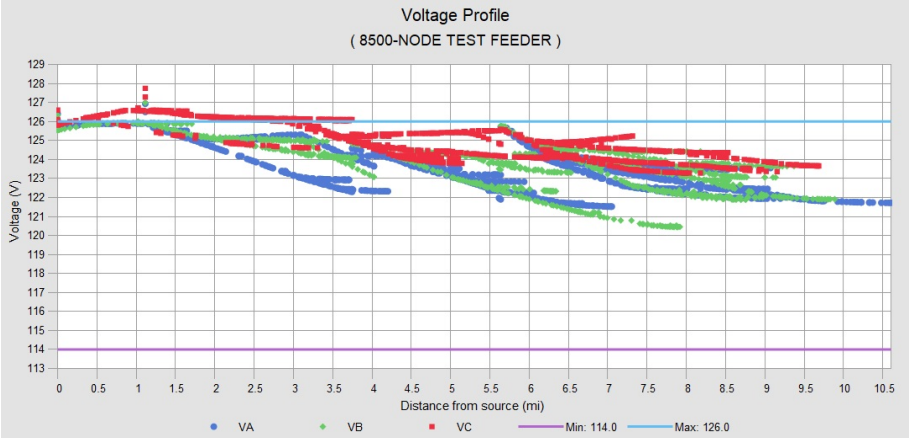

(b) N-G_{NS} Voltage profile without mitigation.

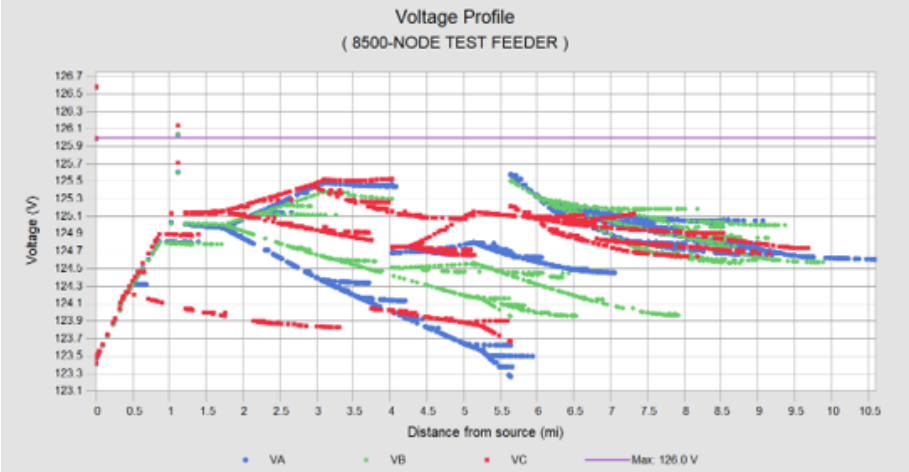

(c) O-G_{NS} Voltage profile without mitigation.

Figure 5.3: Voltage Profiles for G_{NS} Case

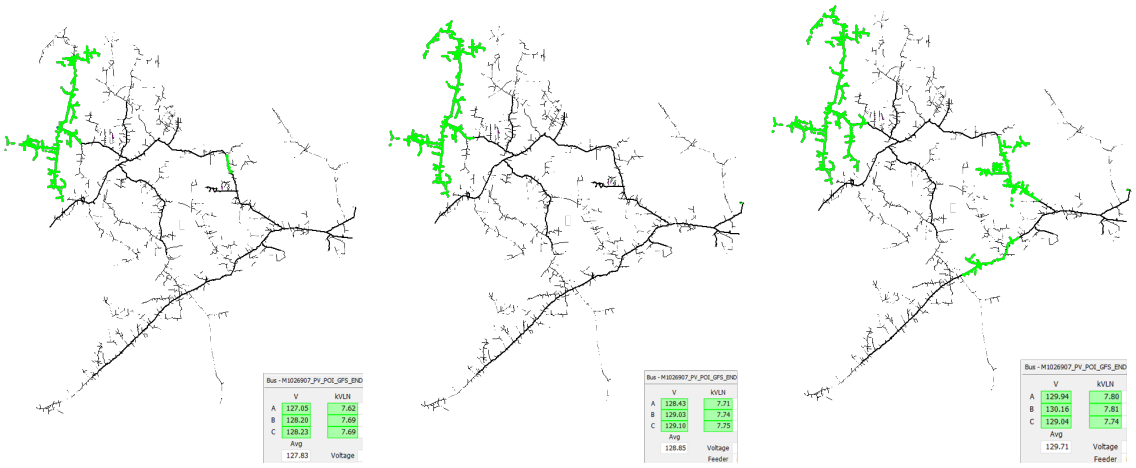

(a) P-G_{FS} (b) N-G_{FS} (c) O-G_{FS}

Figure 5.4: Circuit Condition showing the Voltage Rise at G_{FS} for Different Loading Conditions

Quantitative results, summarized in Table 5.1, indicate that without mitigation, the G_{FS} scenario exhibits significant overvoltage. Under Peak load, the maximum feeder voltage reaches 128.23 V for G_{FS} and 125.85 V for G_{NS}. This overvoltage at G_{FS} is driven by the high feeder impedance, which amplifies the voltage rise from the 10 MVA PV injection, as modeled by Equation 3.2. Under Normal load, voltages escalate to 129.10 V at G_{FS} and 125.57 V at G_{NS}, reflecting reduced demand that exacerbates PV surplus effects. The most severe violation occurs during Off-Peak conditions, where the feeder voltage at G_{FS} peaks at 130.15 V, exceeding the ANSI C84.1 limit of 126 V, due to minimal load (15

Table 5.1: Voltage Impact Analysis – Different Scenarios

Scenarios	**Mitigation Required**	**Feeder V_{max}**
P-B	-	125.71 V
P-G_{FS}	-96.90% PF	128.23 V (Without Mitigation) / 125.56 V (With Mitigation)
P-G_{NS}	None Required	125.85 V
N-B	-	125.94 V
N-G_{FS}	-95.60% PF	129.10 V (Without Mitigation) / 125.85 V (With Mitigation)
N-G_{NS}	None Required	125.57 V
O-B	-	125.27 V
O-G_{FS}	-93.20% PF	**130.15 V** (Without Mitigation) / 125.86 V (With Mitigation)
O-G_{NS}	None Required	125.58 V

Mitigation using a fixed PF approach reduces overvoltage effectively. For instance, a PF of -96.90% at P-G_{FS} lowers the voltage to 125.56 V, and -93.20% at O-G_{FS} brings it to 125.86 V, both within limits. Figures 5.5 illustrate these mitigated profiles, showing a consistent voltage profile below 126 V across all nodes. However, the fixed PF method requires scenario-specific adjustments, with the most aggressive setting (-93.20%) needed for the Off-Peak case due to its severe overvoltage.

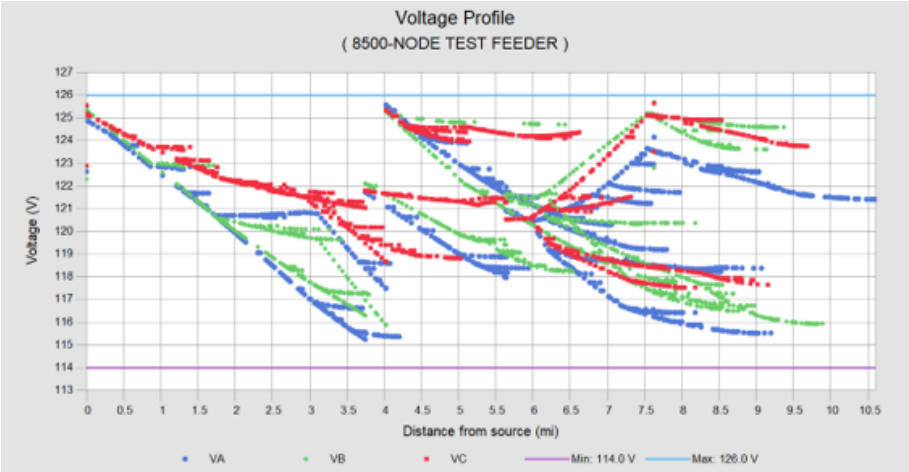

(a) P-G_{FS} Voltage profile with mitigation (Fixed PF).

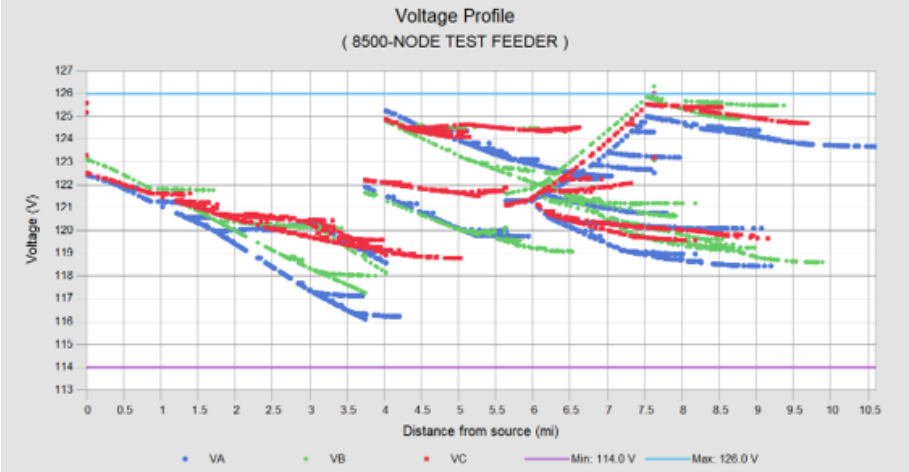

(b) N-G_{FS} Voltage profile with mitigation (Fixed PF).

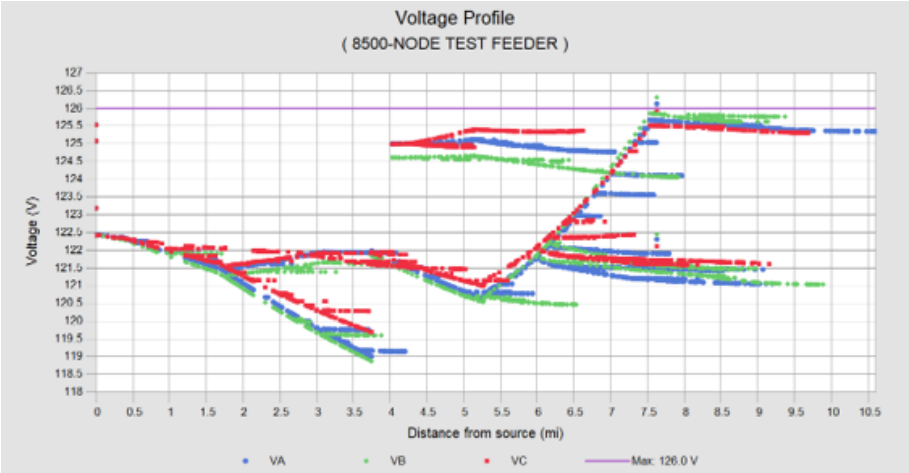

(c) O-G_{FS} Voltage profile with mitigation (Fixed PF).

Figure 5.5: Voltage Profiles for G_{FS} Case After Mitigation (Fixed PF)

5.1.1 Advanced Mitigation: Volt-VAR Settings

As outlined in Chapter FOUR, Volt-VAR operation offers a dynamic alternative to fixed PF mitigation. IEEE Std 1547-2018 [11] permits Distributed Energy Resources (DERs) to compensate up to 44% of their nameplate apparent power rating for voltage regulation through reactive power injection or absorption.

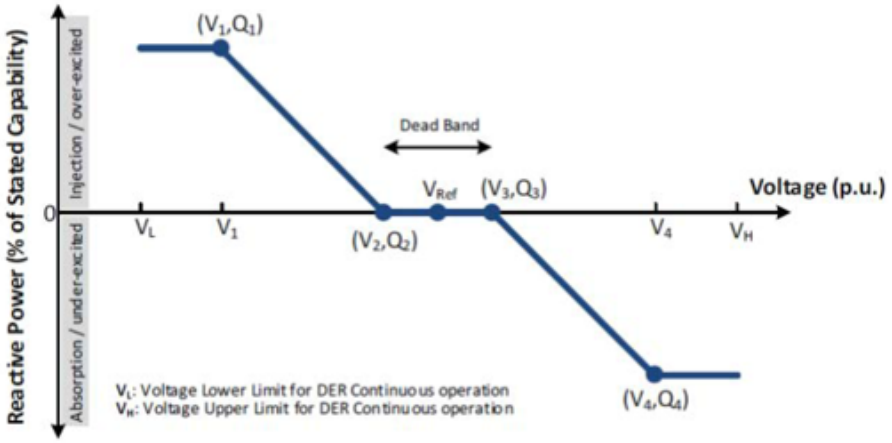

Figure 5.6: IEEE example of volt/VAR curve

The proposed Volt-VAR curve (*with operation points in Volt-VAR curve as shown in Figure 5.6*), as depicted in Figure 5.7, is defined as follows:

- $V_1, Q_1 = 0.99 \text{ pu}\,(118.8\,\text{V}), +44\%$
- $V_2, Q_2 = 1.01 \text{ pu}\,(121.2\,\text{V}), 0\%$
- $V_3, Q_3 = 1.03 \text{ pu}\,(123.6\,\text{V}), 0\%$
- $V_4, Q_4 = 1.05 \text{ pu}\,(126.0\,\text{V}), -44\%$

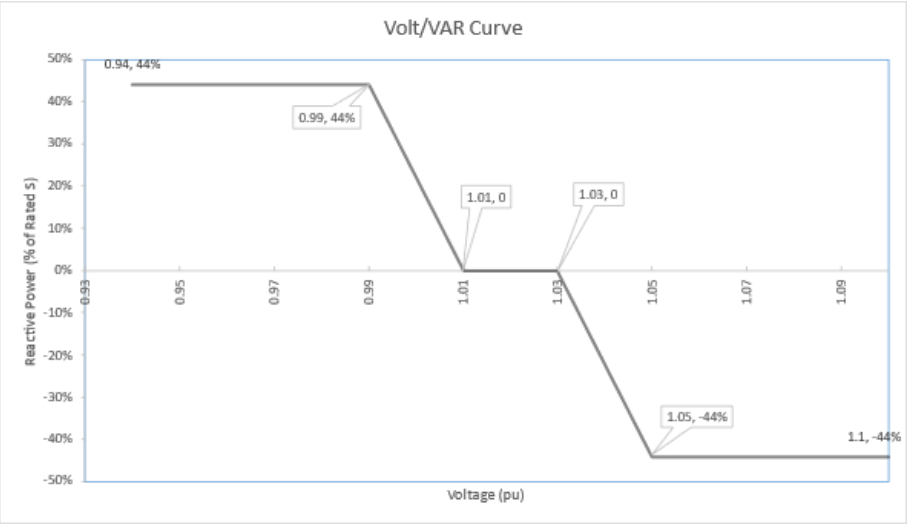

Figure 5.7: The proposed Volt-VAR curve.

Table 5.2 compares the proposed Volt-VAR settings with the default settings specified in IEEE 1547-2018. The proposed settings adjust the voltage thresholds to better align with the ANSI C84.1 voltage limits (114–126 V) used in this study, ensuring reactive power injection begins at a higher low-voltage threshold (118.8 V versus 110.4 V) and absorption starts at a lower high-voltage threshold (126.0 V versus 129.6 V). This results in a more conservative deadband (121.2 V to 123.6 V) compared to the default (117.6 V to 122.4 V) with steeper regulation region slope, maintaining voltage stability within acceptable limits.

Table 5.2: Comparison of Default and Proposed Volt-VAR Settings

Parameter	Default Settings (IEEE 1547-2018)	Proposed Settings
V_1	0.92 p.u. (110.4 V)	0.99 p.u. (118.8 V)
Q_1	+44% (injection)	+44% (injection)
V_2	0.98 p.u. (117.6 V)	1.01 p.u. (121.2 V)
Q_2	0%	0%
V_3	1.02 p.u. (122.4 V)	1.03 p.u. (123.6 V)
Q_3	0%	0%
V_4	1.08 p.u. (129.6 V)	1.05 p.u. (126.0 V)
Q_4	-44% (absorption)	-44% (absorption)

Table 5.3 compares the PF requirements for fixed PF and Volt-VAR methods. Volt-VAR requires slightly higher PF values (e.g., -97.22% vs. -96.90% for P-G_{FS}, -94.83% vs. -93.20% for O-G_{FS}), reflecting its dynamic adjustment to feeder loading. This adaptability ensures voltage remains below 126 V, as shown in Figures 5.8, enhancing efficiency and supporting higher PV penetration.

Table 5.3: Voltage Impact Analysis – Different Scenarios with Advanced Mitigation

Scenarios	**Fixed PF Method**	**PF with Volt-VAR**
P-B	–	–
P-G_{FS}	-96.90%	-97.22%
P-G_{NS}	None Required	–
N-B	–	–
N-G_{FS}	-95.60%	-96.49%
N-G_{NS}	None Required	–
O-B	–	–
O-G_{FS}	-93.20%	-94.83%
O-G_{NS}	None Required	–

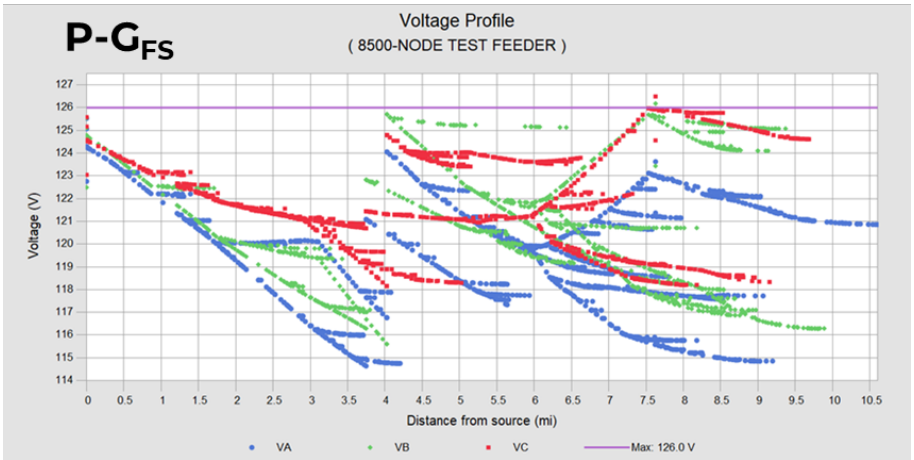

(a) P-G_{FS} Voltage profile with Volt-VAR mitigation.

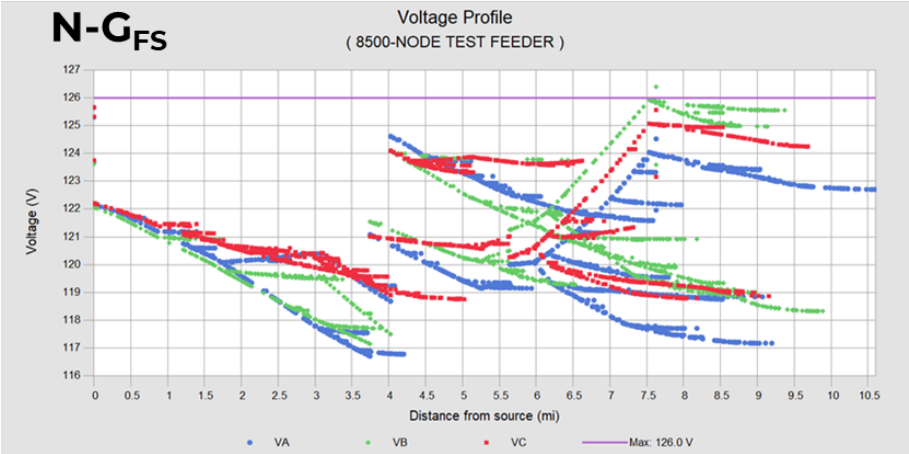

(b) N-G_{FS} Voltage profile with Volt-VAR mitigation.

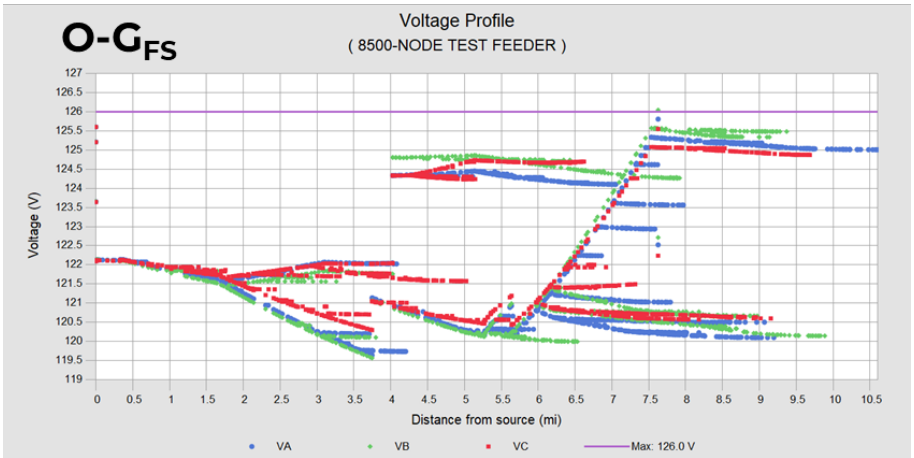

(c) O-G_{FS} Voltage profile with Volt-VAR mitigation.

Figure 5.8: Voltage Profiles for G_{FS} Case After Mitigation (Volt-VAR)

While Volt-VAR operation demonstrates superior performance in these simulations, its practical implementation faces notable challenges. Inverter kVA capability limitations, may limit effectiveness in scenarios with extreme voltage excursions or when supporting large PV capacities, potentially requiring oversized inverters or additional reactive power sources. Significant reactive power compensation along with the active power injection may cause overloading of line devices between POI and substation or undervoltage in the circuit during peak load conditions. Furthermore, coordination with legacy utility devices, such as switchable capacitors and line voltage regulators, introduces complexity. In the IEEE 8500-node feeder, the rapid response of smart inverters (e.g., adjusting VAR within miliseconds) contrasts with the slower mechanical operation of regulators (e.g., tap changes over multiple seconds), risking oscillatory behavior or tap wear if not synchronized. Although these issues were not observed in the steady-state results here—due to locked tap settings in CYMDIST—they highlight potential complexities during real-world deployment, particularly in networks with extensive legacy infrastructure.

5.2 Voltage Flicker/RVC Analysis Under Different Scenarios

A Voltage Change Analysis was conducted to assess the instantaneous voltage fluctuations (flicker) resulting from a sudden 75% drop in PV output, a scenario that simulates the loss of the PV system. IEEE Std 1547-2018 [11] specifies that voltage flicker at the Point of Interconnection (POI) during transitions from full output to no output (and vice versa) must not exceed 3%, while voltage changes at substations and in-series line regulators should remain within half their bandwidth, typically $\leq 1.5\,\text{V}$. This analysis, performed using CYMDIST, evaluates the RVC impact across Peak, Normal, and Off-Peak conditions at the PV POI and regulating devices (Feeder Reg, LREG#2, LREG#3, LREG#4) for G_{FS} and G_{NS} scenarios.

Without mitigation, the RVC results, depicted in Figures 5.9 and 5.10, reveal significant violations, particularly at G_{FS}. Table 5.4 shows that the PV POI at G_{FS} experiences an RVC of 10.85% under Peak load, far exceeding the 3% limit, due to high feeder impedance amplifying the sudden power drop. This is contrasted by G_{NS}, where the RVC is only 1.30% (Table 5.5), benefiting from lower impedance. At regulating devices, G_{FS} under Peak load shows a ΔV of 5.84 V at LREG#2, exceeding the 1.5 V limit, indicating potential stress on voltage control equipment.

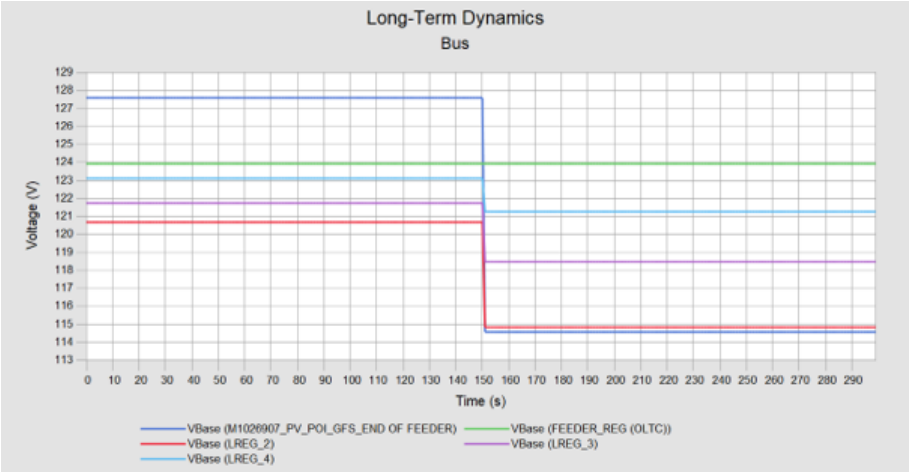

(a) P-G_{FS} Voltage Change at PV POI, Feeder Reg, LREG#2, LREG#3, and LREG#4 during 75% drop of PV.

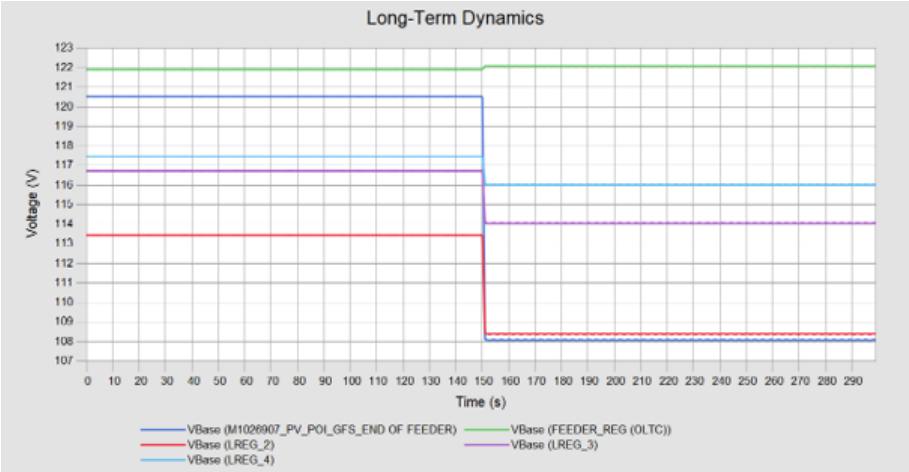

(b) N-G_{FS} Voltage Change at PV POI, Feeder Reg, LREG#2, LREG#3, and LREG#4 during 75% drop of PV.

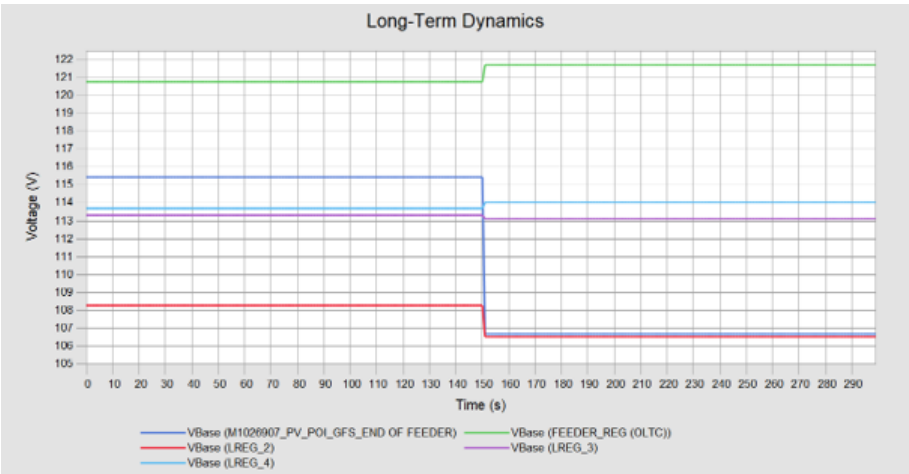

(c) O-G_{FS} Voltage Change at PV POI, Feeder Reg, LREG#2, LREG#3, and LREG#4 during 75% drop of PV.

Figure 5.9: Flicker/RVC Analysis for G_{FS} Scenarios (Without Mitigation)

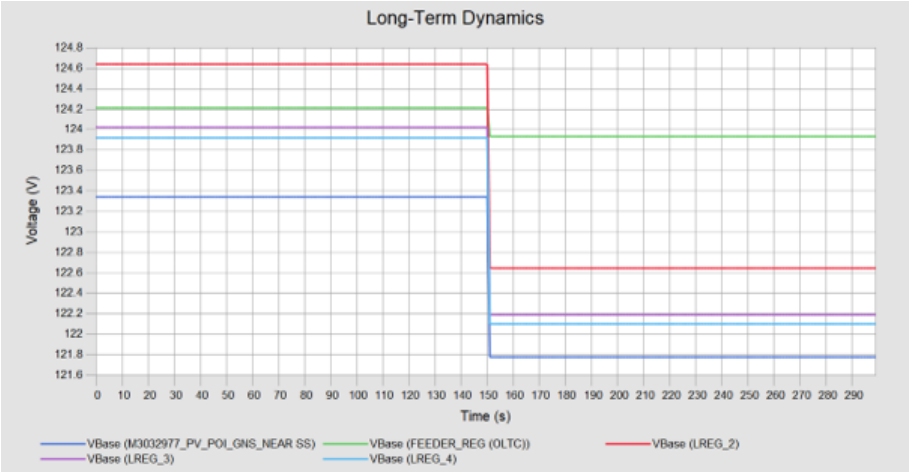

(a) P-G_{NS} Voltage Change at PV POI, Feeder Reg, LREG#2, LREG#3, and LREG#4 during 75% drop of PV.

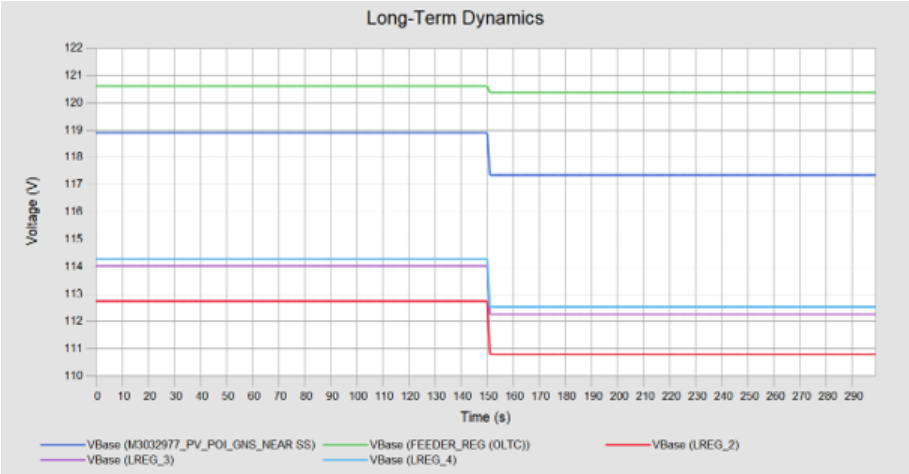

(b) N-G_{NS} Voltage Change at PV POI, Feeder Reg, LREG#2, LREG#3, and LREG#4 during 75% drop of PV.

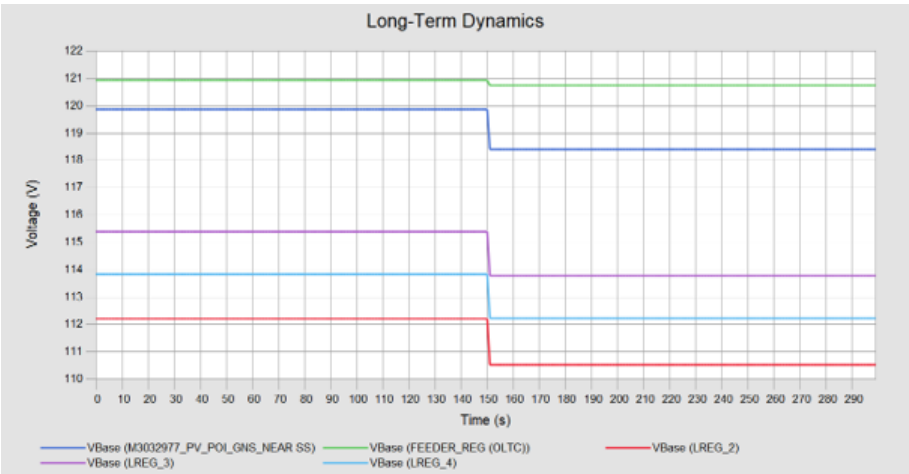

(c) O-G_{NS} Voltage Change at PV POI, Feeder Reg, LREG#2, LREG#3, and LREG#4 during 75% drop of PV.

Figure 5.10: Flicker/RVC Analysis for G_{NS} Scenarios (Without Mitigation)

Table 5.4: Flicker/RVC Analysis – Without Mitigation (G_{FS} Scenarios)

Monitoring Location	ΔV (P-G_{FS})	ΔV (N-G_{FS})	ΔV (O-G_{FS})	Limit
PV POI	**10.85%**	10.39%	7.31%	3%
Feeder Reg	0.00 V	0.17 V	0.94 V	1.5 V
LREG #2	5.84 V	5.06 V	1.75 V	1.5 V
LREG #3	3.26 V	2.70 V	0.19 V	1.5 V
LREG #4	1.85 V	1.43 V	0.34 V	1.5 V

Table 5.5: Flicker/RVC Analysis – Without Mitigation (G_{NS} Scenarios)

Monitoring Location	ΔV (P-G_{NS})	ΔV (N-G_{NS})	ΔV (O-G_{NS})	Limit
PV POI	1.30%	1.28%	0.97%	3%
Feeder Reg	0.29 V	0.23 V	0.18 V	1.5 V
LREG #2	1.99 V	1.93 V	1.69 V	1.5 V
LREG #3	1.84 V	1.77 V	1.61 V	1.5 V
LREG #4	1.82 V	1.75 V	1.61 V	1.5 V

Mitigation was applied to address the worst RVC violation observed at P-G_{FS} (10.85% at the PV POI), with results presented in Table 5.6 and Figure 5.11. The strategy involved adjusting the PV system's Power Factor (PF) to absorb reactive power, reducing ΔV to within limits. At the PV POI, a PF of -98.20% lowered the RVC to 2.72% for P-G_{FS}, and -99.00% reduced it to 2.77% for O-G_{FS}, both below the 3% threshold. For LREG#2, where ΔV was initially 5.84 V, a PF of -99.20% (P-G_{FS}) and -99.90% (O-G_{FS}) reduced it to 1.00 V and 1.06 V, respectively, meeting the 1.5 V limit. Other regulators (Feeder Reg, LREG#3, LREG#4) required no additional mitigation, with ΔV values ranging from 0.39 V to 1.30 V, well within limits, indicating the upstream PF adjustments were sufficient.

Table 5.6: Flicker/RVC Analysis – With Mitigation (P-G_{FS} and O-G_{FS} Scenarios)

Monitoring Location	**Mitigation (P-G_{FS})**	ΔV **(P-G_{FS})**	**Mitigation (O-G_{FS})**	ΔV **(O-G_{FS})**	**Limit**
PV POI	-98.20% PF	2.72%	-99.00% PF	2.77%	3%
Feeder Reg		1.30 V		1.19 V	1.5 V
LREG #2	-99.20% PF	1.00 V	-99.90% PF	1.06 V	1.5 V
LREG #3		0.44 V		0.39 V	1.5 V
LREG #4		0.88 V		0.78 V	1.5 V

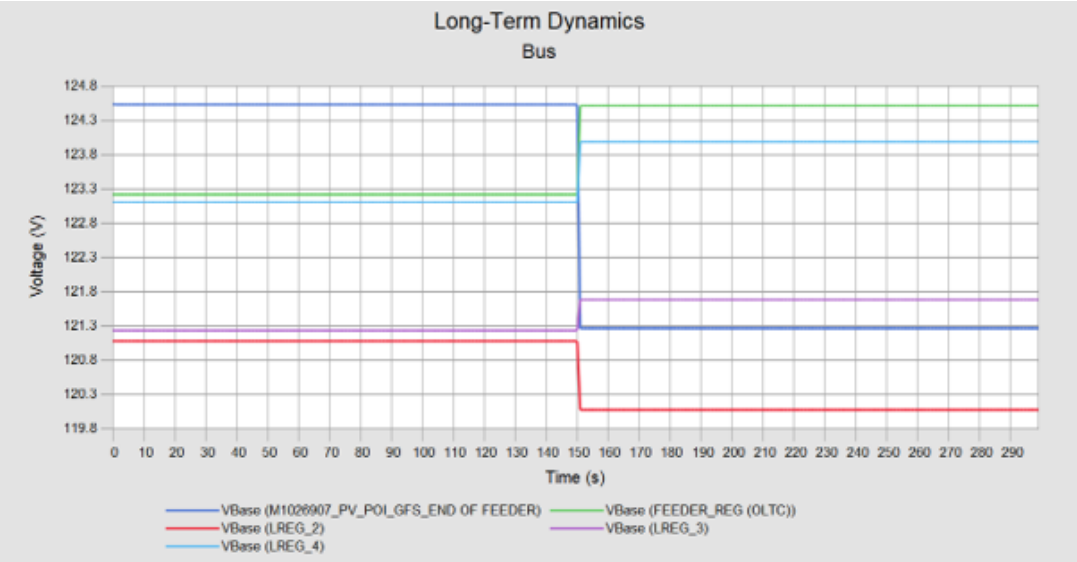

(a) P-G_{FS} Voltage Change at PV POI, Feeder Reg, LREG#2, LREG#3, and LREG#4 after mitigation.

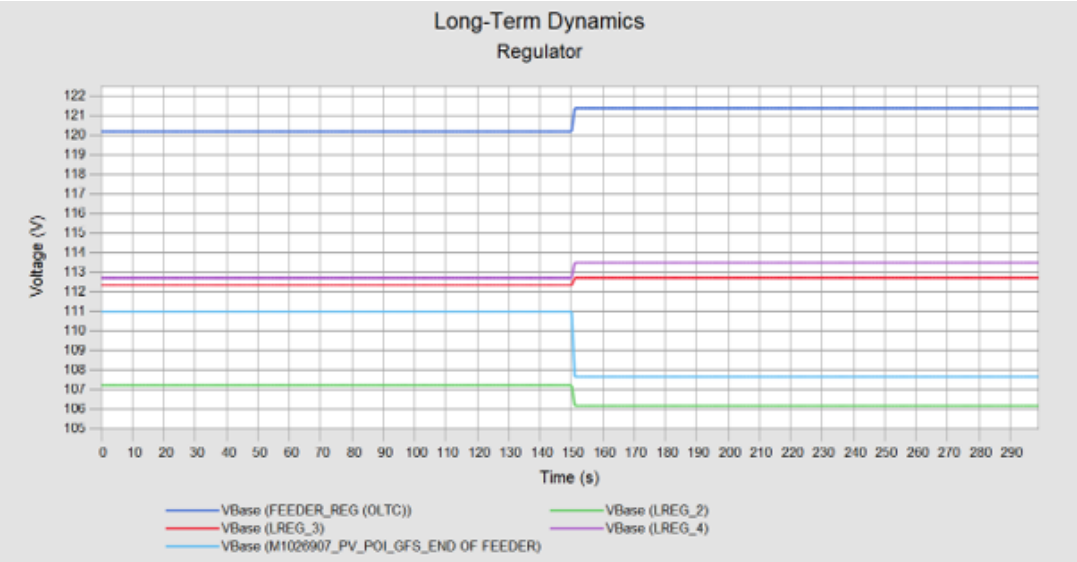

(b) O-G_{FS} Voltage Change at PV POI, Feeder Reg, LREG#2, LREG#3, and LREG#4 after mitigation.

Figure 5.11: Flicker/RVC Analysis for G_{FS} Scenarios (With Mitigation)

5.2.1 Effects of R/X Ratio

The voltage rise and RVC mechanisms are strongly influenced by the R/X ratio, which varies with PV location. The voltage change is modeled as:

- **Without PV:**

$$\Delta V = V_1 - V_2 = \frac{R_{\mathrm{LN}} P_{\mathrm{L}} + X_{\mathrm{LN}} Q_{\mathrm{L}}}{V_2}$$

- **With PV:**

$$\Delta V = V_1 - V_2 = \frac{[R_{\text{LN}}(P_{\text{L}} - P_{\text{PV}}) + X_{\text{LN}}(Q_{\text{L}} - Q_{\text{PV}})]}{V_2}$$

When $P_{\text{PV}} > P_{\text{L}}$, a higher R/X ratio (e.g., 0.55 at G_{FS}) amplifies voltage rise and RVC due to increased feeder impedance (R_{LN} and X_{LN}).

Table 5.7: Effects of R/X ratios on Voltage Rise and RVC - Summary

Location	**R/X Value**	**Vmax @ POI (Scenario)**	**Max. ΔV @ POI (Scenario)**
GFS POI	0.55	130.15 V (O-G_{FS})	10.85% (P-G_{FS})
GNS POI	0.19	125.58 V (O-G_{FS})	1.30% (P-G_{NS})

Table 5.7 shows that G_{FS} (R/X = 0.55) reaches a maximum voltage of 130.15 V during O-G_{FS}, exceeding the 126 V limit, while G_{NS} (R/X = 0.19) peaks at 125.58 V, within limits. The higher R/X ratio at G_{FS} exacerbates both steady-state overvoltage and RVC, particularly under low-load conditions. Furthermore, the analysis reveals that both overvoltage and RVC are minimal in the GNS case, where the R/X ratio is smaller (0.19) compared to the GFS case (0.55), highlighting the significant influence of R/X ratio on voltage stability. Notably, RVC is worst during peak loading conditions in the GFS case, with a maximum ΔV of 10.85%, while overvoltage is most severe during peak loading, reaching 130.15 V, underscoring the interdependence of loading conditions, PV placement location (R/X ratio), and the need to study RVC and steady-state voltage rise simultaneously. This interdependence is critical because mitigation strategies that address voltage rise during off-peak conditions may leave flicker unacceptable during peak load, necessitating a balanced approach to ensure grid reliability across all operating scenarios.

Recommendation: Strategic PV placement near the substation (G_{NS}) is recommended to minimize voltage impacts, leveraging lower impedance and R/X ratios.

5.3 Integrated Analysis and Discussion

The integrated analysis of steady-state voltage and RVC/flicker reveals a complex interplay of factors influencing PV integration. Steady-state overvoltage is most severe at G_{FS} during Off-Peak conditions (130.15 V, Table 5.1), driven by excess PV power against minimal load, amplified by the high R/X ratio (0.55). Mitigation with

fixed PF (-93.20%) or Volt-VAR (-94.83%) effectively reduces this to 125.86 V and maintains voltage below 126 V across all nodes (Figures 5.5 and 5.8). Conversely, the worst RVC violation occurs at P-G_{FS} (10.85%, Table 5.4), due to high impedance and power variability during a 75% PV drop. Mitigation with PF adjustments lowers RVC at the PV POI and at existing regulating devices, meeting the 3% and 1.5 V limits (Table 5.6, Figure 5.11).

This divergence highlights that steady-state and dynamic voltage issues peak under different conditions—Off-Peak for overvoltage and Peak for RVC—necessitating a simultaneous analysis for both effects. Fixed PF provides a straightforward solution but lags the ability of scenario-specific tuning, while Volt-VAR offers dynamic adaptability, slightly increasing PF (e.g., -97.22% vs. -96.90% for P-G_{FS}) but optimizing reactive power use across loading conditions. The R/X ratio's role is critical, with G_{FS}'s 0.55 ratio exacerbating both phenomena compared to G_{NS}'s 0.19, underscoring the importance of PV placement.

These findings suggest that PV integration strategies must account for both steady-state and dynamic impacts to ensure compliance with standards (e.g., ANSI C84.1, IEEE 1547-2018) and grid reliability. The success of mitigation at G_{FS} indicates that smart inverter controls can support high PV penetration, but placement near the substation (G_{NS}) remains optimal to minimize voltage challenges.

CHAPTER SIX: CONCLUSION AND RECOMMENDATION

This thesis has investigated the voltage impacts of Voltage Source Converter (VSC)-based Distributed Energy Resources (DERs), specifically photovoltaic (PV) systems, in primary distribution networks, addressing the critical challenges of steady-state overvoltage and rapid voltage change (RVC). Through simulations on the IEEE 8500-node test feeder using CYMDIST, the study analyzed the effects of PV placement, feeder impedance (R/X ratio), and loading conditions on voltage stability, revealing that placing PV systems near substations significantly reduces both steady-state voltage rise and RVC ($V_{\max}$ at POI in O-G_{NS} case = 125.14 V and RVC, $\Delta V_{\max}$ at POI in P-G_{NS} case = 1.30%), maintaining voltage profiles within ANSI C84.1 limits (114–126 V) and RVC within IEEE 1547-2018 limits, even at high PV penetration levels for the given test feeder, while placement far from the substation introduced severe voltage violations ($V_{\max}$ at POI in O-G_{FS} case = 130.15 V and RVC, $\Delta V_{\max}$ at POI in P-G_{FS} case = 10.85%), necessitating increased mitigation efforts. Both fixed power factor (PF) and Volt-VAR operations, as smart inverter capabilities, were evaluated, with fixed PF applied first to assess voltage impact mitigation, followed by a practical Volt-VAR curve with appropriate settings for performance comparison, demonstrating that Volt-VAR operation, aligned with IEEE 1547-2018 standards, is highly effective due to its ability to dynamically adjust to a non-unity power factor, whereas fixed PF operation showed limited adaptability under dynamic load variations due to its static nature. The study highlights the distinct behavior of voltage rise and RVC, with steady-state voltage rise being most severe during low load scenarios ($V_{\max}$ at POI in O-G_{FS} case = 130.15 V) and RVC most pronounced during peak load (ΔV at POI in P-G_{FS} case = 10.85%, underscoring the necessity of evaluating VSC-based PV system impacts across all loading scenarios to ensure comprehensive voltage management in high-DER networks.

For engineers and utilities aiming to enhance grid reliability in high-DER distribution networks, strategic PV placement near substations is recommended to minimize steady-state voltage rise and RVC, leveraging lower feeder impedance and R/X ratios to maintain voltage stability. Additionally, utilizing smart inverter capabilities to implement constant power factor operation or adopting Volt-VAR operation, using practical settings such as a deadband between 121.2 V and 123.6 V and reactive power limits of ±44% of the inverter's nameplate rating, can mitigate voltage violations and support high PV penetration cost-effectively, offering a robust alternative to traditional infrastructure upgrades. Furthermore, developing adaptive control

strategies that adjust smart inverter settings based on real-time feeder conditions can further optimize voltage regulation dynamically across diverse load scenarios, ensuring long-term grid stability.

Despite these findings, challenges remain in optimizing Volt-VAR settings for diverse feeder configurations, necessitating future research into adaptive Volt-VAR strategies that integrate real-time monitoring and machine learning for predictive control to enhance voltage regulation, while addressing inverter capability limitations (e.g., the 44% reactive power constraint) and coordination with legacy devices like switchable capacitors and line voltage regulators to mitigate risks of hunting behavior. Investigating the combined effects of multiple DERs, such as PV systems and Battery Energy Storage Systems (BESS), particularly the voltage effects of BESS charging on undervoltage conditions, can complement the current focus on PV export and provide a more holistic understanding of VSC-based DG integration. Additionally, conducting thermal overload analyses to assess infrastructure constraints when PV systems are far from the substation (G_{FS}), and performing studies using real-world utility feeders with time-series data and distributed smaller-scale PV systems, will improve the accuracy and applicability of these findings, further strengthening the resilience of modern grids for sustainable renewable energy integration.

REFERENCES

[1] A. Awad, D. Turcotte, and T. H. M. El-Fouly, "Impact assessment and mitigation techniques for high penetration levels of renewable energy sources in distribution networks: Voltage-control perspective," *Journal of Modern Power Systems and Clean Energy*, vol. 10, pp. 450–462, Mar 2022.

[2] E. A. Hamza, B. E. Sedhom, and E. A. Badran, "Impact and assessment of the overvoltage mitigation methods in low-voltage distribution networks with excessive penetration of pv systems: a review," *IET Energy Systems Integration*, vol. 2, no. 1, pp. 1–14, Mar 2022.

[3] M. M. Haque and P. Wolfs, "A review of high pv penetrations in lv distribution networks: Present status and impacts," *Renewable and Sustainable Energy Reviews*, vol. 62, pp. 1195–1208, Sep 2016.

[4] J. O. Petinrin, "Impact of renewable generation on voltage control in distribution systems," *Renewable and Sustainable Energy Reviews*, vol. 65, pp. 770–783, Nov 2016.

[5] V. Sharma, M. H. Haque, S. M. Aziz, and T. Kauschke, "Reducing overvoltage-induced pv curtailment through reactive power support of battery and smart pv inverters," *IEEE Access*, vol. 12, pp. 123 995–124 008, 2024.

[6] O. A. Balogun, Y. Sun, and P. A. Gbadega, "Coordination of smart inverter-enabled distributed energy resources for optimal pv-bess integration and voltage stability in modern power distribution networks: A systematic review and bibliometric analysis," *e-Prime - Advances in Electrical Engineering, Electronics and Energy*, vol. 10, p. 100800, 2024. [Online]. Available: https://www.sciencedirect.com/science/article/pii/S2772671124003802

[7] R. F. Arritt and R. C. Dugan, "The ieee 8500-node test feeder," in *IEEE PES T&D 2010*, 2010, pp. 1–6.

[8] R. Seguin, J. Woyak, D. Costyk, J. Hambrick, and B. Mather, "High-penetration pv integration handbook for distribution engineers," National Renewable Energy Laboratory (NREL), Technical Report NREL/TP-5D00-63114, January 2016. [Online]. Available: https://www.nrel.gov/publications

[9] A. N. S. I. (ANSI), "American national standard for electric power systems and equipment – voltage ratings (60 hertz)," 2007, archived 27 July 2007 at the Wayback Machine. NEMA. Access may require purchase. [Online]. Available: https://webstore.ansi.org/Standards/NEMA/NEMAC8412007R2012

[10] Institute of Electrical and Electronics Engineers (IEEE), *IEEE Standard for Interconnection and Interoperability of Distributed Energy Resources with Associated Electric Power System Interfaces*, Std. 1547-2003, 2003. [Online]. Available: https://standards.ieee.org/standard/1547-2003.html

[11] I. of Electrical and E. E. (IEEE), "Ieee standard for interconnection and interoperability of distributed energy resources with electric power systems," 2018. [Online]. Available: https://standards.ieee.org/standard/1547-2018.html

[12] E. F. Fuchs and M. A. S. Masoum, *Power Quality in Power Systems and Electrical Machines*. Burlington, MA: Academic Press, 2008.

[13] R. K. Varma, *Impacts of High Penetration of Solar PV Systems and Smart Inverter Developments*. John Wiley & Sons, Ltd, 2021, ch. 1, pp. 1–34. [Online]. Available: https://onlinelibrary.wiley.com/doi/abs/10.1002/9781119214236.ch1

[14] R. K. Varma, *Smart Inverter Functions*. John Wiley & Sons, Ltd, 2021, ch. 2, pp. 35–71. [Online]. Available: https://onlinelibrary.wiley.com/doi/abs/10.1002/9781119214236.ch2

[15] R. K. Varma, *Modeling and Control of Three-Phase Smart PV Inverters*. John Wiley & Sons, Ltd, 2021, ch. 3, pp. 73–106. [Online]. Available: https://onlinelibrary.wiley.com/doi/abs/10.1002/9781119214236.ch3

[16] R. K. Varma, *PV-STATCOM*. John Wiley & Sons, Ltd, 2021, ch. 4, pp. 107–144. [Online]. Available: https://onlinelibrary.wiley.com/doi/abs/10.1002/9781119214236.ch4

[17] R. K. Varma, *PV-STATCOM Applications in Distribution Systems*. John Wiley & Sons, Ltd, 2021, ch. 5, pp. 145–204. [Online]. Available: https://onlinelibrary.wiley.com/doi/abs/10.1002/9781119214236.ch5

[18] R. K. Varma, *PV-STATCOM Applications in Transmission Systems.* John Wiley & Sons, Ltd, 2021, ch. 6, pp. 205–300. [Online]. Available: https://onlinelibrary.wiley.com/doi/abs/10.1002/9781119214236.ch6

[19] R. K. Varma, *Increasing Hosting Capacity by Smart Inverters – Concepts and Applications.* John Wiley & Sons, Ltd, 2021, ch. 7, pp. 301–368. [Online]. Available: https://onlinelibrary.wiley.com/doi/abs/10.1002/9781119214236.ch7

[20] R. K. Varma, *Control Coordination of Smart PV Inverters.* John Wiley & Sons, Ltd, 2021, ch. 8, pp. 369–429. [Online]. Available: https://onlinelibrary.wiley.com/doi/abs/10.1002/9781119214236.ch8

[21] R. K. Varma, *Emerging Trends with Smart Solar PV Inverters.* John Wiley & Sons, Ltd, 2021, ch. 9, pp. 431–464. [Online]. Available: https://onlinelibrary.wiley.com/doi/abs/10.1002/9781119214236.ch9

[22] Y. Wan, J. Yan, T. Chu, Y. Li, K. Yuan, and K. Zhang, "A two-layer adaptive control strategy for photovoltaic power in different scenarios," in *2023 3rd International Conference on Energy Engineering and Power Systems (EEPS)*, July 2023, pp. 84–94.

[23] S. Sitompul, K. Shimomukai, and G. Fujita, "Enhancement of volt-var control using voltage sensitivity in grid-connected photovoltaics system," in *2022 IEEE PES Innovative Smart Grid Technologies - Asia (ISGT Asia)*, Nov 2022, pp. 46–50.

APPENDIX A: SYSTEM MODELLING DATA

10 MVA PV Modelling in CYMDIST

The following figures provide supplementary data, including PV Inverter, Transformer, and ECG modelling used in the analysis in this thesis.

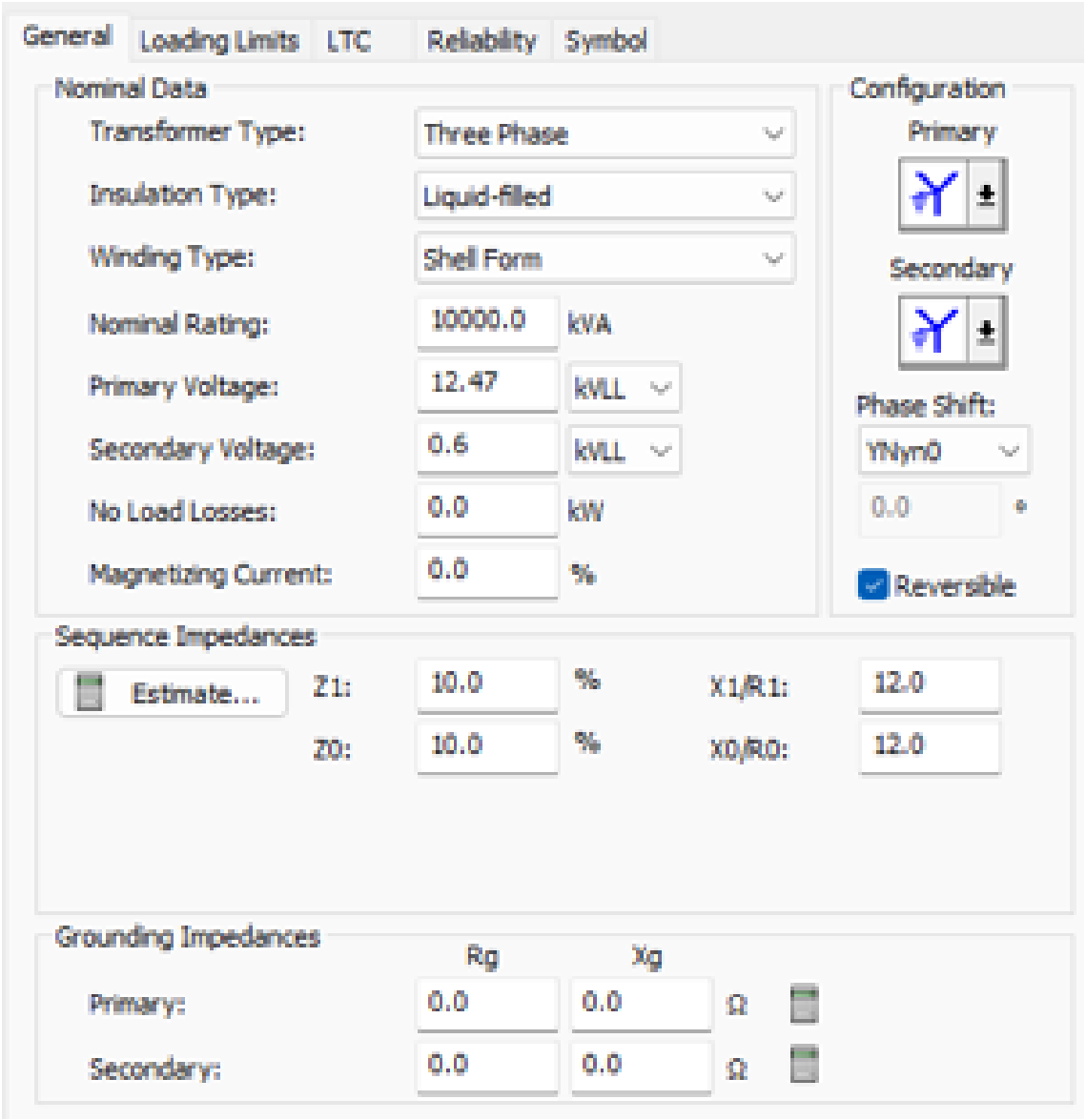

Figure A.12: PV GSU Transformer Modelling

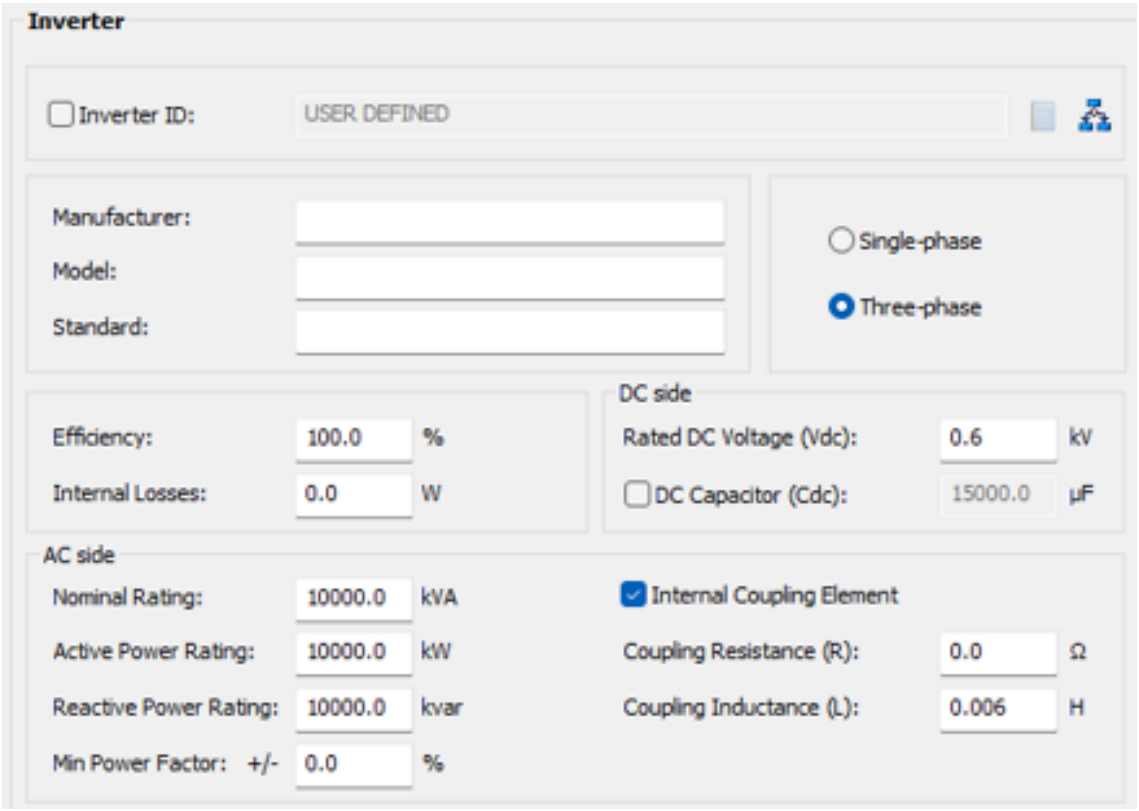

Figure A.13: PV Inverter Modelling

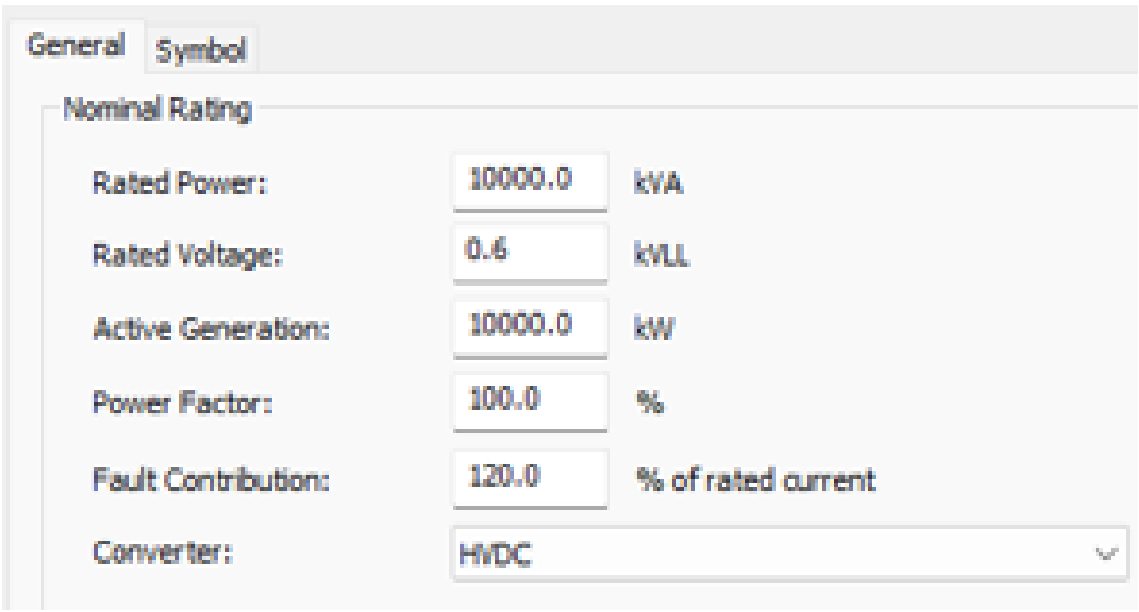

Figure A.14: ECG Modelling

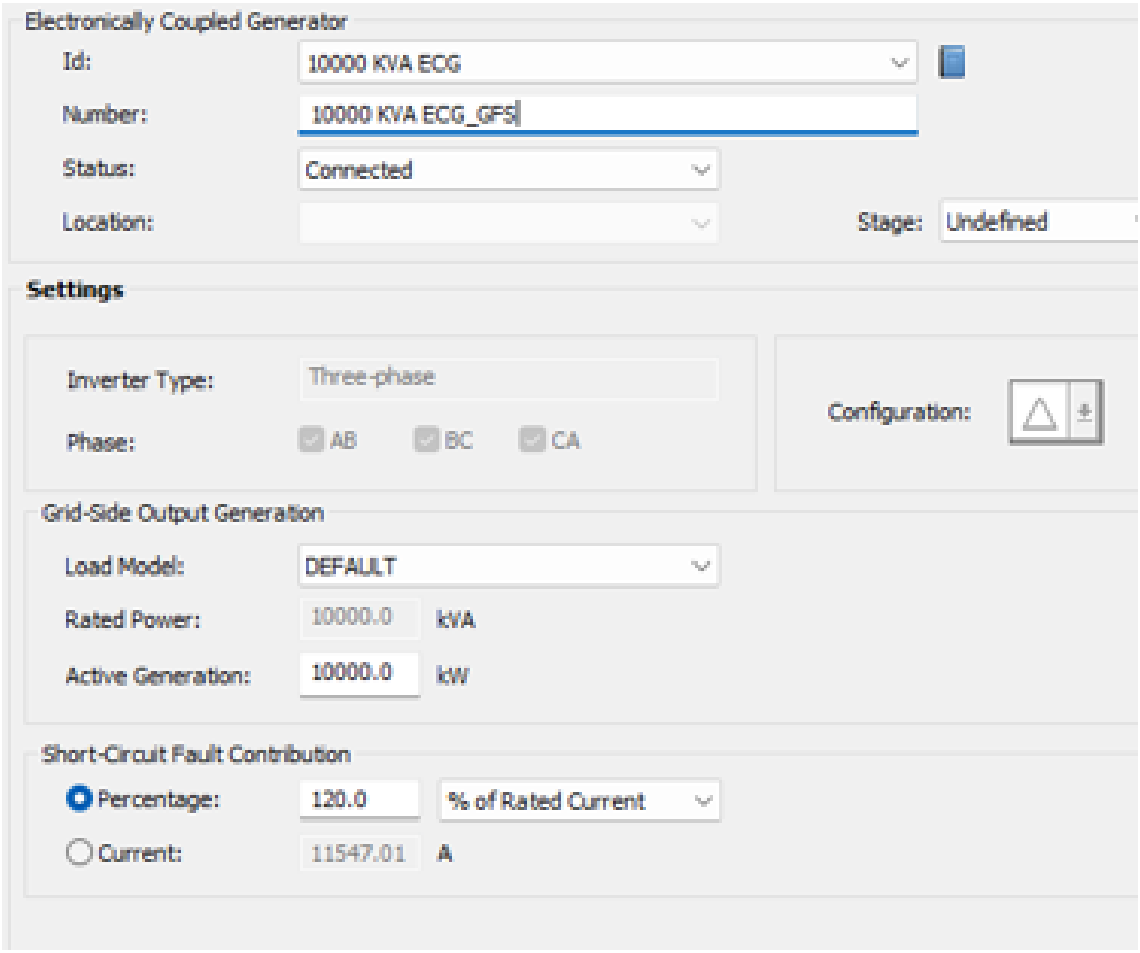

Figure A.15: ECG Modelling - continued

Existing Feeder Devices Settings

The following figures provide supplementary data, including Feeder Devices Settings and simulation settings, to support the analysis in this thesis.

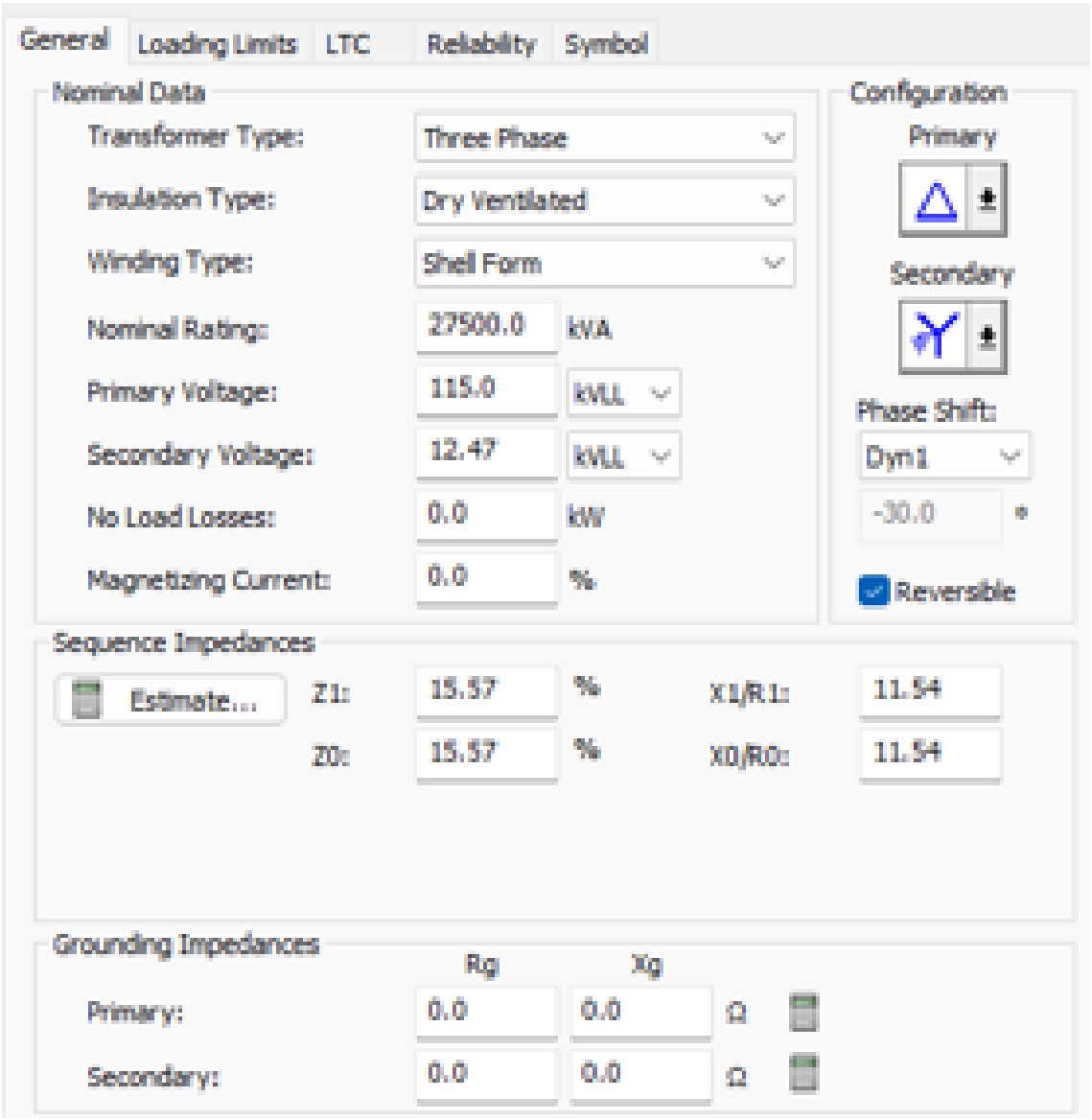

Figure A.16: Substation Transformer Settings

Network Id	Section Id	Equipment Id	Phase	Status	From Node	Bank Type	Type	Cap. Control	Close at/ Trip at (kVAR)	Total Cap. kvar (kvar)	Cap. kvar A (kvar)	Cap. kvar B (kvar)	Cap. kvar C (kvar)	kV (kVLN)	Losses (kW)	Interrupting rating (A)	Config
8500-NODE TEST FEEDER	CAPBANK1	CAPBANK1	ABC	Connected	R42247	Single-phase	Switched	Var	200/ -300	900.0	300.0	300.0	300.0	7.20	0.0	600.0	Yg
8500-NODE TEST FEEDER	CAPBANK0	CAPBANK0	ABC	Connected	R42246	Single-phase	Switched	Var	150/ -226	1200.0	400.0	400.0	400.0	7.20	0.0	600.0	Yg
8500-NODE TEST FEEDER	CAPBANK2	CAPBANK2	ABC	Connected	R20185	Single-phase	Switched	Var	150/ -225	900.0	300.0	300.0	300.0	7.20	0.0	600.0	Yg
8500-NODE TEST FEEDER	CAPBANK3	CAPBANK3	ABC	Connected	R18242	Three-phase	Fixed	Manual	N/A	900.0	300.0	300.0	300.0	7.20	0.0	600.0	Yg

Figure A.17: Capacitors in the feeder - settings

Network Id	Section Id	Equipment Id	Equipment No	Phase	kV (kVLN)	Option	Reverse Mode	VsetA (V)	VsetB (V)	VsetC (V)	Bandwidth (V)	RevVsetA (V)	RevVsetB (V)	RevVsetC (V)
8500-NODE TEST FEEDER	FEEDER_REG	FEEDER_REG	FEEDER_REG (OLTC)	ABC	7.20	Regulator terminal	Co-generation	124.00	124.00	124.00	3.00	122.00	122.00	122.00
8500-NODE TEST FEEDER	VREG_2	VREG2	LREG_2	ABC	7.20	Regulator terminal	Co-generation	124.00	124.00	124.00	3.00	120.00	120.00	120.00
8500-NODE TEST FEEDER	VREG_3	VREG3	LREG_3	ABC	7.20	Regulator terminal	Co-generation	124.00	124.00	124.00	3.00	122.00	122.00	122.00
8500-NODE TEST FEEDER	VREG_4	VREG4	LREG_4	ABC	7.20	Regulator terminal	No reverse	124.00	124.00	124.00	3.00	126.00	126.00	126.00

Figure A.18: Regulators in the feeder - settings

APPENDIX B: PUBLICATION

Conference paper

[IOEGC16] Editor Decision

2025-04-06 01:25 AM

Upendra Bhattarai, Sujan Adhikari,

We are pleased to inform you that your manuscript titled "Voltage Impact Analysis for VSC-Based DGs Connected to the Primary Distribution System" submitted to 16th IOE Graduate Conference is **Accepted** for presentation in the Conference as well as inclusion in the Peer-Reviewed Proceedings. Please note that inclusion in hard copy proceedings is contingent upon your timely response to further edits, if any, during the publication process.

With Warm Regards,
IOEGC-16 Editorial Team

IOE Graduate Conference
[Placeholder for Publication Information]

Voltage Impact Analysis for VSC-Based DGs Connected to the Primary Distribution System

Upendra Bhattarai[a], Sujan Adhikari[b]

[a] *Department of Electrical Engineering, Pulchowk Campus, Institute of Engineering, Tribhuvan University, Nepal* , [b] *Hillside College of Engineering, Balkumari, Kathmandu*

[a] 079mspse024.upendra@pcampus.edu.np , [b] easujan@gmail.com

Abstract

This paper investigates the voltage regulation challenges posed by Voltage Source Converter (VSC)-based Photovoltaic (PV) Distributed Energy Resources (DERs) in primary distribution systems, focusing on voltage rise and rapid voltage changes (flicker). Utilizing the IEEE 8500-node test feeder, the study analyzes the impacts of PV placement (near the substation, G_{NS}, and far from the substation, G_{FS}), loading conditions (Peak, Normal, and Off-Peak), and feeder impedance (R/X ratio) under steady-state conditions. Key findings reveal that voltage rise is most severe during Off-Peak loads at G_{FS}, reaching 130.15 V and exceeding ANSI C84.1 limits, while flicker peaks at 10.85% under Peak loads at G_{FS}, breaching IEEE Std 1547-2018 thresholds. The analysis highlights the heightened vulnerability of G_{FS} due to higher R/X ratios (0.55 versus 0.19 at G_{NS}), underscoring the importance of PV placement and loading conditions in grid stability. These insights recommend interconnecting DERs closer to substations to lower the chances of voltage disturbances in the primary distribution system.

Keywords

Voltage Source Converter (VSC), Distributed Energy Resources (DERs), Distributed Generations (DGs), Photovoltaic (PV) Systems, Battery Energy Storage Systems (BESS), Voltage Rise, Voltage Flicker, Rapid Voltage Change (RVC), Volt-VAR Optimization (VVO), Smart Inverter Control, Primary Distribution System, Power Quality, Reactive Power Control, Point of interconnection (POI), IEEE 8500-Node Test Feeder.

1. Introduction

1.1 Background

The integration of renewable energy sources (RES) into modern power distribution systems has accelerated significantly, driven by global efforts to reduce carbon emissions and enhance energy sustainability. Among these, Photovoltaic (PV) systems and Battery Energy Storage Systems (BESS), interfaced through Voltage Source Converters (VSCs), have emerged as key Distributed Energy Resources (DERs) within primary distribution networks. These VSC-based DGs offer substantial benefits, including reduced reliance on fossil fuels and improved grid flexibility to accommodate variable loads. However, their intermittent generation profiles introduce pronounced challenges in voltage regulation, particularly in the context of high penetration levels. Two critical issues dominate this domain: voltage rise, resulting from excess power injection during periods of low demand, and rapid voltage changes, often manifesting as voltage flicker, triggered by abrupt fluctuations in PV output due to environmental or grid-related factors. Addressing these phenomena is essential to ensure grid stability, power quality, and compliance with operational standards in contemporary distribution systems.

1.2 Related Work and Literature Review

A substantial body of research has investigated the voltage regulation challenges associated with Voltage Source Converter (VSC)-based Distributed Generations (DGs), particularly Photovoltaic (PV) systems, in distribution networks. Awad et al. [1] explored the mechanisms underlying voltage rise in high-PV-penetration scenarios, demonstrating that excessive active power injection into weak distribution feeders, marked by elevated impedance, leads to significant overvoltage, especially under low-load conditions. Similarly, Hamza et al. [2] assessed the impact of PV power surplus on voltage profiles, identifying substantial deviations in rural feeders with long lines and high impedance during periods of reduced demand. On the topic of rapid voltage changes, Haque and Wolfs [3] conducted a thorough examination of voltage flicker, linking these fluctuations to sudden PV output variations induced by cloud cover, which degrade power quality and affect sensitive equipment in distribution systems. Sharma et al. [4] proposed a method to reduce overvoltage-induced PV curtailment

in distribution networks by leveraging reactive power support from battery and smart PV inverters, focusing on an 11-kV feeder in South Australia. Fuchs and Masoum [5] provide a foundational text on power quality in distribution systems, offering insights into voltage rise and flicker mitigation, which remain relevant for modern high-DER networks.

Recent studies have also emphasized the role of network parameters in these phenomena. Petinrin and Shaaban [6] analyzed the influence of feeder impedance and PV location on voltage rise, noting that placements farther from substations exacerbate voltage deviations due to higher resistance and reactance. Seguin et al. [7] further highlighted the significance of loading conditions and feeder topology, identifying peak and off-peak scenarios as critical periods for flicker and overvoltage, respectively, in high-DER networks. Despite these contributions, a detailed investigation into the combined effects of PV placement, feeder impedance (e.g., R/X ratio), and varying loading conditions on voltage rise and flicker, particularly in large-scale distribution systems like the IEEE 8500-node test feeder, remains underexplored. This study addresses this gap by focusing on these factors to deepen the understanding of voltage challenges in modern distribution networks with significant DER integration.

1.3 Objectives and Scope

This study concentrates on the voltage impact analysis of Voltage Source Converter (VSC)-based Distributed Generations (DGs), specifically PV systems, within primary distribution systems. The primary objectives are to examine the causes and consequences of voltage rise under various feeder conditions, assess their steady-state implications, and evaluate the effectiveness of mitigation strategies. The analysis employs the IEEE 8500-node test feeder as a simulation framework, providing a realistic representation of large-scale distribution networks. Three distinct loading conditions—Peak, Normal, and Off-Peak—are considered, reflecting 100%, 60%, and 15% of the feeder's peak load, respectively, with PV output maintained at a constant full capacity of 10 MVA across all scenarios.

In practice, PV generation varies with environmental factors, and feeder loading fluctuates over time. However, this study intentionally adopts fixed values for both PV output and loading in each scenario to represent worst-case conditions. The rationale is that mitigating voltage rise under these extreme cases—where PV generation is maximized and loading ranges from minimal to peak—ensures the proposed solutions remain effective across intermediate operating states. The scope is thus limited to steady-state phenomena, excluding transient dynamics, to focus on persistent voltage regulation challenges. By identifying the causes and effects of voltage rise and rapid voltage changes and evaluating their implications under varying operating conditions, this work aims to deliver practical engineering insights for enhancing grid reliability in modern distribution systems with high DER penetration.

1.4 Voltage Impact Analysis

1.4.1 Voltage Flicker: Causes and Impact

Voltage flicker, interchangeably referred to as Rapid Voltage Change (RVC) in subsequent sections of this paper, denotes short-term voltage fluctuations in distribution systems arising from rapid variations in PV generation. These fluctuations primarily stem from two sources: sudden shading due to cloud coverage, which induces abrupt reductions in PV output and corresponding power swings, and grid faults, such as short circuits or line tripping, which prompt immediate PV disconnections and significant voltage drops. The magnitude of these changes can be approximated as $\Delta V \approx (R \cdot \Delta P + X \cdot \Delta Q)/V_n$ [5], where R and X are the feeder resistance and reactance, ΔP and ΔQ represent the changes in active and reactive power due to PV variability, and V_n is the nominal voltage. The impacts of voltage flicker are multifaceted, degrading power quality by causing perceptible flickering in lighting systems, which diminishes customer satisfaction, and inducing malfunctions in sensitive industrial and medical equipment due to voltage instability. Furthermore, sustained flicker levels exceeding thresholds, such as the 3% limit at the Point of Interconnection specified by IEEE Std 1547-2018 [8], may result in regulatory non-compliance, exposing PV owners to penalties and necessitating robust mitigation measures to maintain grid reliability.

1.4.2 Voltage Rise: Causes and Impact

Voltage rise occurs when excess active power from PV systems is injected into the grid, exceeding local demand. This is particularly significant in weak rural distribution feeders, where high impedance amplifies voltage deviations. The effect of connection of distributed generation systems on the voltage of a distribution network is explained in paper [6].

Figure 1 shows a simple distribution system with both load and PV generation.

The voltage change along a feeder without external generation (PV) can be expressed as:

$$\Delta V = V_1 - V_2 = \frac{R_{LN} P_L + X_{LN} Q_L}{V_2} \tag{1}$$

where P_L, Q_L are the active and reactive power loads, and

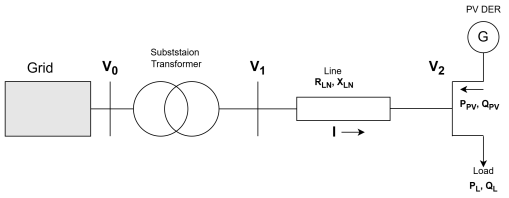

Figure 1: Distribution system with load and PV Generation.

R_{LN}, X_{LN} represent feeder impedance.

When a PV is connected in the distribution system, the voltage equation modifies to:

$$\Delta V = V_1 - V_2 = \frac{(R_{LN}(P_L - P_{PV}) + X_{LN}(Q_L - Q_{PV}))}{V_2} \quad (2)$$

Now, when the generation from PV systems is higher than the power consumed by the load, ΔV given by equation 2 becomes negative, or in other words, the voltage at the load side becomes higher than that at source side. That means, when $P_{PV} > P_L$, the feeder experiences voltage rise, violating grid standards such as IEEE Std 1547-2018 [8] and ANSI C84.1 [9].

This voltage rise is more prominently seen when the PV is interconnected further away from the source, because at those cases the value of R_{LN} and X_{LN} are high. So, when a PV system is connected close to the source, it does not cause much rise in voltage but the same system placed at the end of the network may cause serious overvoltage issues. This phenomenon is further explained and proved in the *Results and Discussion* Section.

1.4.3 Mitigation Strategies

Various strategies have been developed to address voltage regulation challenges in distribution systems with Voltage Source Converter (VSC)-based Photovoltaic (PV) Distributed Energy Resources (DERs). This study exclusively employs non-unity power factor (PF) mitigation to evaluate the level of intervention required across different scenarios, such as mitigating rapid voltage changes (RVC) under Peak load with PV far from the substation (P-G_{FS}) and voltage rise during Off-Peak load with PV far from the substation (O-G_{FS}). Conventional methods, including capacitor banks, offer reactive power compensation but are limited by their lack of dynamic adaptability, rendering them less suitable for rapidly varying PV outputs. Network reinforcements, such as upgrades to thicker conductors and voltage regulators, provide a structural solution but are often prohibitively expensive, potentially discouraging investment in renewable energy initiatives like PV DERs. Fixed power factor operation, specifically non-unity PF, enables DERs to operate at a predetermined lagging power factor, allowing the consumption of reactive power to reduce voltage deviations, as illustrated by the relationship in Equation 2, where absorbing reactive power decreases the second term, thereby lowering voltage rise. However, this approach can curtail active power output, imposing economic burdens on PV owners to resolve grid violations, such as those observed in P-G_{FS} RVC and O-G_{FS} voltage rise scenarios. Advanced techniques, such as Volt-VAR Optimization (VVO), which dynamically adjust reactive power, are not implemented in this study but could provide more efficient mitigation options.

2. Methodology

2.1 System Modeling and Simulation Setup

This study uses the **IEEE 8500-node test feeder** as a benchmark system to analyze voltage regulation challenges in large-scale distribution networks. This realistic test feeder, containing approximately 8500 nodes and 4800 buses, enables rigorous assessment of power flow, loss minimization, and grid stability, making it a valuable tool for evaluating smart inverter control and Volt-VAR optimization strategies in modern high-DER environments.

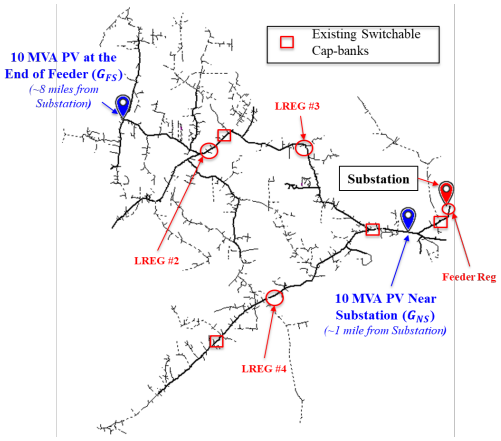

Figure 2: IEEE 8500-node test feeder with Existing Devices and New DGs (PV) Location.

Simulation Parameters:

- **Software:** CYME, Python (CYMPY libraries).
- **DER Configurations:** VSC-based PV and BESS.
- **Loading Scenarios:** Peak, normal, and off-peak conditions.
- **100% PV Penetration Level**

The Peak Loading in the standard feeder is at 11.836 MVA at 99.60% PF, which is considered as 100% loading.

Normal & off-Peak Loading are considered 60% & 15% of the peak loading respectively. The DG (PV) output is considered as 10 MVA and is modelled at 12.47 kV voltage level along the feeder at two different locations: near the substation and along the end of the feeder, as shown in the Figure 2. The 10 MVA PV output is assumed as 100% PV penetration considering the Generation equal to the Peak Load. The voltages shown in this paper will be on the standard base voltage of 120 V, which is considered as the nominal voltage.

2.2 Case Study Scenarios

The study evaluates different PV placement scenarios under varying loading conditions. Table 1 presents the case study scenarios analyzed considering varying loading condition and different DGs placement location along the primary distribution feeder.

Table 1: Case Study Scenarios Based on PV Placement and Loading Conditions

Loading	PV Placement	Scenario Name
Peak (P)	No PV (Off) (B)	P-B
	PV Far from Substation (G_{FS})	P-G_{FS}
	PV Near Substation (G_{NS})	P-G_{NS}
Normal (N)	No PV (Off) (B)	N-B
	PV Far from Substation (G_{FS})	N-G_{FS}
	PV Near Substation (G_{NS})	N-G_{NS}
Off-Peak (O)	No PV (Off) (B)	O-B
	PV Far from Substation (G_{FS})	O-G_{FS}
	PV Near Substation (G_{NS})	O-G_{NS}

Figure 2 illustrates the two PV placement scenarios considered and the name and location of existing feeder regulating devices.

2.3 Evaluation Metrics

The DG's impact on distribution circuit voltage was evaluated through steady-state and voltage change (flicker) analyses. The steady-state analysis was used to verify that circuit voltage remained within the acceptable 114-126 volt range (120-volt base) at the distribution transformer's high side during normal operation, ensuring reliable customer service. The voltage limits are in accordance with ANSI C84.1 [9]. The rapid voltage change analysis assessed the instantaneous voltage fluctuations (flicker) at the Point of Interconnection (POI) upon sudden project output transitions (full to no output and vice versa), with a limit of ≤ 3%. This analysis also examined voltage changes at the substation and in-series line regulators, requiring them to be ≤ half of their bandwidths (typically 1.5 V). The rapid voltage change (RVC) limits are in accordance with IEEE Std 1547-2018 [8].

- **Voltage deviations:** Percentage voltage rise above the standard nominal voltage (≤5%)
- **Power quality improvements:** Voltage flicker within limits at POI (≤3%) and existing regulating equipment (≤ half of the bandwidth).

3. Results and Discussion

3.1 Voltage Impacts Under Different Scenarios

The simulation results, derived from the IEEE 8500-node test feeder under Peak, Normal, and Off-Peak loading conditions, reveal distinct voltage profiles for VSC-based PV integration. These profiles, illustrated in Figures 3, 4, 5, 6, 7, 8, 9, 10, and 11, highlight the steady-state voltage impacts across PV placement scenarios—no PV (B), PV far from the substation (G_{FS}), and PV near the substation (G_{NS}) without mitigation.

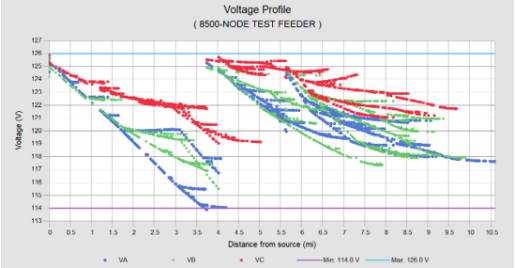

Figure 3: P-B Voltage profile without mitigation.

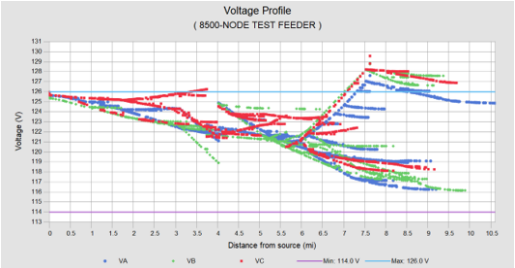

Figure 4: P-G_{FS} Voltage profile without mitigation.

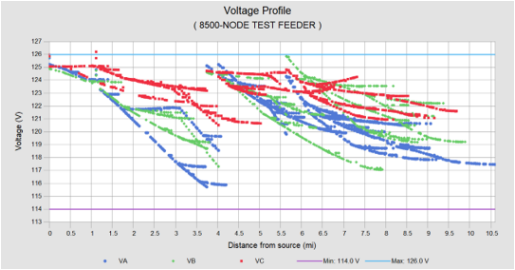

Figure 5: P-G_{NS} Voltage profile without mitigation.

Under Peak load conditions, the maximum feeder voltage without mitigation reaches 128.23 V for G_{FS} and

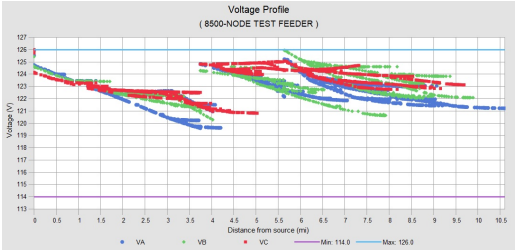

Figure 6: N-B Voltage profile without mitigation.

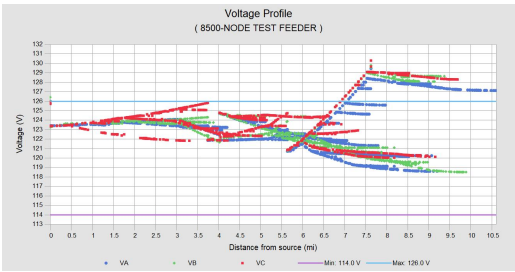

Figure 7: N-G_{FS} Voltage profile without mitigation.

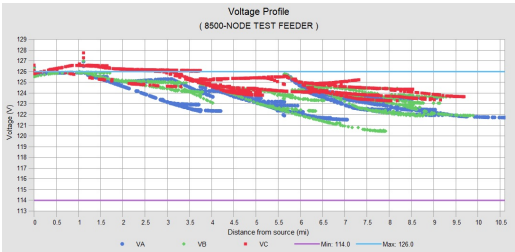

Figure 8: N-G_{NS} Voltage profile without mitigation.

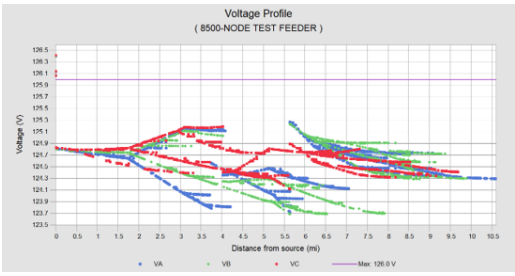

Figure 9: O-B Voltage profile without mitigation.

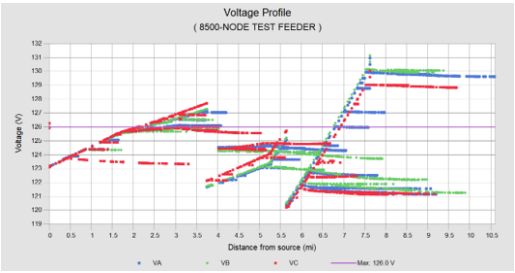

Figure 10: O-G_{FS} Voltage profile without mitigation.

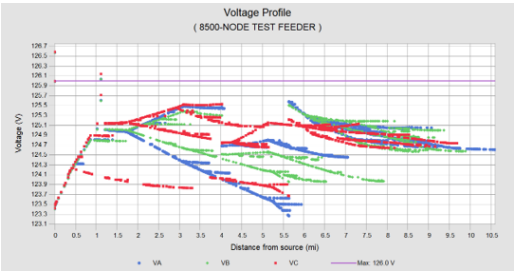

Figure 11: O-G_{NS} Voltage profile without mitigation.

125.85 V for G_{NS}, as summarized in Table 2. This overvoltage, particularly at G_{FS}, is attributed to the high impedance of long feeders amplifying the effect of excess PV power injection, as modeled in Equation 2. For Normal load conditions, voltages escalate to 129.10 V at G_{FS} and 125.57 V at G_{NS}, reflecting increased sensitivity to PV surplus due to reduced demand. In Off-Peak conditions, the most severe voltage rise occurs, with a maximum of 130.15 V at G_{FS}, exceeding ANSI C84.1 limits (114-126 V on a 120 V base) [9], due to minimal load offsetting the constant 10 MVA PV output. These results underscore the critical influence of feeder loading and PV location on voltage stability, with G_{FS} exacerbating overvoltage due to higher R/X ratios, as detailed in Table 5.

3.2 Voltage Flicker/RVC Analysis Under Different Scenarios

The Rapid Voltage Change (RVC) analysis, conducted without mitigation, examines instantaneous voltage fluctuations resulting from a 75% drop in PV output, as depicted in Figures 12, 13, 14, 15, 16, and 17. This analysis focuses on voltage changes at the PV Point of Interconnection (POI) and feeder regulating devices (Feeder Reg, LREG#2, LREG#3, LREG#4) under Peak, Normal, and Off-Peak conditions.

Under Peak load, G_{FS} exhibits the highest RVC at the PV POI, reaching 10.85%, significantly exceeding the 3% limit specified by IEEE Std 1547-2018 [8], as shown in Table 3. This is attributed to the increased impedance

Table 2: Voltage Impact Analysis – Different Scenarios

Loading Condition	Scenarios	Mitigation Required to Pass	Feeder V_{max}
Peak (P)	P-B	-	125.71 V
	P-G_{FS}	-96.90% PF	128.23 V (Without Mitigation) / 125.56 V (With Mitigation)
	P-G_{NS}	None Required	125.85 V
Normal (N)	N-B	-	125.94 V
	N-G_{FS}	-95.60% PF	129.10 V (Without Mitigation) / 125.85 V (With Mitigation)
	N-G_{NS}	None Required	125.57 V
Off-Peak (O)	O-B	-	125.27 V
	O-G_{FS}	-93.20% PF	130.15 V (Without Mitigation) / 125.86 V (With Mitigation)
	O-G_{NS}	None Required	125.58 V

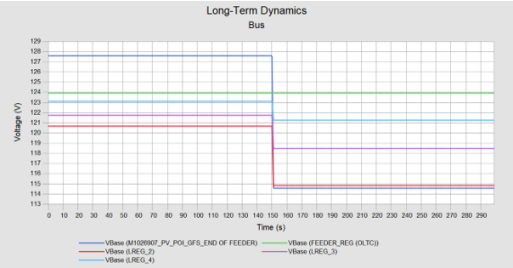

Figure 12: P-G_{FS} Voltage Change at PV POI, Feeder Reg, LREG#2, LREG#3, and LREG#4 during 75% drop of PV.

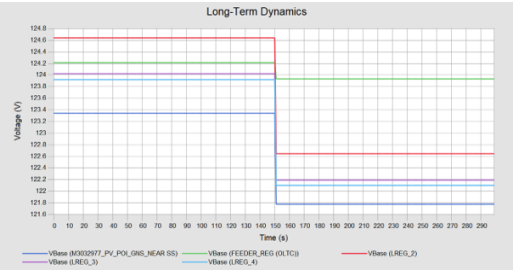

Figure 13: P-G_{NS} Voltage Change at PV POI, Feeder Reg, LREG#2, LREG#3, and LREG#4 during 75% drop of PV.

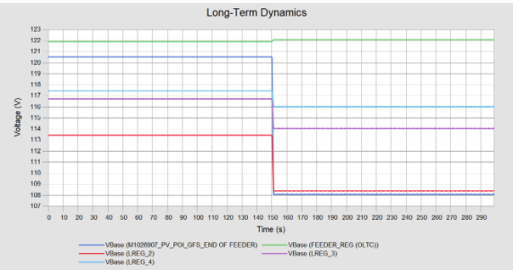

Figure 14: N-G_{FS} Voltage Change at PV POI, Feeder Reg, LREG#2, LREG#3, and LREG#4 during 75% drop of PV.

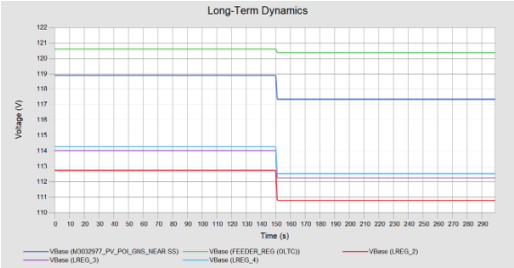

Figure 15: N-G_{NS} Voltage Change at PV POI, Feeder Reg, LREG#2, LREG#3, and LREG#4 during 75% drop of PV.

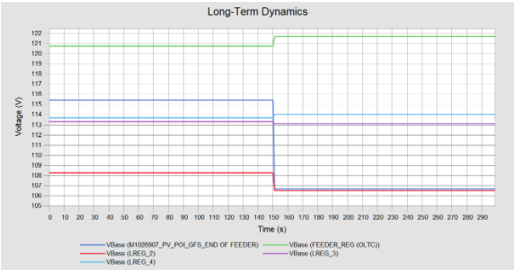

Figure 16: O-G_{FS} Voltage Change at PV POI, Feeder Reg, LREG#2, LREG#3, and LREG#4 during 75% drop of PV.

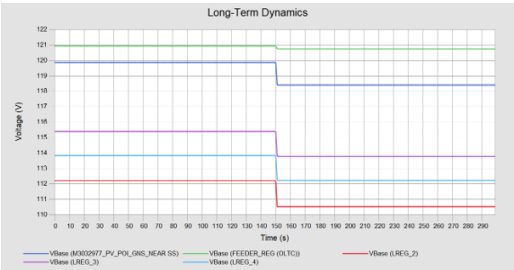

Figure 17: O-G_{NS} Voltage Change at PV POI, Feeder Reg, LREG#2, LREG#3, and LREG#4 during 75% drop of PV.

and power variability at the feeder end, amplifying sudden drops in PV generation. At G_{NS}, the RVC is mitigated to 1.30%, reflecting lower impedance and proximity to the substation. Similar trends are observed under Normal and Off-Peak loads, with G_{FS} showing 10.39% and 7.31% RVC at the POI, respectively, compared to 1.28% and 0.97% at G_{NS}. At feeder regulating devices, voltage changes remain within 1.5 V (half the bandwidth) for most scenarios, except at G_{FS} under Peak load, where LREG#2 experiences 5.84 V, indicating potential regulatory stress.

Table 3: Flicker/RVC Analysis – Without Mitigation (G_{FS} Scenarios)

Monitoring Location	ΔV (P-G_{FS})	ΔV (N-G_{FS})	ΔV (O-G_{FS})	Limit
PV POI	10.85%	10.39%	7.31%	3%
Feeder Reg	0.00 V	0.17 V	0.94 V	1.5 V
LREG #2	5.84 V	5.06 V	1.75 V	1.5 V
LREG #3	3.26 V	2.70 V	0.19 V	1.5 V
LREG #4	1.85 V	1.43 V	0.34 V	1.5 V

Table 4: Flicker/RVC Analysis – Without Mitigation (G_{NS} Scenarios)

Monitoring Location	ΔV (P-G_{NS})	ΔV (N-G_{NS})	ΔV (O-G_{NS})	Limit
PV POI	1.30%	1.28%	0.97%	3%
Feeder Reg	0.29 V	0.23 V	0.18 V	1.5 V
LREG #2	1.99 V	1.93 V	1.69 V	1.5 V
LREG #3	1.84 V	1.77 V	1.61 V	1.5 V
LREG #4	1.82 V	1.75 V	1.61 V	1.5 V

These findings suggest that PV placement at G_{FS} heightens susceptibility to flicker, particularly under high-load conditions, due to the combined effects of feeder impedance and PV power dynamics. The R/X ratio, as summarized in Table 5, further explains this behavior, with G_{FS}'s 0.55 ratio contributing to greater voltage sensitivity compared to G_{NS}'s 0.19 ratio.

Table 5: Summary table for relation of PV Location, R/X ratio and feeder loading

Location	R/X Value	Vmax Value @ POI (Scenario)
G_{FS} POI	0.55	130.15 V (O-G_{FS})
G_{NS} POI	0.19	125.14 V (O-G_{NS})

3.3 Key Observations from Case Studies

The analysis, guided by the voltage rise model in Equation 2, provides critical insights into the voltage regulation challenges of Voltage Source Converter (VSC)-based Photovoltaic (PV) systems within the IEEE 8500-node test feeder. The following observations, derived from simulation results, highlight the influence of feeder characteristics and operational conditions on voltage behavior:

- **Peak Load Conditions:** PV systems located far from the substation (G_{FS}) exhibit the highest rapid voltage change (RVC) at the Point of Interconnection (POI), reaching 10.85% under Peak load, as documented in Table 3. This heightened flicker susceptibility is attributed to increased feeder impedance and power variability, amplifying sudden PV output drops. In contrast, PV near the substation (G_{NS}), as documented in Table 4 shows a reduced RVC of 1.30%, reflecting lower impedance and proximity to the source, with a maximum feeder voltage of 125.85 V, as noted in Table 2.
- **Normal Load Conditions:** Under Normal load, G_{FS} continues to demonstrate elevated RVC values, reaching 10.39% at the POI, while G_{NS} maintains lower fluctuations at 1.28%, per Tables 3 and 4. Steady-state voltages at G_{FS} peak at 129.10 V, and at G_{NS} at 125.57 V, indicating persistent voltage rise sensitivity to PV placement and reduced demand, as detailed in Table 2.
- **Off-Peak Load Conditions:** During Off-Peak conditions, voltage rise is most severe at G_{FS}, with a maximum feeder voltage of 130.15 V, exceeding ANSI C84.1 limits (114-126 V on a 120 V base) [9], as shown in Table 2. This overvoltage results from excess PV power injection against minimal load, exacerbated by the higher R/X ratio of 0.55 at G_{FS} compared to 0.19 at G_{NS}, per Table 5. RVC at G_{FS} is reduced to 7.31%, while G_{NS} shows only 0.97%, indicating lower flicker risk near the substation.

These observations, supported by Tables 2, 3, 4, and 5 emphasize the critical role of PV placement, feeder impedance (R/X ratio), and loading conditions in determining voltage rise and flicker severity, providing a foundation for strategic DER interconnection to enhance grid reliability.

4. Conclusion

This paper presented the voltage regulation challenges from Voltage Source Converter (VSC)-based Photovoltaic (PV) Distributed Energy Resources (DERs) in primary distribution systems using the IEEE 8500-node test feeder. It was revealed that the voltage rise peaks at 130.15 V during Off-Peak conditions at G_{FS}, exceeding ANSI C84.1 limits, while flicker reaches 10.85% under Peak load at G_{FS}, surpassing IEEE Std 1547-2018 thresholds. PV placement far from the substation (G_{FS}) worsens both issues due to higher R/X ratios (0.55 vs. 0.19 at G_{NS}), whereas proximity to the substation (G_{NS}) lowers the impact. These findings highlight the need to study the steady-state voltage rise and RVC of PV DERs simultaneously at all feeder loading conditions and

recommend connecting DERs closer to substations to reduce the likelihood of voltage disturbances and enhance grid stability.

References

[1] A. Awad, D. Turcotte, and T. H. M. El-Fouly. Impact assessment and mitigation techniques for high penetration levels of renewable energy sources in distribution networks: Voltage-control perspective. *Journal of Modern Power Systems and Clean Energy*, 10:450–462, Mar 2022.

[2] E. A. Hamza, B. E. Sedhom, and E. A. Badran. Impact and assessment of the overvoltage mitigation methods in low-voltage distribution networks with excessive penetration of pv systems: a review. *IET Energy Systems Integration*, 2(1):1–14, Mar 2022.

[3] M. M. Haque and P. Wolfs. A review of high pv penetrations in lv distribution networks: Present status and impacts. *Renewable and Sustainable Energy Reviews*, 62:1195–1208, Sep 2016.

[4] Vanika Sharma, Mohammed H. Haque, Syed Mahfuzul Aziz, and Travis Kauschke. Reducing overvoltage-induced pv curtailment through reactive power support of battery and smart pv inverters. *IEEE Access*, 12:123995–124008, 2024.

[5] Ewald F. Fuchs and Mohammad A. S. Masoum. *Power Quality in Power Systems and Electrical Machines*. Academic Press, Burlington, MA, 2008.

[6] J. O. Petinrin. Impact of renewable generation on voltage control in distribution systems. *Renewable and Sustainable Energy Reviews*, 65:770–783, Nov 2016.

[7] Rich Seguin, Jeremy Woyak, David Costyk, Josh Hambrick, and Barry Mather. High-penetration pv integration handbook for distribution engineers. Technical Report NREL/TP-5D00-63114, National Renewable Energy Laboratory (NREL), January 2016.

[8] Institute of Electrical and Electronics Engineers (IEEE). Ieee standard for interconnection and interoperability of distributed energy resources with electric power systems, 2018.

[9] American National Standards Institute (ANSI). American national standard for electric power systems and equipment – voltage ratings (60 hertz), 2007. Archived 27 July 2007 at the Wayback Machine. NEMA. Access may require purchase.

APPENDIX C: PLAGIARISM TEST REPORT

Upendra Bhattarai

079MSPSE024_MSc_Thesis_Upendra_For_Plagiarism.pdf

Tribhuvan University

Document Details

Submission ID
trn:oid:::3117:450092398

Submission Date
Apr 18, 2025, 1:36 AM GMT+5:45

Download Date
Apr 18, 2025, 1:38 AM GMT+5:45

File Name
079MSPSE024_MSc_Thesis_Upendra_For_Plagiarism.pdf

File Size
3.2 MB

63 Pages

14,131 Words

76,822 Characters

11% Overall Similarity

The combined total of all matches, including overlapping sources, for each database.

Match Groups

- **128** Not Cited or Quoted 8%
  Matches with neither in-text citation nor quotation marks
- **29** Missing Quotations 2%
  Matches that are still very similar to source material
- **8** Missing Citation 1%
  Matches that have quotation marks, but no in-text citation
- **1** Cited and Quoted 0%
  Matches with in-text citation present, but no quotation marks

Top Sources

6% Internet sources
9% Publications
0% Submitted works (Student Papers)

Integrity Flags

0 Integrity Flags for Review

No suspicious text manipulations found.

Our system's algorithms look deeply at a document for any inconsistencies that would set it apart from a normal submission. If we notice something strange, we flag it for you to review.

A Flag is not necessarily an indicator of a problem. However, we'd recommend you focus your attention there for further review.

Match Groups

- **128** Not Cited or Quoted 8%
  Matches with neither in-text citation nor quotation marks
- **29** Missing Quotations 2%
  Matches that are still very similar to source material
- **8** Missing Citation 1%
  Matches that have quotation marks, but no in-text citation
- **1** Cited and Quoted 0%
  Matches with in-text citation present, but no quotation marks

Top Sources

6% Internet sources
9% Publications
0% Submitted works (Student Papers)

Top Sources

The sources with the highest number of matches within the submission. Overlapping sources will not be displayed.

1	Publication	Olufunke Abolaji Balogun, Yanxia Sun, Peter Anuoluwapo Gbadega. "Coordinatio... <1%
2	Publication	Rajiv K. Varma. "Smart Solar PV Inverters with Advanced Grid Support Functionali... <1%
3	Internet	www.nrel.gov <1%
4	Publication	Yanghui Wan, Jiahao Yan, Tianfeng Chu, Yaping Li, Kun Yuan, Kaifeng Zhang. "A T... <1%
5	Publication	Yuan Liu, Renke Huang, Wei Du, Ankit Singhal, Zhenyu Huang. "Highly-Scalable Tr... <1%
6	Publication	Parthasarathy, Hari Krishna Achuthan. "A Unified Mode Selection Framework for ... <1%
7	Internet	export.arxiv.org <1%
8	Internet	www.mdpi.com <1%
9	Publication	Ahmed Y. Hatata, Eman. O. Hasan, Mohammed A. Alghassab, Bishoy E. Sedhom. "... <1%
10	Internet	doaj.org <1%

11 Publication
Ismail Bendaas, Salim Bouchakour, Saliha Boulahchiche, Abdelhak Razagui et al. ... <1%

12 Publication
Ahmed S. A. Awad, Dave Turcotte, Tarek H. M. EL-Fouly, Alexandre Prieur. "Impact... <1%

13 Internet
dx.doi.org <1%

14 Publication
R. F. Arritt, R. C. Dugan. "The IEEE 8500-node test feeder", IEEE PES T&D 2010, 2010 <1%

15 Publication
Sanni, Mubeenah Titilola. "Voltage Profile Control of Active Distribution Networks... <1%

16 Internet
hdl.handle.net <1%

17 Internet
tigerprints.clemson.edu <1%

18 Publication
Nicholas Jacobs, Shamina Hossain-McKenzie, Deepu Jose, Danish Saleem et al. "A... <1%

19 Publication
Sandro Sitompul, Ken Shimomukai, Goro Fujita. "Enhancement of Volt-VAR Contr... <1%

20 Publication
Tooryan, Fatemeh. "A Techno-Economical Optimization of Distributed Generators... <1%

21 Publication
Daisuke Iioka, Kenichi Kusano, Takahiro Matsuura, Hiromu Hamada, Teru Miyaza... <1%

22 Internet
ilkogretim-online.org <1%

23 Internet
ir.lib.uwo.ca <1%

24 Internet
www.hindawi.com <1%

25 Internet
dspace.mit.edu <1%

26 Publication
Singh, Sanjeev, and Bhim Singh. "Passive filter design for a 12-pulse converter fed... <1%

27 Publication
Rajiv K Varma, Vatandeep Singh. "Review of Studies and Operational Experiences ... <1%

28 Internet
sc.osti.gov <1%

29 Internet
www.semanticscholar.org <1%

30 Publication
K. P. Schneider. "Voltage control devices on the IEEE 8500 node test feeder", IEEE ... <1%

31 Publication
Venkatesan, N.. "Residential Demand Response model and impact on voltage pro... <1%

32 Internet
exaly.com <1%

33 Internet
habib.edu.pk <1%

34 Publication
Musaed Alrashidi, Saifur Rahman. "A bi-level optimization method for voltage con... <1%

35 Internet
www.researchgate.net <1%

36 Publication
"Intelligent Data Engineering and Automated Learning – IDEAL 2018", Springer Sc... <1%

37 Publication
Kocar, Ilhan, Jean Mahseredjian, Ulas Karaagac, Gurkan Soykan, and Omar Saad. ... <1%

38 Publication
Modi, Pramod S.. "An Investigation on Harmonics and Active / Reactive Power of ... <1%

39 Publication
Vanika Sharma, Mohammed H. Haque, Syed Mahfuzul Aziz, Travis Kauschke. "Sm... <1%

40 Publication
Gandhi, Oktoviano. "Reactive Power Support Using Photovoltaic Systems: Techno... <1%

41 Publication
Kun Huang, Fuhai Chi, Zhenlan Dou, Zhongguang Yang, Ming Fu, Cheng Liu. "Stab... <1%

42 Publication
Shriram Srinivasarangan Rangarajan, Jayant Sharma, C. K. Sundarabalan. "Novel ... <1%

43 Internet
vdoc.pub <1%

44 Publication
Henrique P. Correa, Flavio H. T. Vieira, Lina P. G. Negrete. "Double Pilot Node Dec... <1%

45 Internet
econpapers.repec.org <1%

46 Internet
ouci.dntb.gov.ua <1%

47 Internet
www.kscst.org.in <1%

48 Publication
Chakraborty, Sudipta, Anderson Hoke, and Blake Lundstrom. "Evaluation of multi... <1%

49 Publication
Emmanuel, Michael, and Ramesh Rayudu. "Evolution of dispatchable photovoltai... <1%

50 Publication
Haque, M. Mejbaul, and Peter Wolfs. "A review of high PV penetrations in LV distri... <1%

51 Internet
ir.mksu.ac.ke <1%

52 Internet
mpce.info <1%

53 Internet
www.etasr.com <1%

54 Internet
www.osti.gov <1%

55 Publication
Leandro Ramos de Araujo. "Power-flow analysis of the IEEE8500-Node Test Feede... <1%

56 Publication
Leonard Mukwekwe, Chitra Venugopal, Innocent E. Davidson. "A review of the im... <1%

57 Internet
mdpi-res.com <1%

58 Internet
vtechworks.lib.vt.edu <1%

59 Publication
D. Lin, E.F. Fuchs. "Real-Time Monitoring of Iron-Core and Copper Losses of Transf... <1%

60 Publication
Juan M. Lujano-Rojas, Rodolfo Dufo-López, José L. Bernal-Agustín, José A. Domíng... <1%

61 Publication
Karthikeyan M., Manimegalai D., Karthikeyan Rajagopal. "Enhancing voltage cont... <1%

62 Publication
Kelsey A.W. Horowitz, Bryan Palmintier, Barry Mather, Paul Denholm. "Distributio... <1%

63 Publication
Mora, Sergio Basilio Sepúlveda. "Renewable Energy Grid Integration and Resilien... <1%

64 Publication
Paulo Radatz, Celso Rocha, Matthew Rylander, Jeff Smith, Nelson Kagan. "Distribu... <1%

65 Publication
Schneider, Kevin P., Jason C. Fuller, and David P. Chassin. "Multi-State Load Model... <1%

66 Publication
Sibin Mohan, Syeed Hasan, Yafet Gebremariam, Rajiv K Varma. "Increasing Hosti... <1%

67 Publication
Sultan S. AlKaabi, Vinod Khadkikar, H. H. Zeineldin. "Incorporating PV Inverter Co... <1%

68 Publication
Sunderman, W., R. Dugan, and B. Seal. "Advanced inverter controls for distribute... <1%

69 Publication
W. H. Kersting. "Center tapped transformer and 120/240 volt secondary models", ... <1%

70 Internet
acris.aalto.fi <1%

71 Internet
cimug.ucaiug.org <1%

72 Internet
ntnuopen.ntnu.no <1%

73 Internet
phd.mater.uni-mate.hu <1%

74 Publication
Bryan Palmintier, Blake Lundstrom, Sudipta Chakraborty, Tess Williams, Kevin Sc... <1%

75 Publication
Giraldez Miner, Julieta. "Customer and System Impacts of Grid Support Functions ... <1%

76 Publication
M. Pantos, F. Gubina. "Allocation of production to consumers", The IEEE Region 8 ... <1%

77 Publication
Nishant Bilakanti, Frank Lambert, Deepak Divan. "Integration of Distributed Ener... <1%

78 Publication
Paradis, Dominic, Farid Katiraei, and Barry Mather. "Comparative analysis of time... <1%

79 Publication
Renata Mota Martins, Zedequias Machado Alves, Gustavo Marchesan, Ghendy Ca... <1%

80 Internet
silo.pub <1%

81 Publication

"Energy Informatics", Springer Science and Business Media LLC, 2025 <1%

82 Publication

Dilini Almeida, Jagadeesh Pasupuleti, Janaka Ekanayake. "Assessing the Performa... <1%

83 Publication

Oytun Babacan, William Torre, Jan Kleissl. "Siting and sizing of distributed energy... <1%

84 Publication

Sarineh Hacopian Dolatabadi, Maedeh Ghorbanian, Pierluigi Siano, Nikos D. Hatzi... <1%

85 Publication

Williams, Tess, Jason Fuller, Kevin Schneider, Bryan Palmintier, Blake Lundstrom, ... <1%